NTNU
Norwegian University of Science and Technology
Department of Marine Technology

MASTER THESIS

Title:	Delivered:
Time-domain simulation of floating wind power plants in irregular seas	June 9, 2011
	Availability: Restricted
Student: Ine-Therese Binner	**Number of pages:** Report: 49 Total: 79

Abstract:

As the limited fossil energy sources become empty, new sources for energy need to be exploited. One such renewable energy is wind energy. The wind energy potential is high offshore, and is therefore a beneficial location to place wind power plants. Europe has very large areas of seabed with a suitable water depth and sea floor. However, due to a number of reasons, the available shallow area for bottom-fixed offshore wind farms is limited. One must therefore exploit the possibility of wind turbines at large water depths. Here, floating solutions must be introduced. As it is not possible to perform model tests which comply with the scaling laws for both the aerodynamic and wave forces, the design of floating wind turbines is highly dependent on precise numerical tools to find the optimal technical solutions.

The main loads on an offshore structure come from the environmental, waves, wind and current, with waves as the most important. Thus, it is very important to simulate waves correctly so that their effects on the structures have an adequate degree of accuracy. Fast Fourier Transform (FFT) is normally used for linear analysis when simulating irregular waves. However, the computational requirements will become prohibitive when performing a nonlinear analysis on floating offshore structures, and therefore is another method for representation of the wave spectrum desirable. The purpose of this thesis is to contribute to the verification of an alternative method, the *Equal Area Principle (EAP)*. The adequacy of the equal area method is tested on a bottom-fixed, vertical cylinder and the SWAY turbine.

The models are implemented in the nonlinear structural analysis program, USFOS. The accuracy of the USFOS command, *SpoolWave* employed on SWAY has also been examined, and is found to be satisfactory.

According to present observations the equal area method is not recommended to be used on fixed structures because of the non-consistent trend in the results. Regarding the SWAY turbine, the equal area method gives satisfactory results, and is therefore considered valid when used on floating solutions.

Key words:

Stochastic Processes and Statistical Parameters

Fast Fourier Transform and Equal Area Method

SWAY Turbine, Fixed Cylinder

Advisors:

Professor Jørgen Amdahl

Tore Holmås

MASTER THESIS 2011
for
Stud. Techn. Ine-Therese Binner

Time-domain simulation of floating wind power plants in irregular seas

Tidsplananalyse av flytende vindkraftverk i irregulær sjø

As the limited, fossil energy sources become empty, new sources for energy need to be exploited. One such source is wind energy. Most wind turbines today are installed on-shore, and in many regions the remaining on-shore sites are limited. There is often a conflict between installation wind turbines and other use of the area, for example noise, visual "pollution" etc.
One solution to this may be to put the wind turbines offshore where the wind energy potential is high. Relative shallow water areas will be utilized first with bottom-fixed installations.
As large areas offshore have water depths more than 50-70m, which is the limit for bottom-fixed structures, floating solutions will have to be introduced.

As it is not possible to perform model tests which comply with the scaling laws for both the aerodynamic and wave forces, the design of floating wind turbines is highly dependent on precise numerical tools to find the optimal technical solutions. This paper addresses some central aspects in the design of floating wind turbines. One such tool is vpOne, which has performs time domain integrated the servo-aero-hydroelastic system.

A challenge with time-domain analysis is the representation of the sea spectrum. For linear analysis and small displacements is common to use fast Fourier transform (FFT) of the sea spectrum. In order to avoid repetition of the wave history several thousand of uniformly spaced wave components may be needed. For floating structures large horizontal motions the computational requirements will become prohibitive by using FFT. An alternative top FFT is to use few wave components based on equal area principle. This implies that emphasis is placed on the energy rich parts of the wave spectrum. The accuracy of this method must be demonstrated. The purpose of this work is to check contribute to the verification of the method.

The following topics should be addressed:

1. Perform time domain static and dynamic simulation of a single bottom fixed, vertical cylinder subjected to Morrison based wave forces. The cylinder diameter shall be varied so that the loads are either mass dominated or drag dominated. The eigenperiod of the cylinder shall be varied be in regions with high energy and low energy. Simulations shall be carried out with both with constant frequency width and the equal area method. The number of wave components shall be varied.

2. Compare the statistical properties of the simulated histories and assesses the adequacy of using the constant area method. The required number of wave components shall also be addressed.

3. Perform a statistical comparison of the two methods for FLS and ULS characteristic response for the SWAY turbine concept and a bottom fixed (jacket) turbine.

4. Conclusions and recommendation for further work.
   Literature studies of specific topics relevant to the thesis work may be included.

The work scope may prove to be larger than initially anticipated. Subject to approval from the supervisors, topics may be deleted from the list above or reduced in extent.

In the thesis the candidate shall present his personal contribution to the resolution of problems within the scope of the thesis work.

Theories and conclusions should be based on mathematical derivations and/or logic reasoning identifying the various steps in the deduction.

The candidate should utilise the existing possibilities for obtaining relevant literature.

Thesis format
The thesis should be organised in a rational manner to give a clear exposition of results, assessments, and conclusions. The text should be brief and to the point, with a clear language. Telegraphic language should be avoided.

The thesis shall contain the following elements: A text defining the scope, preface, list of contents, summary, main body of thesis, conclusions with recommendations for further work, list of symbols and acronyms, references and (optional) appendices. All figures, tables and equations shall be numerated.

The supervisors may require that the candidate, in an early stage of the work, presents a written plan for the completion of the work. The plan should include a budget for the use of computer and laboratory resources which will be charged to the department. Overruns shall be reported to the supervisors.

The original contribution of the candidate and material taken from other sources shall be clearly defined. Work from other sources shall be properly referenced using an acknowledged referencing system.

The report shall be submitted in two copies:
- Signed by the candidate
- The text defining the scope included
- In bound volume(s)
- Drawings and/or computer prints which cannot be bound should be organised in a separate folder.
- The report shall also be submitted in pdf format along with essential input files for computer analysis, spreadsheets, Matlab files etc. in digital format

Deadline:, June 14, 2011

Contact person at Aker Offshore Partner: Tore Holmås

Trondheim, January 17, 2011

Jørgen Amdahl
Professor

Preface

This report is the result of my master thesis work at the Department of Marine Technology at the Norwegian University and Science and Technology (NTNU). The master thesis is the last part of the Master of Science degree and counts for 30 credits.

The thesis work has been about time-domain simulation of fixed and floating structures in irregular seas. The main focus has been on testing the adequacy of an alternative method of simulating waves, the *Equal Area Principle*. The goodness of the *SpoolWave* command in USFOS has also been tested with the equal area principle on the SWAY turbine.

Some problems were encountered during this process which led to some delays. The simulations on the fixed cylinder were first performed with a duration of three hours. But the computer program USFOS has a limited number of frequencies available for splitting the wave spectrum, leading to too few components to divide the wave spectrum satisfactory considering Fast Fourier Transform. All analyses were therefore performed over again with a duration of one thousand seconds. It was also necessary to run all analyses on the SWAY turbine again to avoid results that came from the initial transient response.

First I would like to thank my supervisor Professor Jørgen Amdahl for his help and encouragement throughout the semester.

Next, I would like to thank Tore Holmås from Aker Offshore Partner for running a great number of analyses on the SWAY turbine.

I would also like to thank Zhen Gao for teaching me the basics of the MATLAB toolbox, WAFO.

……..

Ine-Therese Binner

Summary

As the limited fossil energy sources become empty, new sources for energy need to be exploited. One such renewable energy is wind energy. The wind energy potential is high offshore, and is therefore a beneficial location to place wind power plants. The dimensions of offshore wind turbines are relatively larger than onshore wind turbines. Traditionally, offshore wind turbines are bottom fixed and installed in relatively shallow waters. Europe has very large areas of seabed with a suitable water depth and sea floor. However, shipping lanes, fishing banks, bird migration zones, defense testing grounds and recreational interest all tend to limit the area potentially available for offshore wind farms. Taking these limitations into account, there are not sufficient shallow water areas for large-scale offshore wind farms. One must therefore exploit the possibility of wind turbines at large water depths. Here, floating solutions must be introduced. As it is not possible to perform model tests which comply with the scaling laws for both the aerodynamic and wave forces, the design of floating wind turbines is highly dependent on precise numerical tools to find the optimal technical solutions.

The main loads on an offshore structure come from the environmental, waves, wind and current, with waves as the most important. Thus, it is very important to simulate waves correctly so that their effects on the structures have an adequate degree of accuracy. Fast Fourier Transform (FFT) is normally used for linear analysis when simulating irregular waves. However, the computational requirements will become prohibitive when performing a nonlinear analysis on floating offshore structures, and therefore is an alternative method for representation of the wave spectrum desirable. The purpose of this thesis is to contribute to the verification of an alternative method, the *Equal Area Principle (EAP)*, i.e. the main objective is to compare the Equal Area Principle method against Fast Fourier Transform.

The thesis is divided into two main parts where the first part deals with the adequacy of the equal area method on a single bottom fixed, vertical cylinder. The second part compares the equal area method with FFT on the floating structure, the SWAY turbine. The assessment of the validity of the equal area method is based upon results from the following quantities; the mean, the standard deviation and the extreme values plotted in Gumbel probability papers. 90 percentile estimate of the Gumbel distributions are also used for comparison.

The models are implemented in the nonlinear structural analysis program, USFOS. The accuracy of the USFOS command, *SpoolWave* employed on SWAY has also been examined, and is found to be satisfactory.

The relevant statistical parameters for the resulting surface elevations have also been investigated. The simulated waves should approach a Gaussian process. The distribution has the following characteristics; a mean value of 0, standard deviation of 3, skewness of 0, and a kurtosis of 3. Both methods produce a good wave profile, i.e. satisfactory parameters, except the kurtosis. FFT produces a kurtosis value less than 3 and less than the equal area method. EAP produces in fact "better" parameters than FFT. The mean extremes of surface elevation from FFT and EAP are respectively lower and higher than the theoretical value. However, the deviations are not significant, and FFT and EAP results in a satisfactory, asymptotically Gaussian distribution.

Considering the results for the fixed cylinder, the equal area method gives both conservative and non-conservative response in comparison to FFT, i.e. the tendency of the equal area method is not predictable. Safety factors are proposed in the conclusions if employing EAP. However, according to present observations the equal area method is not recommended to be used on fixed structures because of the non-consistent trend in the results.

Several response quantities have been studied when checking the adequacy of the equal area method on the SWAY turbine. The equal area method always produces higher responses than FFT, i.e. the equal area method is conservative when employed on the SWAY turbine. However, the difference between the two methods is minor. This suggests that the equal area method is valid when employing a potential correction factor. These are proposed in conclusions.

The simulations have been carried out with a duration of one thousand seconds, and twenty samples from each case are available for comparison. Because of statistical uncertainty, the information basis may be too small to justify firm conclusions. It is therefore recommended to carry out more simulations with longer duration before final conclusions are made.

Table of Contents

Figures

Tables

Nomenclature

An attempt has been made to explain all symbols the first time they appear in each chapter. Here follows a list explaining the most important symbols and abbreviations.

Latin Symbols

α	Gumbel parameter
α	Damping coefficient
β	Damping coefficient
β	Frequency ratio
γ_1	Skewness
γ_2	Kurtosis
$\delta()$	Phase angle associated with response
ε	Phase angle
ϵ	Phase angle
λ	Damping ratio
μ^n	Moments
$\bar{\mu}^n$	Central Moments
ξ	Surface elevation
ξ_A	Wave Amplitude
ρ	Water density
σ	Standard deviation
σ^2	Variance
ϕ	Phase angle
ω	Frequency (rad/s)

Greek Symbols

A	Added mass
A_j	Wave amplitude
a_x	Horizontal water particle acceleration
C	Damping matrix
C_D	Drag coefficient
C_M	Mass coefficient
D	Diameter
E()	Expectation value
f()	Probability density distribution
f	Hertz (s^{-1})
F()	Cumulative density function
dF	Total wave force per unit length
H_s	Significant wave height
$\lvert H() \rvert$	Transfer function
K	Stiffness matrix
k	Stiffness
M	Mass matrix
m	Mass
m_o	Second standardized moment
N	Number

R	External forces
r	Response
S()	Wave spectrum
T_i	Transfer function
T_n	Natural period
T	Time
t	Time
u	Horizontal water particle velocity
u	Gumbel parameter
x	Stochastic variable
dz	Unit length in z direction

Abbreviations

CDF	Cumulative distribution function
EAP	Equal Area Method
FFT	Fast Fourier Transform
PDF	Probability density function
RAO	Response amplitude operator
ULS	Ultimate limit state

1 Introduction

As fossil energy sources become empty, new sources for energy need to be exploited. One such source is wind energy. The wind energy potential is high offshore. Traditionally, offshore wind turbines are installed on relatively shallow waters. However, due to a number of reasons, the potentially available shallow area for offshore wind turbines is limited. One needs therefore to exploit the possibility of wind turbines at larger depths. When the water depth is large, floating solutions must be introduced where horizontal deformations are large. In a linear analysis, the Fast Fourier Transform (FFT) is commonly used for simulating irregular waves. However, here, the computational requirements will become prohibitive, and an alternative method for representation of the wave spectrum is desirable. An option is using a method based on the *equal area principle* with few wave components. The accuracy of this method has not yet been fully demonstrated.

Thesis Outline

The purpose of this Thesis is to contribute to the verification of the alternative method to simulate waves, the *Equal Area Principle* (EAP). The main objective of this thesis is to compare the Equal Area Method against Fast Fourier Transform. The main loads on an offshore structure come from environmental, waves, wind and current, with waves as the most dominating. Thus, it is very important to simulate waves correctly so that their effects on the structures have an adequate degree of accuracy.

The thesis is divided into two main parts where the first part deals with the adequacy of the equal area method on a fixed offshore structure, a single bottom fixed, vertical cylinder. The latter part compares the equal area method upon FFT on the floating structure, the SWAY turbine.

When comparison of two methods is made, several statistical parameters must be checked. Chapter 2 gives an overview and explanation of these parameters together with a short introduction of the methods, FFT and EAP, and stochastic processes.

Chapter 3 describes the performance of a time-domain static and dynamic simulation of the fixed cylinder subjected to Morison based wave forces. The computer program, USFOS is used throughout this project for the analyses. Chapter 4 gives a short description of the program.

Chapter 5 contains all results from the time-domain analyses of the fixed cylinder together with discussion of the results. A temporary conclusion of the adequacy of the equal area method is made in Chapter 6.

Chapter 7 gives an introduction of the SWAY concept and outlines the performance and results for the dynamic analyses of the turbine in USFOS. Discussion around the results is found in Chapter 8.

Further reduction of computer time can be possible by using a command, *SpoolWave* in USFOS. Verification of this command is attempted in Chapter 9.

Chapter 10 contains the conclusion of this work and Chapter 11 gives recommendations for further work.

2 Time-Domain Analysis

A challenge with time-domain analysis is to get a correct representation of the sea spectrum. It is common to use Fast Fourier transform (FFT) for representation of the sea spectrum. But in order to avoid repetition of the wave history and to describe the peak accurately, several thousand of uniformly spaced wave components may be necessary. Therefore, the computational requirements will become prohibitive concerning nonlinear analyses. An alternative is to use few wave components based on the equal area principle (EAP). In this case the area in the spectrum is kept constant as the name implies, in contrast to FFT.

This chapter gives a description of FFT and EAP, together with the theory regarding statistical parameters and extreme value distribution that is used to assess the adequacy of the equal area method.

2.1 Simulation of Irregular Sea

The irregular sea is generated by Fast Fourier Transform of the wave spectrum. This gives a finite set of discrete wave components. Each component is expressed as a harmonic wave amplitude, angular frequency and random phase angle. The surface elevation of the irregular sea is approximated by superposition of all extracted harmonic wave components with random phase angles between 0 and 2π. Refer equation 2-1 and Myrhaug (2007).

$$\boldsymbol{\xi(t) = \sum_{n=1}^{N} \xi_{An} \cos(\omega_n t + k_n x + \phi_n)} \qquad \textbf{(2-1)}$$

Where:

ξ_{An}	Amplitude of harmonic wave number n
ω_n	Angular frequency of harmonic component n
k_n	Wave number for harmonic component n
ϕ_n	Random phase angle for harmonic component n

The wave amplitude of each harmonic component is determined by the wave spectrum

$$\boldsymbol{\zeta_{An} = \sqrt{2 \int_{\omega_{l,n}}^{\omega_{u,n}} S(\omega_n) \mathrm{d}\omega}} \qquad \textbf{(2-2)}$$

Where $S(\omega_n)$ is a given value in the wave spectrum, and $\omega_{l,n}$ $\omega_{u,n}$ represents the lower and upper angular frequency limit for wave component n. Two methods are available for the integration term, refer USFOS Hydrodynamics (SINTEF marintek 2010).

2.1.1 FFT – Fast Fourier Transform

The traditional method, FFT calculates the wave amplitude with same resolution in frequency, giving different amplitudes for each calculation.

$$\boldsymbol{\omega_{u,n} - \omega_{l,n} = \Delta\omega = \frac{\omega_u - \omega_l}{N} = constant} \qquad \textbf{(2-3)}$$

Where ω_u and ω_l are the upper and lower limit for the integration of the wave energy spectrum, refer Figure 2-1. The number of components, N must be sufficiently large in order to avoid repetition of the wave history. A minimum number of harmonic components are given by $\Delta\omega \leq \pi/T$, where T is the simulation time, refer Langen (1979).

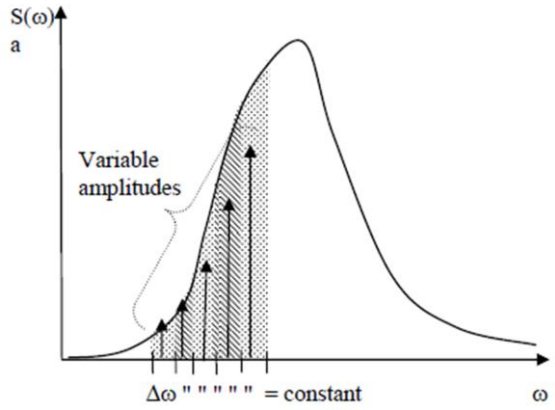

Figure 2-1 Illustration of irregular sea state generation with FFT (USFOS Hydrodynamics 2010)

2.1.2 EAP – Equal Area Method

The equal area method adjusts the frequency limits so that each component contains the same amount of energy, resulting in equal wave amplitudes for each calculation. This is illustrated in Figure 2-2 and shown in equation 2-4. Number of components that are required in EAP is not as strict because of the variable resolution in frequency. The following periods of the sine curves are not harmonically related and the series repeats only after a long time, refer USFOS Hydrodynamics (SINTEF marintek 2010).

$$\zeta_{An} = \sqrt{2\int_{\omega_{l,n}}^{\omega_{u,n}} S(\omega)\mathrm{d}\omega} = \sqrt{\frac{2\int_{\omega_l}^{\omega_u} S(\omega_n)\mathrm{d}\omega}{N}} = constant \qquad \textbf{(2-4)}$$

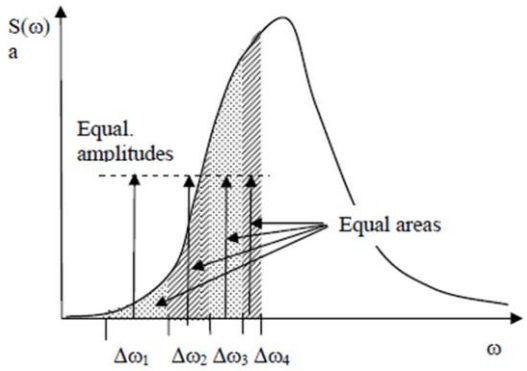

Figure 2-2 Illustration of irregular sea state generation with EAP (USFOS Hydrodynamics 2010)

The above methods give a deterministic spectral amplitude, i.e. only random phase and non-random generation of amplitudes. A stochastic process with only random phase is asymptotically Gaussian. Use of this equation in a time simulation will always produce a spectrum equal to S(ω) and thus some randomness of the real wave system will be lost according to M. J. Tucker et al. (1984). In reality the amplitude should be random resulting in a Gaussian distribution.

Due to the idealization one has to some extent lost contact with reality, and the adequacy of this idealization regarding the actual problem is essential with respect to reliability of the decisions that are to be made. To quantify this sort of uncertainty is in general rather difficult.

2.2 Statistical Parameters

Spectral analysis of stochastic processes carried out in the frequency domain is a prerequisite for predicting properties of stochastic processes (Leira 2010). A detailed description of a stochastic variable, such as a wave profile is achieved by characteristic quantities given by higher order moments. It is important to evaluate various parameters of a stochastic process such as those representing the measure of mean, variance, asymmetry and peakedness of the probability distribution. Haver (2010) states that in practice it is usually assumed that the variations in characteristics are much slower than the variations in the sea surface itself. Due to this realization, the stochastic process can for short time periods considered as being a realization of a stationary process.

For a total description of a stochastic variable by its moments, one must in general include an infinite number of moments. In practice, this is impossible, and the methods available for describing a variable by moments are based on inclusion only of moments up to a certain order. This implies that one only have an approximate description. However, the mean value and the variance are the most important characteristic quantities for a variable. If the variable is normally distributed, such as a wave profile, the second order moments give a complete description of the variable, refer Leira (2010). Moments and central moments are defined below:

Moments: $$\mu_x^{(n)} = \int_{-\infty}^{\infty} x^n f_x(x) dx \quad \textbf{(2-5)}$$

Central moments: $$\bar{\mu}_x^{(n)} = \int_{-\infty}^{\infty} (x - \mu_x)^n f_x(x) dx \quad \textbf{(2-6)}$$

Where:

x	Variable X
$f_x(x)$	Probability density function for a variable

2.2.1 Expectation Value

The expectation value represents the "center of gravity" for the distribution (Leira 2010), where X is the stochastic variable. The mean is the expected value for a random variable.

$$\mu_x^{(1)} = E[X] = \int_{-\infty}^{\infty} x f_x(x) dx \quad \textbf{(2-7)}$$

This value is zero for a normal distribution.

2.2.2 The Variance

The variance is used in order to express the spreading of the distribution (Leira 2010). The standard deviation is the square root of the variance. Figure 2-3 illustrates the center of gravity and standard deviation for a normal distribution.

$$\bar{\mu}_x^{(2)} = \sigma_x^2 = Var[X] = \int_{-\infty}^{\infty} (x - \mu_x)^2 f_x(x) dx \quad \textbf{(2-8)}$$

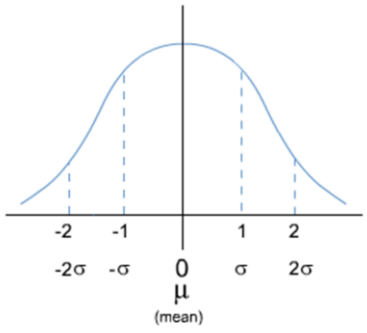

Figure 2-3 Normal distribution with sketch of standard deviation and mean

2.2.3 Skewness

The skewness gives a description of the asymmetry of a distribution around its mean. The skewness of a random variable X is the third standardized moment (Leira 2010), and defined as:

$$\gamma_1 = \frac{\bar{\mu}_x^{(3)}}{(\bar{\mu}_x^{(2)})^{3/2}} = \frac{\bar{\mu}_x^{(3)}}{\sigma_x^3} \qquad \textbf{(2-9)}$$

This value is zero for a normal distribution. Figure 2-4 illustrates different shapes for distributions with variable skewness.

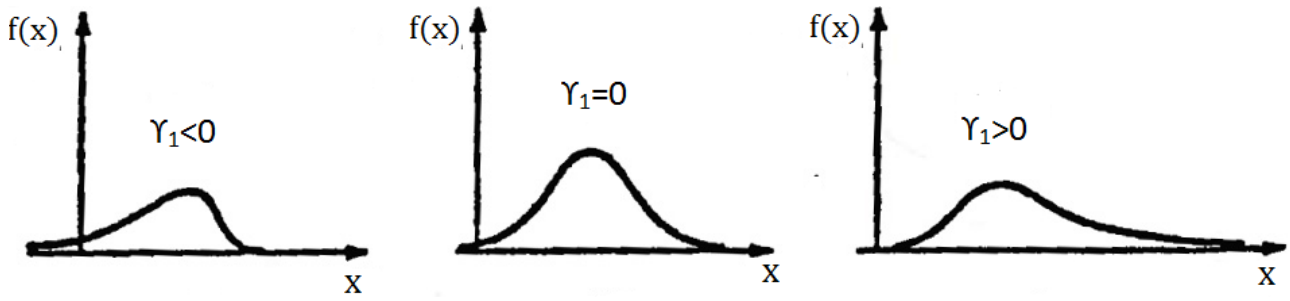

Figure 2-4 Illustration of distributions with different skewness

2.2.4 Kurtosis

Kurtosis is the measurement of the "peakedness" of the probability distribution. The kurtosis coefficient is also called the fourth standardized moment (Leira 2010) and is defined as:

$$\gamma_2 = \frac{\bar{\mu}_x^{(4)}}{(\bar{\mu}^{[2]})^2} = \frac{\bar{\mu}_x^4}{\sigma_x^4} \qquad \textbf{(2-10)}$$

This value is three for a normal distributed variable. Refer Figure 2-5 for illustration.

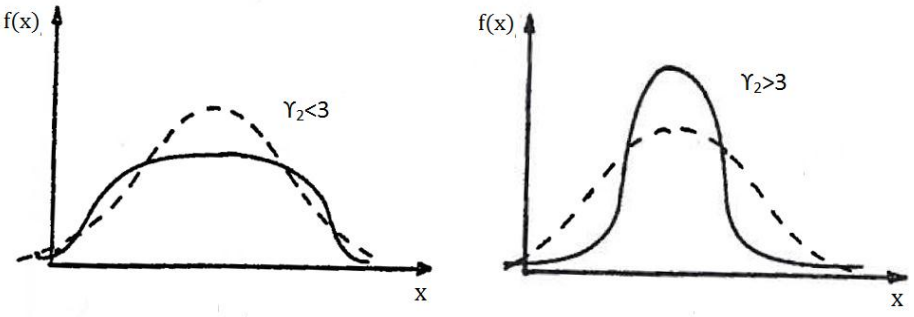

Figure 2-5 Illustration of distributions with different kurtosis

2.3 Extreme value statistics and Distribution

A quantity of high interest is the maximum value from a sample of a stochastic process. The distribution of the largest maxima from each sample is very important when it comes to analysis. The following assumptions are made in this thesis, refer (Leira 2010).

- All wave peaks are identically Rayleigh-distributed.
- All maxima are statistically independent and identically distributed.

2.3.1 The Gumbel Distribution

The Rayleigh distribution together with normal, log-normal, exponential, Weibull and Rice distributions result in an asymptotic Gumbel extreme value distribution, and is the most common extreme value distribution. The Gumbel cumulative density function (CDF) and probability density function (PDF) are defined as:

$$\boldsymbol{F_y(y) = \exp(-e^{-\alpha(y-u)})} \qquad \textbf{(2-11)}$$

$$\boldsymbol{f_y(y) = \alpha \exp(-\alpha(y-u) - e^{-\alpha(y-u)})} \qquad \textbf{(2-12)}$$

Where:

y	Sample maxima
α	Gumbel parameter
u	Gumbel parameter

Gumbel Probability Paper

Gumbel probability paper is based on the linearization of the cumulative distribution function shown in equation 2-11. Selecting a system with x as the horizontal axis and $y=-\ln[-\ln(F_y(y))]$ as the vertical axis, the Gumbel distribution will result in a straight line, i.e. the coordinate system is a Gumbel probability paper (Leira 2010).

Plotting the extreme values in a probability paper is a subjective method for verification of a selected distribution. This is due to the fact that it is not possible to establish any objective criteria for how large deviations from the straight line that can be accepted until the postulated distribution is rejected for a given significance level according to Leira (2010). However, the method represents a very simple and efficient tool for preliminary assessment of a tentative model. Accordingly, it is frequently applied in practical applications. Refer equation 2-13 for transformation to the Gumbel paper:

$$\boldsymbol{-\ln[-\ln[F_y(y)] = G_y(y) = \alpha(y-u) = \alpha y - b} \qquad \textbf{(2-13)}$$

Where:

α	Slope of straight line
b	Crossing of the axis

The cumulative density function F_i from an available sample is given by:

$$\boldsymbol{F_i = \frac{i}{1+N_y}} \qquad \textbf{(2-14)}$$

Where:

i	Number of samples within a given level
N_y	Total number of samples

2.3.2 Extreme value predictions

Provided that the number of samples is sufficiently large for identifying the tail behavior of the distribution, one can obtain extreme values in a Gumbel Probability Paper corresponding to a priory given exceedance probability. The duration of simulation should also be sufficiently long. In practice it is important to remember that there is considerable variability from sample to sample and whether the estimator is biased or not, i.e. there are scatter around the "true" value, refer Haver (2010). Various results may also come from different calculations of the Gumbel parameters α and b. They can be established from the moments from the distribution or by regression (Leira 2010). In this thesis, the parameter estimation is done by fitting the straight line to the empirical distribution functions in the diagrams and using the relations to relate parameters to intercept and slopes of the estimated lines, refer WAFO Tutorial (2000).

3 Time-Domain Simulation on a Fixed Cylinder

This chapter describes the performance of a time-domain static and dynamic simulation of a single bottom fixed, vertical cylinder subjected to Morison based wave forces. Simulations are carried out with FFT and the equal area method. Number of wave components is constant considering FFT and varied in the latter. The computer program USFOS is used when performing the time-domain simulations. Chapter 4 gives a description of the program.

The wave loads are chosen to be either mass dominated or drag dominated. This results in four separate analyses where comparison of FFT and equal area principle will be made. The following are:

- Static analysis when loads are mass dominated
- Static analysis when loads are drag dominated
- Dynamic analysis when loads are mass dominated
- Dynamic analysis when loads are drag dominated

When comparing two different methods, an adequate number of samples must be available. Twenty samples from each method with corresponding components in the four cases have been chosen to be a satisfying number. Statistical properties calculated from wave elevation time histories will be compared and evaluated, together with the extreme value distribution for wave elevation, wave load and overturning moment.

Running this many simulations is time consuming, and to automatize this process, Cygwin has been made use of. Cygwin is a Linux-like environment and command-line interface for Windows.

3.1 Case Study

The simulations of waves in USFOS have duration of one thousand seconds, T=1000s. FFT is executed with 1000 components while the number of wave components in the equal area method is varied between 30, 60 and 90 components. Morison's equation displayed in equation 3-1 is used to calculate wave forces on the structure (Pettersen 2007). The control file and model file for the fixed cylinder is given in Appendix A. Figure 3-1 illustrates the cylinder in USFOS.

$$dF = \rho \frac{\pi D^2}{4} C_M a_x dz + \frac{1}{2} \rho C_D D u|u| dz \qquad \textbf{(3-1)}$$

Where:

dF	Total force per unit cylinder length
ρ	Water density
D	Diameter of cylinder
C_M	Mass coefficient
C_D	Drag coefficient
a_x	Horizontal water particle acceleration
u	Horizontal water particle velocity
dz	Unit length in z direction

The first term represents the inertia force, and the latter, drag force. The cylinder diameter is varied so that the loads are either mass dominated or drag dominated, refer (Pettersen 2007). The wave loads decrease exponentially with water depth. It is therefore important to define number of integration sections to be used in connection with wave load calculation and to subdivide the cylinder in several beam elements to obtain accurate results (USFOS User's Manual 2006). A fine mesh is specified in the water surface where the wave loads are dominating. To save computer time, a coarser mesh is defined with increasing water depth where the wave loads are minor, refer Appendix A.

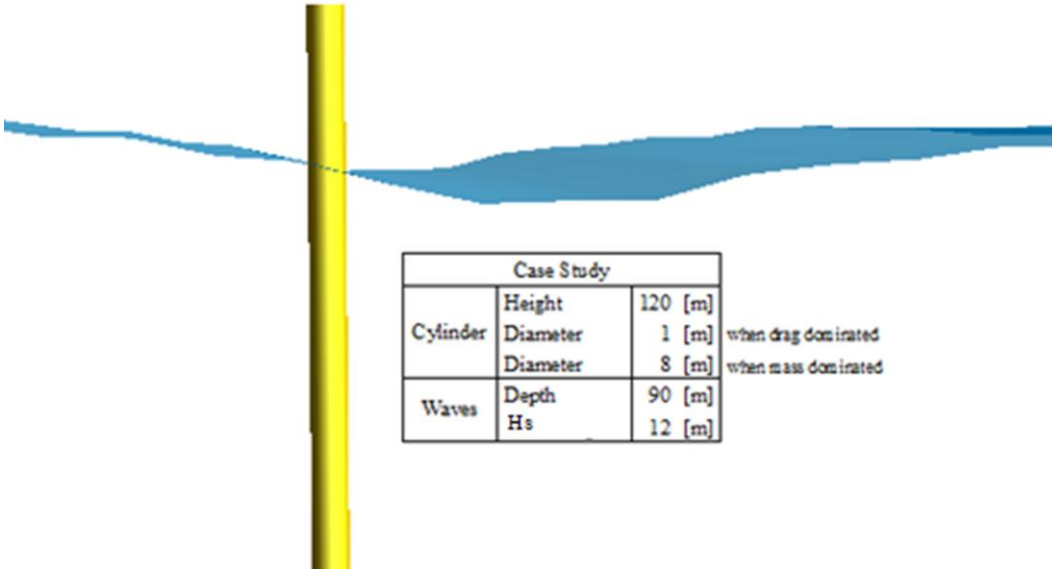

Figure 3-1 Fixed Cylinder in USFOS

The same Jonswap wave spectrum is used throughout the analysis. The gamma parameter in the Jonswap spectrum is set to 3.3 which give a realistic sea state of waves in the North Sea, according to Myrhaug (2007). The frequencies in the wave spectrum vary from $0.04s^{-1}$ to $0.33s^{-1}$ with a top period, T_p=14s, refer Figure 3-2. The water depth is set to 90m and the cylinder is 120m high. Significant wave height is also kept constant throughout the analysis, keeping the surroundings the same at all times.

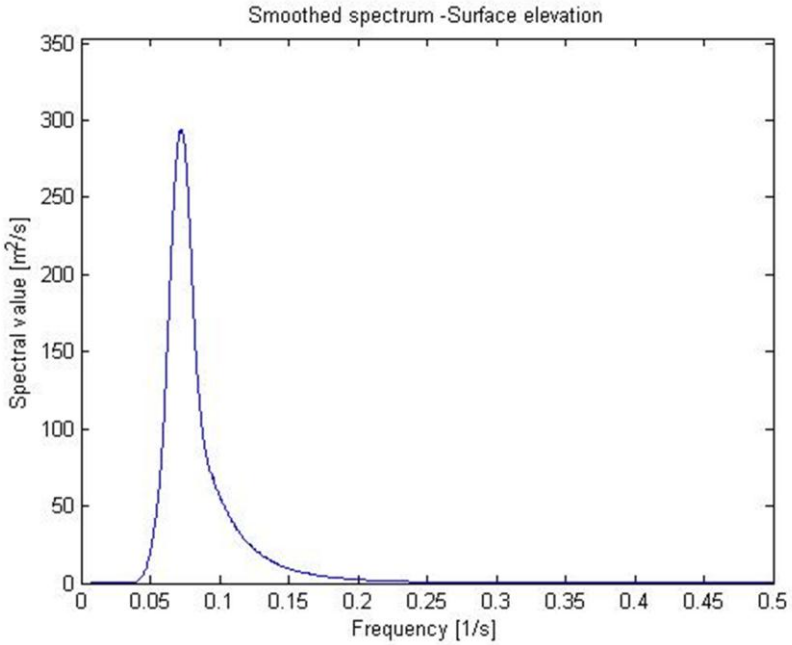

Figure 3-2 Specified wave spectrum

3.2 Static Analysis

In order to get a static behavior the cylinder's E-modulus is set to a value hundred times larger than steel, giving the cylinder hardly any horizontal displacement. The largest natural period is then far below 2s, and the cylinder can be considered as a quasi-static structure (Haver 2010), i.e. one can neglect the mass and damping term in the equation of motion. The equation of equilibrium is given by:

$$\boldsymbol{kr(t) = R(t)} \qquad \textbf{(3-2)}$$

Where:

k	Stiffness
r(t)	Response
R(t)	External/wave forces

3.3 Dynamic Analysis

The dynamic equation of equilibrium is formulated in terms of

$$\boldsymbol{m\ddot{r}(t) + c\dot{r}(t) + kr(t) = R(t)} \qquad \textbf{(3-3)}$$

Where:

m	Mass
c	Damping
k	Stiffness
R(t)	External/wave forces
r(t)	Response

The structural response can for all structures in principle be found by solving the equation of motion. The left hand side of the equation characterizes the mechanical properties of the system, i.e. how the structure responds to the loading, while the right hand side defines external loading. The damping coefficient and stiffness coefficient will generally be of a nonlinear behavior. However, results of sufficient accuracy can be achieved by modeling damping force as a linear function of $\dot{x}$ and the stiffness as a linear function of x, and one can define the problem as a linear mechanical system. Here, the acceptance of using a linear mechanical system is of reasonable accuracy as far as one is not analyzing the structure close to its limiting utilization. A linear model assumes that the structural response stay well within the elastic behavior (Haver 2010).

The response of a structure is dependent on the eigenfrequency of the structure, wave height and period of the wave profile subjected to the structure, refer Larsen (2009). It is therefore important to run the dynamic analyses on the cylinder with different natural periods to check the validity of EAP. The resolution in frequency intervals in the equal area method increases as the energy increases in the wave spectrum and therefore one suspect that large spreading in frequency in the low energy parts may give spurious response of the structure in USFOS. It is essential to investigate these responses to find the adequacy of the equal area method. Refer equation 3-4 for formula of the natural period.

$$\boldsymbol{T_n = 2\pi\sqrt{\frac{m+A}{k}}} \qquad \textbf{(3-4)}$$

Where:

m	Mass
A	Added mass
k	Stiffness

The structure's natural period is dependent of added mass, the natural period increases as the added mass increases. Added mass is dependent of wave frequency, and therefore will different wave height, seed and wave components in USFOS influence the natural period. Calculations of the natural periods must therefore be performed in calm water; significant wave height is set to 0.1m in USFOS. E-modulus and density are altered for obtaining the desired natural periods, keeping the dimensions of the cylinder the same. Structural displacements should not be too large, around 0.5m, keeping the structure in the elastic range, i.e. obtaining a linear mechanical system. This is taken in under consideration when tuning the natural periods. The three different natural periods that are chosen for dynamic analysis are:

- T_n=4.4s Lays in the low energy part of the wave spectrum.
- T_n=8.5s Lays in the mid energy part of the wave spectrum.
- T_n=14.0s Lays in the highest energy part of the wave spectrum.

It should be exercised that the initial transient response has been damped out when finding extreme responses from the dynamic simulation. Startup period is therefore set to eight minutes and is specified in the control file in USFOS.

3.3.1 Damping Actions

The damping coefficient in the equation of motion is one of the most critical parameters to be accounted for. The variables that govern damping forces are generally not as clear as they are for inertia and stiffness forces. Because of this uncertainty, it is most common to use viscous damping or Rayleigh damping, in which it is assumed that the damping matrix is proportional to the mass matrix, **M** and stiffness matrix, **K** (Langen 1979).

$$\boldsymbol{C = \alpha M + \beta K} \qquad \textbf{(3-5)}$$

Since the damping properties are frequency dependent, the identification of valid damping coefficients, α and β is a very complicated task. By assuming the relationship between the damping ratio and natural frequencies, Langen (1979) states that one can estimate the Rayleigh damping coefficients that will approximate the damping for all frequency modes. Here, one are assuming a damping ratio, λ=3%, at the periods 2s (ω_1= 3,14rad/s) and 15s (ω_2= 0,42rad/s), resulting in a damping ratio ranging between 2-3%. The relationship between damping ratio and frequency is calculated in an Excel spreadsheet and is shown in Figure 3-3. Equations used are displayed below:

$$\boldsymbol{\lambda_i = \frac{1}{2}\left(\frac{\alpha_1}{\omega_1} + \alpha_2 \omega_2\right)} \qquad \textbf{(3-6)}$$

Where:

$$\boldsymbol{\alpha_1 = \frac{2\omega_1\omega_2}{\omega_2^2 - \omega_1^2}\left(\lambda_1\omega_2 - \lambda_2\omega_1\right)} \qquad \textbf{(3-6)}$$

$$\boldsymbol{\alpha_2 = \frac{2\left(\lambda_2\omega_2 - \lambda_1\omega_1\right)}{\omega_2^2 - \omega_1^2}} \qquad \textbf{(3-7)}$$

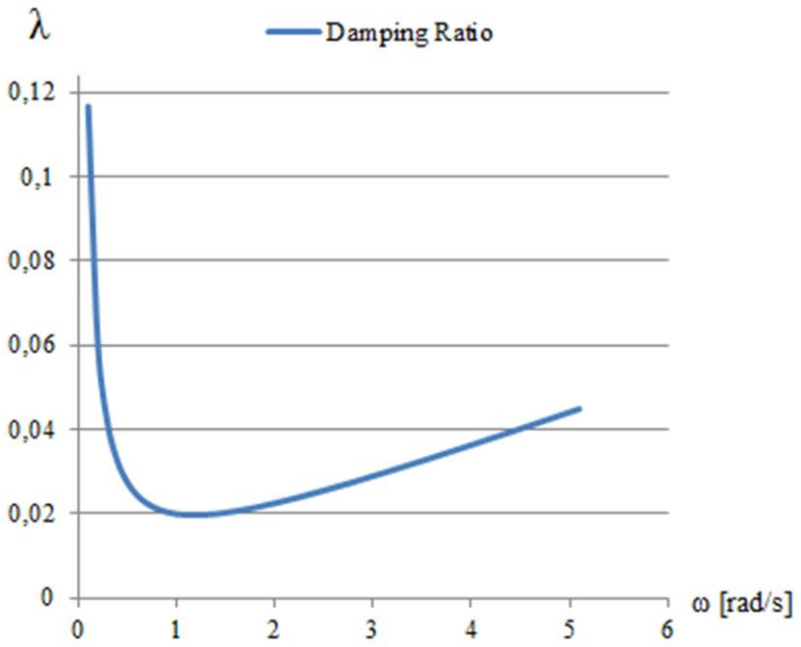

Figure 3-3 Damping as a function of eigenfrequency by proportional damping

4 Brief USFOS Review

This chapter gives a short review of the computer program, USFOS where the analyses are executed. The review focuses on parts which is important for time-domain simulation of irregular waves. Time-domain analysis gives the best prediction of "reality" where dynamic effects, integration to true surface level, buoyancy effects, hydrodynamic damping and other nonlinear effects become significant.

USFOS is a computer program for nonlinear static and dynamic analysis of space frame structures. The collapse process is accurately simulated in USFOS, from the initial yielding, through to the formation of a complete collapse mechanism and the finale toppling of the structure (USFOS Getting Started 2001).

The user may give all input on one file, or distribute the data on two or three .fem files. Usually, all control parameters are specified in the analysis control/head file and structure data are given in a separate file. The data records can be given in an arbitrary order (USFOS User's Manual 2006).

If not noted otherwise, default values are automatically used. For example the mass and drag coefficients are respectably 2.0 and 0.7.

4.1.1 Hydrodynamic Forces and Parameters

USFOS has built in the following wave theories; Airy extrapolated, Airy stretched, Stoke's 5th and stream function theory. Wave loads are calculated up to the momentary sea surface elevation. The user may also specify an irregular wave to be applied to the structure as hydrodynamic forces. This includes specification of different specter types, Jonswap, Pierson-Moscovitz or user defined. One can also select different representations of the sea spectrum, FFT and the equal area method. In order to obtain different time series the user must specify different "seeds" in the command, *wavedata*. Wave load integration points may be specified in connection with wave conditions for a more accurate result. In addition to surface waves, a stationary current can be defined. Refer USFOS User's Manual (2006).

Hydrodynamic forces are calculated according to Morison's equation with nonlinear drag formulation; refer equation 3-1. Loads are applied up to the instantaneous water surface generated by superposition of regular wave components. On the basis of the kinematics of each wave component, the hydrodynamic loads are calculated as a time series with a given time increment and for a given time interval. In a dynamic simulation the wave forces have to be introduced gradually, and the wave is ramped up using a user defined "envelope" (USFOS Hydrodynamics 2010).

The acceleration of the member influences the mass force in Morison's equation. In USFOS, the structure accelerations are transformed to element local axes, before subtraction from the local wave particle accelerations. Added mass are included in the mass term on the left side of the dynamic equation. Added mass intensity for each element is predefined. Motion in and out of water is taken into account on node level, i.e. the mass matrix is constantly updated. Only submerged nodes contribute to the system's added mass, refer USFOS Hydrodynamics (SINTEF marintek 2010).

The hydrodynamic pressure is specified by the command *buoyform panel* and is integrated to the true surface. The resultant of integrating the hydrodynamic pressure is the Archimedes buoyancy force. Integration of the hydrodynamic pressure gives a reduced buoyancy effect during a wave crest an increase of the buoyancy during a wave trough compared to the "Archimedes" (static force) force (USFOS Hydrodynamics 2010).

Buoyancy may be calculated either by determination of the displaced volume or by direct integration of the hydrodynamic – and hydrostatic pressure over the wetted area mentioned above. The buoyancy forces are added to the actual load case or if no load case is specified, added to the *wavedata* load case.

By default all elements are buoyant, but by using the *flooded* command, it is possible to remove buoyancy for selected elements. The *flooded* command has only meaning if *buoyancy* is specified. The current position of the sea surface defines whether an element becomes buoyant or not at any time.

Marine growth can also be implemented and is specified as a thickness addition to element diameter and may be specified by a depth profile, $t_{mg}(z)$. The thickness of the marine growth is based upon the midpoint coordinate of the member and is characterized by its density. In USFOS, the buoyancy counteracts marine growth when the pipe is submerged. The buoyancy disappears and the weight of the marine growth becomes fully effective when the pipe is free of water.

The *SpoolWave* command in USFOS can be used for reduction in computer time, and is applied in this rapport. Further details around the command are found in Chapter 9.

4.1.2 Dynamic Modeling Parameters

The user may choose between a *static* or *dynamic* analysis. If a dynamic analysis is chosen, damping ratio or Rayleigh damping can be specified. In connection with calculation of drag forces, one must specify the command *rel_velo* to account for the relative velocity between the structure and the wave particles.

The input parameter *Dynres* may be considered one of the most important dynamic modeling parameters in USFOS. A Dynres parameter specifies element quantities to be saved every step during a dynamic analysis independent on the 'raf'-file saving interval where structure data, analysis results, and restart data at each load step are found. Results are stored on a separate file and these time histories are accessed from *exact.exe* which is the graphical user interface for USFOS. The dynamic result may refer to node, beam or global result (USFOS User's Manual 2006).

4.1.3 Generally

The loads on the structure are applied in steps, and the system stiffness equations are solved at every step according to the updated Lagrangian formulation. After each step, element forces, nodal coordinates etc. are updated, and plastic hinges are introduced if necessary. In other words, each step forms a full and linear analysis, based on the updated information from all previous analysis steps. A pure incremental procedure is adopted as default. Equilibrium iterations may also be specified by the user (USFOS Getting Started 2001).

Other area of application has not been an important part of this thesis, and will not be taken into more detail. For more details refer USFOS Hydrodynamic (SINTEF marintek 2010), USFOS User's Manual (SINTEF marintek 2006) and Theory Manual (Tore H. Søreide 1993).

5 Discussion and Results from Fixed Cylinder Analyses

To find the accuracy of the equal area method, several statistical properties for the wave profile must be examined from time series of the surface elevation. These are the mean value, standard deviation, skewness, kurtosis and the extreme value distribution. Time series from FFT are treated as the correct solution and results from the equal area principle are compared upon FFT. Extreme values for wave load and overturning moment are also going to be examined.

Results from the static and dynamic analyses are given and discussed in this chapter. Mean values are calculated as $X = \frac{1}{n}\sum_{i=1}^{n} x_i$.

5.1 Verification of Statistical Parameters for the Wave profile

Time series from a wave elevation should approach a Gaussian/normal distribution. A normal distribution has a mean value of zero, skewness value of zero and kurtosis value of three. Refer Chapter 2.2 for more details.

As mentioned previously, a sufficient number of samples must be available to compare the two methods. The static and dynamic simulations have a duration of 1000s. It should be exercised that the initial transient response has been damped out when performing the dynamic simulation. Startup period is therefore set to 500s in the dynamic analysis (T=500s-1500s). A consequence of this is that the wave profile for the same method with same seed and number of components results in two different sea states in the dynamic and static simulation. A consequence of this is more data, and a judgment on the accuracy of methods can more accurately be performed. However, the last 500s in the static simulation and the first 500s in the dynamic simulation will consist of the same wave history, i.e. one cannot compare the resulting wave profiles independently. Though, one can assure that a correct wave profile have been subjected to the cylinder in all dynamic and static simulations. The estimates will generally be subjected to random error. Short term variability will always be present, as one will observe from the deviations of the wave elevation from the dynamic and static analysis.

Simulations for the equal area method are carried out with 30, 60 and 90 components. FFT is carried out with a requisite number of 1000 components in order to avoid repetition of wave history according to Langen (1979).

5.2 Results

Time series from USFOS are analyzed in MATLAB for calculation of the statistical parameters of the wave profile. The mean, maximum, minimum, standard deviation, skewness and kurtosis are built-in MATLAB functions. To assure that the calculation is correct, the global maximum is asked for in both USFOS and MATLAB. The maximum wave elevations are identical and one can therefore conclude that the calculations in MATLAB are correct. Refer Appendix B for script.

The Gumbel probability papers are obtained using the MATLAB toolbox, WAFO. WAFO contains MATLAB routines for statistical analysis and simulation of random waves and random loads (WAFO-Group 2000). The used WAFO routines, *wgumbplot.m* and a built-in function that calculates the Gumbel parameters are given in Appendix B. An extreme value for a given percentile can be found from these Gumbel parameters.

Take notice that the built-in function *log* in MATLAB refers to the natural logarithm, *ln*.

5.2.1 Wave Profile Results

Table 5-1 gives a total overview of the mean maximum for the statistical parameters from the two methods. Each method with corresponding components is run 20 times. Refer Appendix C for total summary of each sample.

Table 5-1 Overview of Statistical Parameters

Overview of mean values from Static Simulation						
Method	Number of comp.	Mean	Standard Deviaton	Kurtosis	Skewness	Max Surf. Elev [m]
EAP	30	0,00	2,99	2,92	0,01	9,97
EAP	60	0,00	2,95	2,92	0,02	9,83
EAP	90	0,00	2,97	2,93	0,02	9,75
FFT	1000	0,00	2,99	2,73	-0,01	9,00

Overview of mean values from Dynamic Simulation						
Method	Number of comp.	Mean	Standard Deviaton	Kurtosis	Skewness	Max Surf. Elev [m]
EAP	30	0,00	2,97	2,96	-0,01	9,78
EAP	60	0,00	3,02	2,89	0,00	9,83
EAP	90	0,00	3,03	2,95	-0,03	10,19
FFT	1000	0,00	3,00	2,77	-0,00	9,34

Table 5-2 Statistical Parameters for Kurtosis (Static Analysis)

Method / **Kurtosis**	EAP, 30comp	EAP, 60comp	EAP, 90comp	FFT, 1000comp
Max	3,47	3,73	3,39	2,96
Min	2,48	2,48	2,65	2,57
STD	0,28	0,27	0,21	0,11
Mean	**2,92**	**2,92**	**2,93**	**2,73**

5.2.2 Extreme Value Distribution for Surface Elevation

The sample extremes are plotted in a Gumbel probability paper to see if the extremes follow a straight line, and large deviations cannot be accepted. 20 samples for each case from the static analysis are plotted in Figure 5-1 to Figure 5-4.

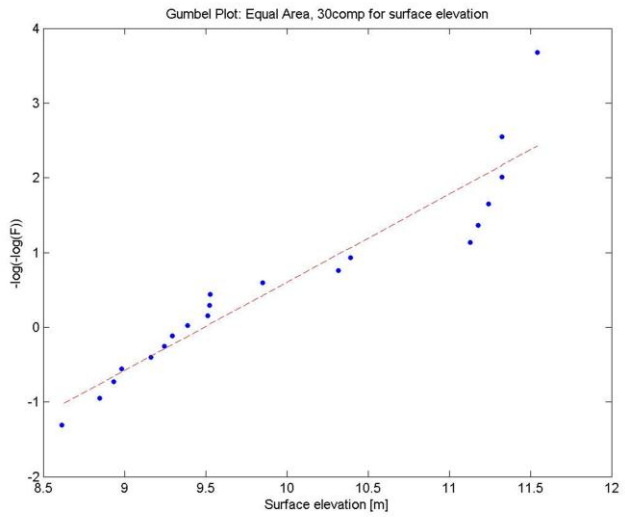

Figure 5-1 Gumbel Plot for Wave Elevation. EAP, 30comp

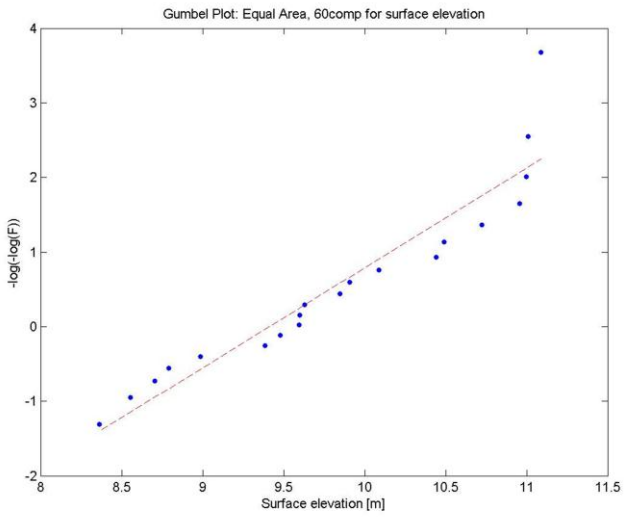

Figure 5-2 Gumbel Plot for Wave Elevation. EAP, 60comp

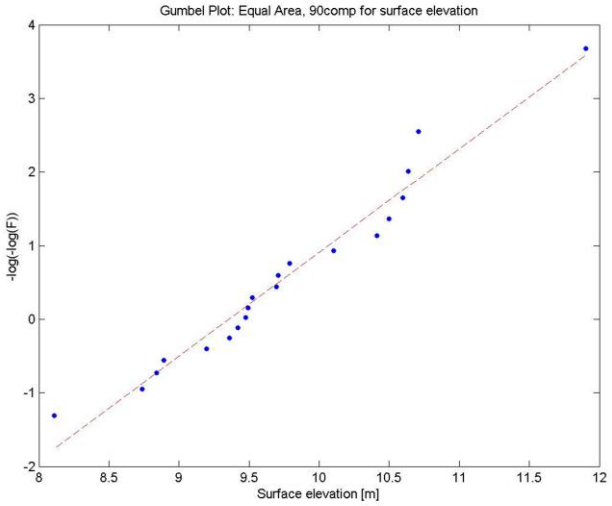

Figure 5-3 Gumbel Plot for Wave Elevation. EAP, 90comp

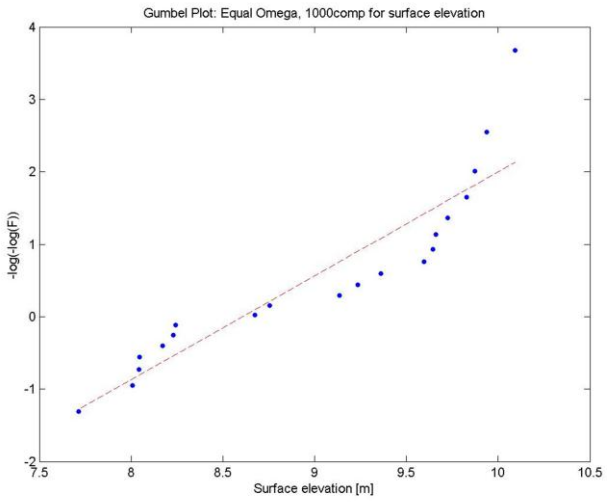

Figure 5-4 Gumbel Plot. for Wave Elevation. FFT, 1000comp

5.3 Discussion of Wave Profile Results

The major loads on an offshore structure are generally those caused by waves and accordingly an adequate description of ocean waves is necessary. This subchapter discusses the results from each statistical parameter one by one. The Gaussian model can be questioned if the results deviate significantly from the correct value.

5.3.1 Mean Value

The mean value function E[x(t)] should be constant independent in the collected data. This value is zero for a wave profile. Observing the mean value from Table 5-1, both methods give satisfactory results.

5.3.2 Standard Deviation

Significant wave height is set to 12m in this case study. Wave peaks are Rayleigh distributed when assuming that the wave process is stationary and normally distributed, and has the following properties (Myrhaug 2007):

$$\boldsymbol{H_S = H_{1/3} = 4\sqrt{m_0} = 4\sigma \;\rightarrow\; \sigma = \frac{H_S}{4} = 3} \qquad \textbf{(5-1)}$$

Where H_s are significant wave height, m_0 second standardized moment and σ the standard deviation. Equation 5-1 gives a standard deviation equal to 3. From Table 5-1, one finds that the requirement for this statistical property for wave elevation is also fulfilled.

5.3.3 Skewness

The skewness coefficient is equal to zero in a normal distribution. When one has assumed ergodic Gaussian process for the wave profile, the skewness property for waves should also equal zero to be satisfactory. The skewness is approximately zero and the requirement is satisfied.

5.3.4 Kurtosis

The kurtosis for a standard normal distribution is 3. The equal area method with different components is closer to 3 than FFT, refer Table 5-1. The Gaussian model should be questioned if the estimate deviates significantly. Here, one must consider if the noticeable deviation from the value 3 considering FFT is within an acceptable range.

5.3.5 Largest Maximum

The process for individual maxima is usually assumed to be narrow banded. This assumption introduces uncertainties into the analysis. However the adequacy of the assumption is assumed to be good enough according to Leira (2010). Assuming that all maxima are identically distributed, and furthermore, that they are statistically independent, then the individual maxima specializes into the well-known Rayleigh distribution (Leira 2010), refer equation 5-2.

$$f_{\xi}(\xi) = \frac{\xi}{\sigma^2}\exp\left\{-\frac{1}{2}\left(\frac{\xi}{\sigma}\right)^2\right\} \qquad \textbf{(5-2)}$$

Where ξ represents wave peaks, and σ the standard deviation. According to Myrhaug (2005), the theoretical extreme value in a period T is given by:

$$\xi_{1/n} = \sigma\left(\sqrt{2\ln(n)} + \frac{0{,}5772}{\sqrt{2\ln(n)}}\right) = \sigma\left(\sqrt{2\ln(T/T_0)} + \frac{0{,}5772}{\sqrt{2\ln(T/T_0)}}\right) = 9{,}36m \qquad \textbf{(5-3)}$$

Where $\xi_{1/n}$ are the global maxima in a sample, n number of wave peaks, T the duration, T_o the zero crossing wave period and σ the standard deviation.

From Table 5-1, it is clear that FFT produces lower extremes than the theoretical value and the equal area method. According to Saha et al. (in press) the peak maxima are dependent on the kurtosis. Kurtosis values for FFT are 2.73 and 2.77 for static analysis and dynamic analysis respectively. A kurtosis less than 3 makes the peak lower and wider around the mean in the probability density function in comparison to the Gaussian probability density function. The extreme values will therefore be underestimated than that obtained using Gaussian process. This complies with the surface elevation extremes presented in Appendix C where one observes a small deviation in the extremes for FFT.

The spectral set of $\Delta\omega$ is larger in the tail regime of spectrum than the peak region of spectrum considering the equal area method. Saha et al. (in press) states that the phenomenon of spikes is bound to occur when a large spectral band is represented by a single frequency. This is somewhat confirmed when investigating surface elevation extremes for EAP found in Appendix C where the standard deviation is larger for EAP. Therefore one should exercise caution for applications to extreme responses with a small number of frequencies.

Conclusion is that the equal area method and FFT are therefore only asymptotically Gaussian, refer 2.1. However, from an engineering point of view, the mentioned methods for simulation of waves are very attractive due to the simplifications they imply on a possible structural response analysis; refer Saha et al. (in press).

One should also be aware of statistical uncertainties with a sample size of only 20 simulations. The standard deviation of kurtosis in Table 5-2 confirms this. The non-consistent trend seen in Table 5-1 between 30, 60 and 90 components in the equal area method also support this statement.

The deviation from the theoretical value is minimal, but the amount of effect this has on the response of the structure is still unknown. When comparing FFT and equal area against each other, the difference between mean extremes can be up to 10%. Therefore, further investigation on the equal area method must be carried out.

5.3.6 Extreme Value Distribution

Figure 5-1 to Figure 5-4 displays the extreme value distribution. A noticeable deviation from the straight line in largest extremes in both methods is observed, except EAP with 90 components. This could be a coincidence when only dealing with twenty samples since one may not expect that EAP with 30 components has approximately the same fitting as EAP with 60 components.

5.4 Wave Load Results from Static Analysis

Table 5-3 shows mean extreme values and standard deviation for wave loads in the static analysis. For a better comprehension of the results, ratio between FFT and EAP is also given and the results are plotted in a Gumbel probability paper, see Figures 5-5 to 5-12. Refer Appendix C for wave load result from each sample.

Table 5-3 Mean and Standard deviation for results from static analysis

Method	Number of comp.	Wave Loads [N]					
		Mass dominated	Ratio	Standard Deviation	Drag dominated	Ratio	Standard deviation
EAP	30	8,89E+06	1,10	1,03E+06	2,00E+05	1,18	3,33E+04
EAP	60	8,66E+06	1,07	6,06E+05	1,95E+05	1,15	2,61E+04
EAP	90	8,73E+06	1,08	7,38E+05	1,97E+05	1,17	2,71E+04
FFT	1000	8,09E+06	1,00	7,93E+05	1,69E+05	1,00	2,52E+04

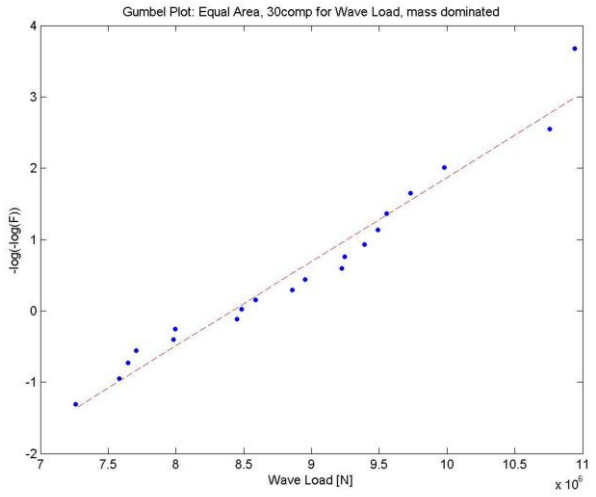

Figure 5-5 Gumbel Plot for Mass dominated Wave Loads. EAP, 30comp

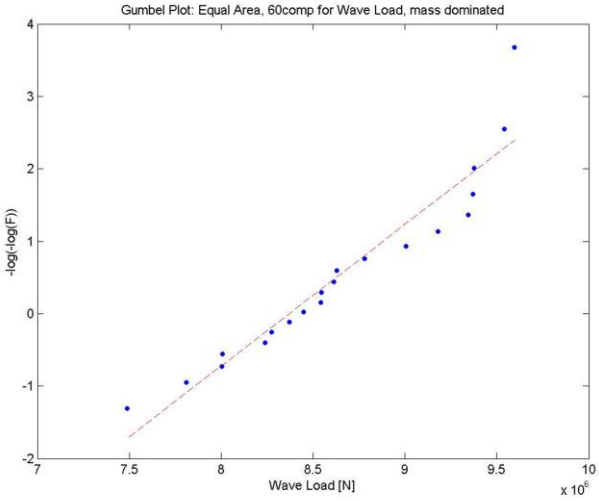

Figure 5-6 Gumbel Plot for Mass dominated Wave Loads. EAP, 60comp

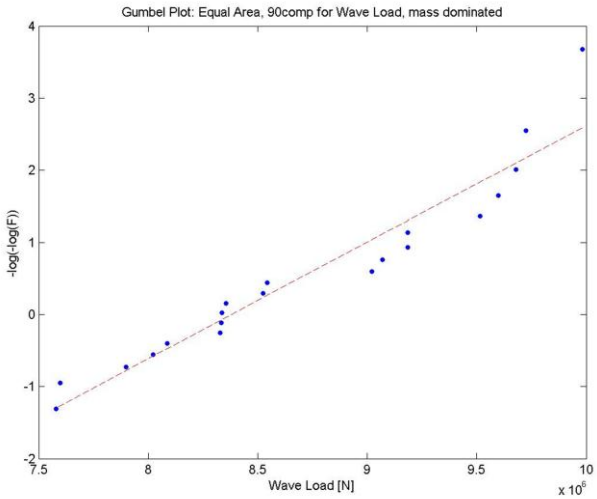

Figure 5-7 Gumbel Plot for Mass dominated Wave Loads. EAP, 90comp

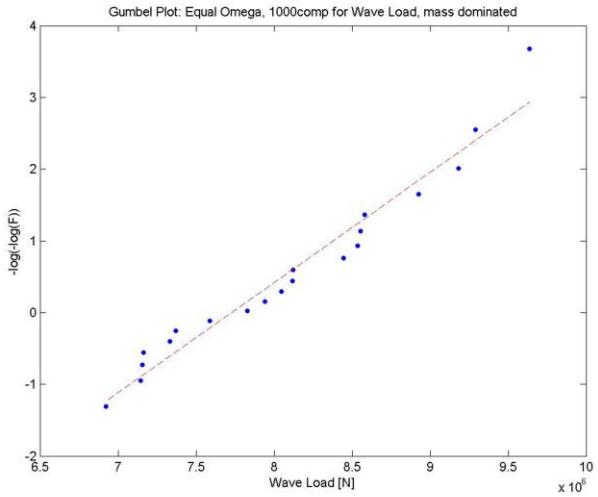

Figure 5-8 Gumbel Plot for Mass dominated Wave Loads. FFT, 1000comp

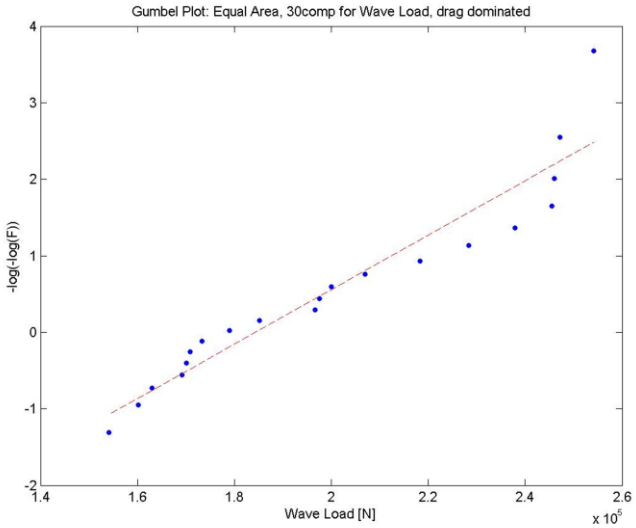

Figure 5-9 Gumbel Plot for Drag dominated Wave Loads. EAP, 30comp

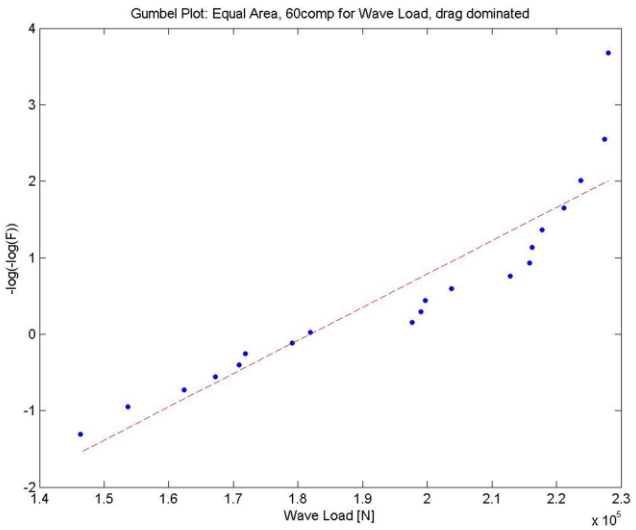

Figure 5-10 Gumbel Plot for Drag dominated Wave Loads. EAP, 60comp

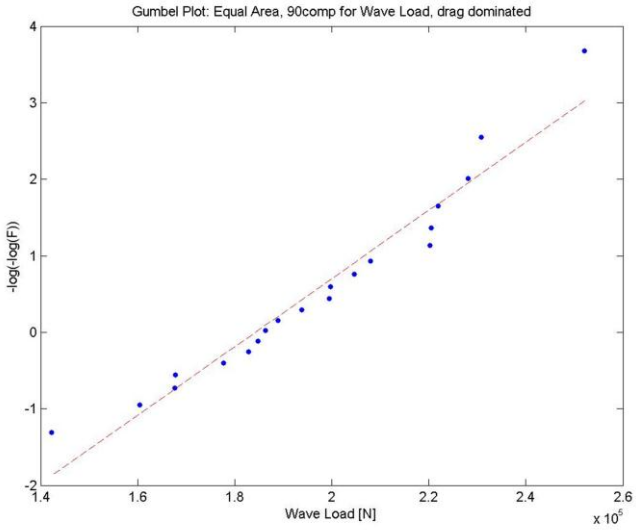

Figure 5-11 Gumbel Plot for Drag dominated Wave Loads. EAP, 90comp

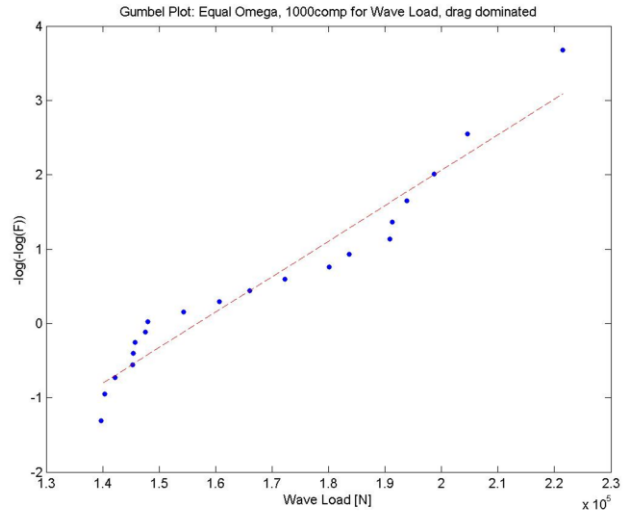

Figure 5-12 Gumbel Plot for Drag dominated Wave Loads. FFT, 1000comp

5.5 Discussion of Wave Load Results from Static Analysis

Mass dominated wave loads from the equal area method gives 7-10% larger results than FFT. Drag dominated loads gives 15-18% larger results. This is a consequence of larger wave amplitudes produced by the equal area method. The velocity squared in the Morison's equation may be the reason for the larger deviation between FFT and the equal area method when wave loads are drag dominated.

There is a noticeable difference in the extent of deviations from the straight line when comparing the Gumbel probability papers for wave load. But the deviations are slightly less when considering plots for mass and drag dominated wave loads than surface elevation, which is preferable considering design. There are no clear difference when comparing deviations from the straight line in the Gumbel plots between FFT and equal area principle. If the deviations are too large is yet to be found. 90 percentile estimates from all plotted distributions are found in Appendix D. These results are used for further discussion and conclusion in Chapter 6.

From Table 5-3, it is clear that the largest standard deviation comes from the equal area method with 30 components. One should therefore be careful using EAP with 30 components because of larger spreading in response per simulation. Also note that EAP with 30 components has better fitting to the straight line than EAP with 60 components. One assumes that this is a result of statistical uncertainty and short term variability.

Considering the difference between FFT and EAP, it should be questioned if the results from the equal area method are within an acceptable range.

5.6 Results from Dynamic Analysis

The dynamic analysis is run with three different natural periods. Response quantities asked for in the dynamic analysis are the maximum surface elevation, wave load and overturning moment. Results are found in Tables 5-4 to 5-7 and in Gumbel probability papers shown in Figures 5-13 to 5-18. The color red represents FFT, and blue, black and green represent the equal area method with 30, 60 and 90 components.

5.6.1 Results when Wave Loads are Mass dominated.

When the wave loads are mass dominated, the first term in Morison equation are governing. Results are given in Table 5-4 and ratio between FFT and the equal area method considering the overturning moment are found in Table 5-5.

Table 5-4 Overview of mean values for mass dominated loads

	Method	Number of comp.	ReacOVTM [Nm]	Wave Load [N]	Surface Elevation [m]
Tn=4,4s	EAP	30	9,50E+08	8,87E+06	9,78
	EAP	60	9,11E+08	8,64E+06	9,83
	EAP	90	8,95E+08	9,15E+06	10,19
	FFT	1000	1,23E+09	8,15E+06	9,34
Tn=8,5s	EAP	30	2,07E+09	8,86E+06	9,78
	EAP	60	2,43E+09	8,65E+06	9,83
	EAP	90	2,65E+09	9,16E+06	10,19
	FFT	1000	2,58E+09	8,16E+06	9,34
Tn=14s	EAP	30	3,94E+09	8,83E+06	9,78
	EAP	60	4,21E+09	8,70E+06	9,83
	EAP	90	4,04E+09	9,14E+06	10,19
	FFT	1000	4,24E+09	8,16E+06	9,34

Table 5-5 Overview of deviation between EAP and FFT of Overturning Moment when loads are mass dominated

	Method	Number of comp.	ReacOVTM [Nm]	Difference
Tn=4,4s	EAP	30	9,50E+08	0,77
	EAP	60	9,11E+08	0,74
	EAP	90	8,95E+08	0,73
	FFT	1000	1,23E+09	1,00
Tn=8,5s	EAP	30	2,07E+09	0,80
	EAP	60	2,43E+09	0,94
	EAP	90	2,65E+09	1,03
	FFT	1000	2,58E+09	1,00
Tn=14s	EAP	30	3,94E+09	0,93
	EAP	60	4,21E+09	0,99
	EAP	90	4,04E+09	0,95
	FFT	1000	4,24E+09	1,00

5.6.2 Results when Wave Loads are Drag Dominated

When wave loads are drag dominated, the second term in Morison equation is governing. Results are found in Table 5-6 and comparison between FFT and the equal area method regarding overturning moment is given in Table 5-7. Ratio between the reaction overturning moment and wave overturning moment is also calculated to get an indication around the ratio between the static and dynamic results. It is not analogous to the transfer function because of the relative velocity in the drag term. However, one would expect larger response amplification when the natural period lay in the peak area of the wave spectrum, and this is confirmed when viewing Table 5-6.

Table 5-6 Overview of mean values for drag dominated loads

	Method	Number of comp.	ReacOVTM [Nm]	WaveOVTM [Nm]	Ratio OVTM	Wave Load [N]	Surface Elevation [m]
Tn4,4s	EAP	30	2,41E+07	1,52E+07	1,61	2,00E+05	9,78
	EAP	60	2,34E+07	1,43E+07	1,67	1,95E+05	9,83
	EAP	90	2,28E+07	1,55E+07	1,49	2,20E+05	10,19
	FFT	1000	2,32E+07	1,32E+07	1,79	1,74E+05	9,34
Tn=8,5s	EAP	30	3,79E+07	1,51E+07	2,57	1,93E+05	9,78
	EAP	60	4,19E+07	1,40E+07	3,13	1,90E+05	9,83
	EAP	90	4,41E+07	1,48E+07	3,05	2,08E+05	10,19
	FFT	1000	4,02E+07	1,35E+07	3,06	1,78E+05	9,34
Tn=14s	EAP	30	6,92E+07	1,34E+07	5,31	1,74E+05	9,78
	EAP	60	7,40E+07	1,23E+07	6,06	1,73E+05	9,83
	EAP	90	7,17E+07	1,37E+07	5,36	1,98E+05	10,19
	FFT	1000	7,58E+07	1,18E+07	6,47	1,81E+05	9,34

Table 5-7 Overview of deviation between EAP and FFT of Overturning Moment when loads are drag dominated

	Method	Number of comp.	ReacOVTM [Nm]	Difference
Tn4,4s	EAP	30	2,41E+07	1,04
	EAP	60	2,34E+07	1,01
	EAP	90	2,28E+07	0,98
	FFT	1000	2,32E+07	1,00
Tn=8,5s	EAP	30	3,79E+07	0,94
	EAP	60	4,19E+07	1,04
	EAP	90	4,41E+07	1,10
	FFT	1000	4,02E+07	1,00
Tn=14s	EAP	30	6,92E+07	0,91
	EAP	60	7,40E+07	0,98
	EAP	90	7,17E+07	0,95
	FFT	1000	7,58E+07	1,00

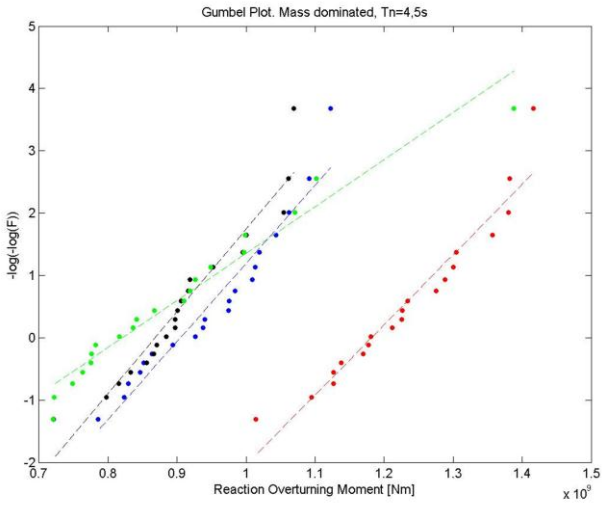

Figure 5-13 Gumbel Plot. FFT vs. EAP. Mass Dominated Wave Loads, Tn=4,4s

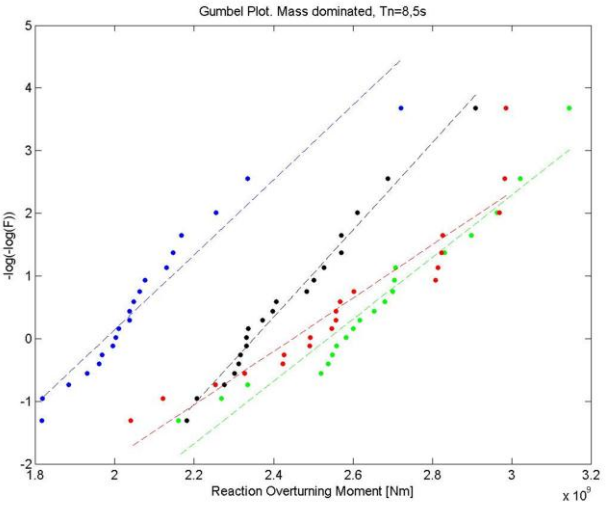

Figure 5-14 Gumbel Plot. FFT vs. EAP. Mass Dominated Wave Loads, Tn=8,5s

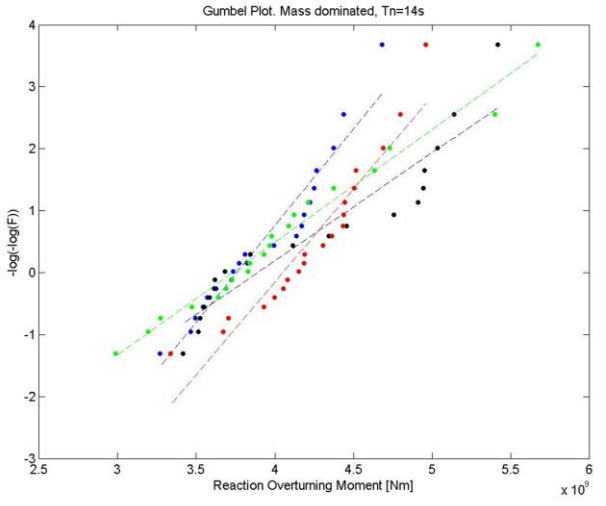

Figure 5-15 Gumbel Plot. FFT vs. EAP. Mass Dominated Wave Loads, Tn=14s

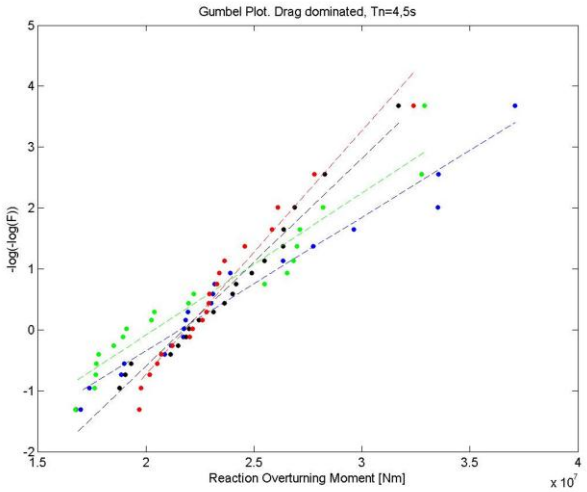

Figure 5-16 Gumbel Plot. FFT vs. EAP. Drag Dominated Wave Loads, Tn=4,4s

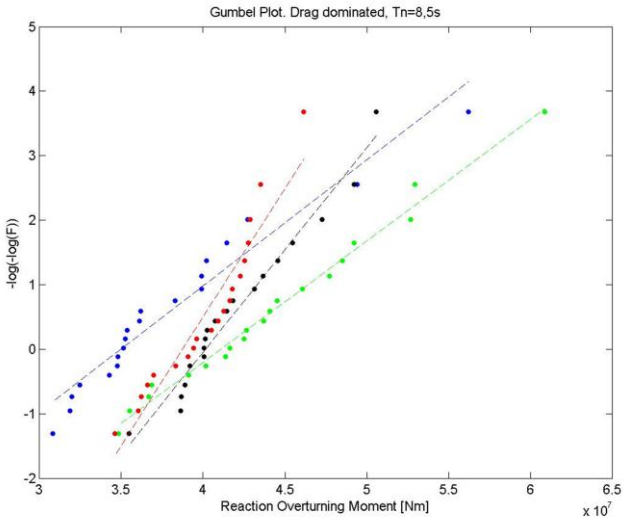

Figure 5-17 Gumbel Plot. FFT vs. EAP. Drag Dominated Wave Loads, Tn=8,5s

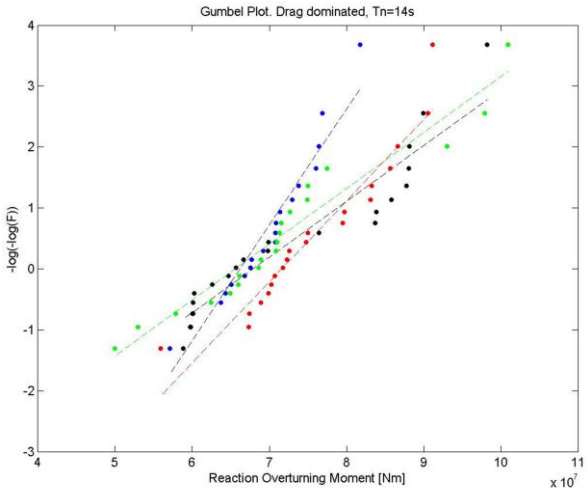

Figure 5-18 Gumbel Plot. FFT vs. EAP. Drag Dominated Wave Loads, Tn=14s

5.7 Discussion of Results from Dynamic Analysis

Table 5-4 and Table 5-6 show mean maximum outcome of overturning moment, wave load and surface elevation. Mean maximum surface elevation is of interest to make sure that one apply the same wave profile in all three cases (T_n=4.4s, T_n=8.5s, T_n=14s). The main interest is the overturning moment that is used as the target quantity to compare the two methods. For a better comparison, Table 5-5 and Table 5-7 show the ratio between the correct answer from FFT and EAP with different number of components.

5.7.1 Mass Dominated Wave Loads

Large deviations in the overturning moment between EAP and FFT are found when the natural period is 4.4s. The straight lines in the Gumbel probability paper in Figure 5-13 illustrate this. The difference is less when the natural periods lay in the more energy rich parts of the wave spectrum. All other cases give rather close results to FFT, except EAP with 30 components when the natural period is 8.5s.

The reason for larger difference in reaction overturning moment when the natural period is small is found when investigating the dissolution of the wave spectrum considering the equal area method. Table 5-8 shows the lower range of wave periods in the wave spectrum for different number of components in EAP.

Table 5-8 Overview of splitting of the Wave spectrum with AEP

Wave Spectrum		
Period, T		
30 comp	**60 comp**	**90 comp**
12,22	9,90	8,83
11,87	9,62	8,59
11,47	9,32	8,34
11,02	9,00	8,07
10,54	8,65	7,77
10,02	8,27	7,44
9,45	7,84	7,06
8,80	7,34	6,62
8,02	6,72	6,08
6,94	5,86	5,33
3,85	3,75	3,61

The spreading in wave periods is large in the low energy parts of the wave spectrum. A consequence of this may be that the waves don't "hit" the natural period of the cylinder resulting in a lower dynamic effect, i.e. lower response amplitude operator (RAO) considering EAP. RAO are effectively transfer functions used to determine the effect that a sea state will have upon the motion of a structure (Haver 2010), refer equation 5-4.

$$\boldsymbol{RAO} = |\boldsymbol{H}(\boldsymbol{\omega})| = \frac{\mathbf{1}}{\boldsymbol{k}((\mathbf{1}-\boldsymbol{\beta}^{\mathbf{2}})+(\mathbf{2}\boldsymbol{\lambda}\boldsymbol{\beta})^{\mathbf{2}})^{\frac{\mathbf{1}}{\mathbf{2}}}} \qquad \textbf{(5-4)}$$

Where:

$\lvert H(\omega)\rvert$	Transfer function (Response amplitude per unit wave amplitude)
k	Stiffness
β	Frequency ratio, ω/ω_0
λ	Damping ratio, $c/2m\omega_0$

Mass dominated wave loads is a linear function of the surface elevation, and one can refer the response as a linear response problem, refer Haver (2010). Linear theory can to a large extent describe the wave-induced motions and loads (Faltinsen 2009). Because of linearity one can get the response to each wave component separately, and write the steady state response as:

$$\boldsymbol{A_j|H(\omega)|\sin(\omega_t t + \delta(\omega_j) + \varepsilon_j)} \quad \textbf{(5-5)}$$

Where:

A_j	Wave amplitude
$\|H(\omega)\|$	Transfer function
ω_t	Frequency
$\delta(\omega_j)$	Phase angle associated with response
ε_j	Random phase angle

Due to linearity, one can superpose the response from all wave components, i.e. one can write

$$\boldsymbol{\sum_{J=1}^{N} A_j|H(\omega)|\sin(\omega_t t + \delta(\omega_j) + \varepsilon_j)} \quad \textbf{(5-6)}$$

The overturning moment is dependent of the global response, and a bad transfer function will result in bad values for the overturning moments. The equal area method gives higher wave loads than FFT and this compensates for a lower dynamic amplification factor. However, the conclusion is that one gets an inadequate transfer function, especially in the low energy parts of the wave spectrum.

5.7.2 Drag Dominated Wave Loads

Deviations in overturning moment between FFT and equal area principle are less when the wave loads are drag dominated, also considering the lowest natural period. Only a few percent between the two methods are observed several places. However, one still observe a 10% difference between FFT and EAP when the natural period is 8.5s and one should exercise caution when dealing with this method.

What is the physical reason for that the drag dominated wave loads gives "better" results? Transfer functions are used when the load is linearly related to the wave process, but this is not valid considering drag forces, refer equation 3-1. When investigating the Morison's equation closer, it is seen that the drag force is proportional to the velocity squared, and the force is not proportional to the wave height since the term u_0^2 enters the equation. Nor is the wave load harmonic since there is a $\sin(\omega t)|\sin(\omega t)|$ term. According to Larsen (2005), frequencies other than the wave frequency will also appear in the nonlinear drag term and is shown in the following equations. Equation for drag force is:

$$\boldsymbol{F_D = \frac{1}{2}\rho C_D D \Delta l[u(t) - \dot{r}]|u(t) - \dot{r}|} \quad \textbf{(5-7)}$$

Where:

ρ	Water density
C_d	Drag coefficient
D	Diameter
Δl	Length section
u(t)	Water particle velocity
$\dot{r}$	Velocity of the pile

Further, one assumes that the wave induced motion are harmonic, $u(t) = u_0 \sin(\omega t)$ and neglect the relative velocity in further equations, refer (C. M. Larsen 2005). The force equation will hence be written as:

$$F_D = C_D^*[u_0 \sin(\omega t)]|u_0 \sin(\omega t)| \quad \textbf{(5-8)}$$

Where:

$$C_D^* = \frac{1}{2}\rho C_D D \Delta l \quad \textbf{(5-9)}$$

The dynamic equilibrium equation can now be written as

$$m\ddot{r} + c\dot{r} + kr = C_D^* u_0^2[\sin(\omega t)]|\sin(\omega t)| = F_o(\sin \omega t)^2 \cdot sign(\sin \omega t) \quad \textbf{(5-10)}$$

Equation 5-10 can be expressed as a Fourier series, which will give following results

$$F(t) = \sum_{i=1}^{\infty} b_n \sin n\omega t \quad \textbf{(5-11)}$$

The Fourier coefficient, b_n can be found as

$$b_n = \frac{2}{T}\int_0^{T/2} F(t) \sin n\omega t \cdot dt = \frac{2F_o}{T}\int_0^{T/2} (\sin \omega t)^2 \cdot \sin n\omega t \cdot dt \quad \textbf{(5-12)}$$

Calculating equation 5-12, the force time function can now be written as

$$F(t) = F_0\left[\frac{8}{3\pi}\sin \omega t - \frac{8}{15\pi}\sin 3\omega t - \frac{8}{105\pi}\sin 5\omega t + \ldots\right] \quad \textbf{(5-13)}$$

Equation 5-13 shows that the drag force contains higher order frequency components than the wave frequency. It is observed that both the second and third term is of considerable amplitude, refer Figure 5-20. If these terms hit a natural period, a considerable dynamic amplification can occur even if the wave frequency, ω and the eigenfrequency are well separated. Here, when the natural period is 4.4s, the term, 3ω may have noticeable effects. Since the top period in the wave spectrum is 14s, the 3ω term is very close to hit this natural period because T_n=4.4s is within a 90% interval of the top period (Haver 2010). Figure 5-19 and Figure 5-20 gives illustrations of the accuracy and importance of the higher frequency terms.

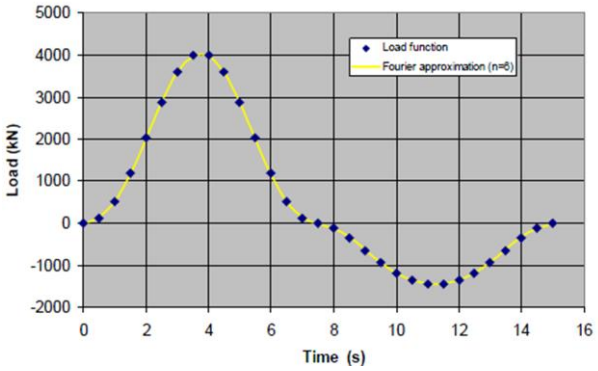

Figure 5-19 Fourier description of total drag load on pile (Haver 2010)

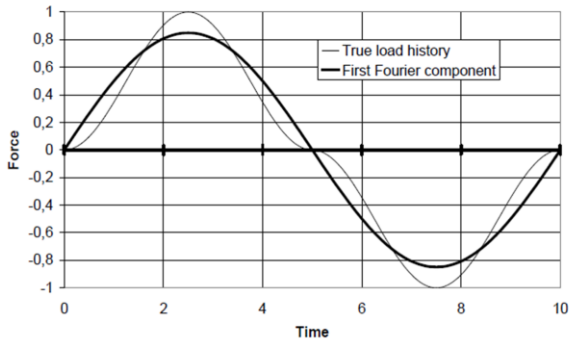

Figure 5-20 True drag force and first Fourier component (C. M. Larsen 2005)

These higher order frequencies may be the reason for obtaining a more accurate result with the equal area method for drag dominated wave loads.

There are also other differences between mass and drag dominated loads that may also be the reason for obtaining better results considering drag dominated wave loads. The maximum drag forces occur during a wave crest and is more concentrated at sea surface while maximum mass force occur during a wave node.

6 Temporary Conclusion

Summing up all the results of statistical parameters of the wave profile, wave loads, and overturning moment, a temporary conclusion of the adequacy of the equal area method can be made. Note that one should be aware of statistical uncertainties with a sample size of only twenty simulations.

6.1.1 Statistical Parameters for the Wave Profile

The simulated waves in the computer program, USFOS should approach a Gaussian process. Here, the Gaussian distribution has the following characteristics; a mean value of 0, standard deviation of 3, skewness of 0, and a kurtosis of 3. The two methods give a satisfactory representation of the sea state when considering the statistical parameters given in Table 5-1 and Figures 5-1 to 5-4. FFT produces a kurtosis value less than 3 and less than the equal area method. However the deviation is not significant and one assumes that it is acceptable to proceed. The equal area method produces a somewhat higher surface elevation, i.e. the equal area method is conservative which is not necessarily so bad.

All in all, one can clearly observe that the wave elevation shows a Gaussian trend by comparing Table 5-1 upon statistical properties for a Gaussian distribution. Similar experiments performed by Saha et al. (in press) show similar results and characteristics and has the same conclusion.

6.1.2 Mass dominated Wave Loads

Higher results in wave loads in the equal area method are produced because of the linear relationship between wave elevation and wave loads. Mass dominated wave loads in the static analysis using the equal area method gives a 7-10% higher result than FFT, and 6-12% higher results are found in the dynamic analysis. Extensive deviations in results are found when considering overturning moment in the dynamic analysis when the natural period is 4.4s. Here, the equal area method gives an overturning moment 23-27% less than the exact value, and lays far away from an acceptable region. Deviations decrease as the natural period goes to the peak period of the wave spectrum. This is not the case when wave loads are drag dominated.

6.1.3 Drag dominated Wave Loads

The equal area method produces 15-18% larger results in drag dominated wave loads in the static analysis. Considering Table 5-6, a difference between FFT and EAP can be as high as 26% when the natural period is 4.4s in the dynamic analysis.

Looking at the target quantity; reaction overturning moment the differences decreases between FFT and EAP. The ratio of overturning moment between FFT and the equal area method is small. This may be because of a too small dynamic amplification factor in the equal area method which compensates for the too high wave load. However, the conclusion is that the large spreading in frequencies of wave components from the equal area methods gives inaccurate response amplitude, especially in the low energy parts of the wave spectrum.

Several reasons for better results considering overturning moment when the wave loads are drag dominated are mentioned. However, one should also consider the possibility that it may just come from a coincidence. The transfer function for mass and drag dominated loads may be equally inaccurate, but the too large drag dominated wave load from the equal area method may compensate better for this.

6.1.4 Summary

The equal area method gives conservative and non-conservative results in comparison to FFT, i.e. there is no consistent trend in the outcome of this method. The equal area method is in other words not predictable.

All ratios between EAP and FFT are given in Table 6-1 and Table 6-2 for a better overview.

Table 6-1 Wave Load Ratio between FFT and EAP results

	EAP	Static	Dynamic		
			Tn=4,4s	Tn=8,5s	Tn=14s
Mass dominated wave loads	30	1,10	1,09	1,09	1,08
	60	1,07	1,06	1,06	1,07
	90	1,08	1,12	1,12	1,12
Drag Dominated wave loads	30	1,18	1,15	1,08	0,96
	60	1,15	1,12	1,07	0,96
	90	1,17	1,26	1,17	1,09

Table 6-2 OVTM Ratio between FFT and EAP

	EAP	Tn=4,4s	Tn=8,5s	Tn=14s
OVTM, mass dominated	30	0,77	0,80	0,93
	60	0,74	0,94	0,99
	90	0,73	1,03	0,95
OVTM, drag dominated	30	1,04	0,94	0,91
	60	1,01	1,04	0,98
	90	0,98	1,10	0,95

From the current results, a correction factor is necessary if one should make use of the equal area method. EAP with 90 components gives the most accurate statistical parameters for a Gaussian distribution, and is therefore preferred. A safety factor using EAP with 90 components should be high enough so that the possibility for underestimation of the response is small. Considering wave loads, no safety factor is necessary. A safety factor regarding the overturning moment however, is necessary.

It is common to make a q-probability estimate of the Gumbel distribution when dealing with extreme responses. These estimates are used to compare the two methods. Appendix D gives estimates of the 90 percentile of all distributions. It should be noted, that if number of samples are small and N ($N=v_oT$ are the number of peaks that depends on the duration T over which the extreme peak distribution is requested) is much smaller than the actual value relevant for design, the linearization of the Gumbel distribution will result in an inaccurate estimate of the probability of exceedance of a design threshold value. This is the case here with a simulation with duration of 1000s and is a drawback in the use of Gumbel fitting procedure.

Assuming that the structure's natural periods and properties are known, a safety factor for overturning moment is proposed when viewing 90 percentile estimates in Appendix D. Results from Table 6-2 are also considered because of the mentioned uncertainty around the extreme percentile estimates.

- Natural period in the low energy part of wave spectrum and mass dominated: 1.35
- Natural period in the high energy part of wave spectrum and mass dominated: 1.10
- Natural period in the low energy part of wave spectrum and drag dominated: 1.05
- Natural period in the high energy part of wave spectrum and drag dominated: 1.05

The mean of surface elevation extremes are largest considering 30 components in the static analysis, whereas 90 components in the dynamic analysis results in largest mean. Spikes are bound to occur when a large spectral band is represented by a single frequency according to Saha et al. (in press). In other words, higher extremes are expected when considering only 30 components. One can assume

that the non-consistent trend between the equal area method with 30, 60 and 90 components is a result of only having twenty samples available, i.e. statistical uncertainty. Same trend is found in wave load and overturning moment because of this. For further work, more samples are required for a final conclusion.

All in all, caution should be exercised if choosing the equal area method and are not recommended, especially considering mass dominated wave loads. Results are not completely satisfying when the method is used with fixed structures. Whether the method can be introduced to floating structures remains to be investigated.

7 Time-Domain simulation on the SWAY Turbine

The main aim of this thesis is to perform a comparison between two methods for simulating waves, the equal area method and the Fast Fourier Transform, treated as the correct solution. It is very important to simulate waves correctly since the main load on an offshore structure comes from waves.

The adequacy of the equal area method is to be tested on both fixed and floating structures. Previous chapters have dealt with results from FFT and EAP when the methods where subjected to a fixed cylinder. This chapter deals with the validity of the equal area method when the floating solution, SWAY is introduced. Statistical comparison of the two methods for an ultimate limit state (ULS) characteristic response will be made. A short outline of the SWAY concept is also given.

7.1 The SWAY Concept

The sway concept consists of a floating spar buoy designed to rise and fall with wave activity. The floating tower is anchored to the seabed with a single pipe and suction anchor. The center of gravity of the tower is located far below the center of buoyancy of the tower. This gives the tower enough stability to withstand large loads produced by the wind turbine installed on the top of the tower, refer Figure 7-1. The concept is unique since the turbine will face downwind when wind hits the rotor. The tower will then tilt around 5-8 degrees. By placing the rotor downwind of the tower the rotor is kept perfectly aligned with the wind. The tower turns around a subsea swivel when the wind changes direction. This makes it possible to strengthen the tower with a tension rod system that results in that the tower is capable of carrying a much larger turbine due to the decreased stresses in the tower. This again is economically favorable (SWAY AS).

Figure 7-1 Illustration of SWAY concept (SWAY AS)

When built, it will be the world's largest turbine standing 160m tall with a rotor diameter of 145m. It will also be the most powerful by generating 10MW.

7.2 Performance of SWAY Analysis

When performing the analyses on the SWAY turbine, ULS characteristic response shall be found. Dynamic effects, integration to true surface level, buoyancy effects, hydrodynamic damping and other nonlinear effects becomes significant, and therefore a time-domain simulation of irregular waves must be chosen to give the best prediction of reality. The dynamic analysis is carried out in USFOS; refer Appendix A for control file and model file. The force in the cardan is of main interest when comparing the two methods. Other important response quantities requested in USFOS for comparison are; displacement and acceleration at the top of the turbine, moment in the tower at sea surface, wave load and surface elevation.

When investigating full plots for response versus time, it is found that the maximum cardan force often occur in the very beginning of the analysis. These too large responses come from the initial transient response that has not been damped out. To avoid these spurious responses, all maximum results are specified to come from 100s to 1000s. A startup period of 100s is shown to be more than enough satisfying when observing the plots for temporal variation for the cardan force. An example of the initial response is given in Figure 7-2.

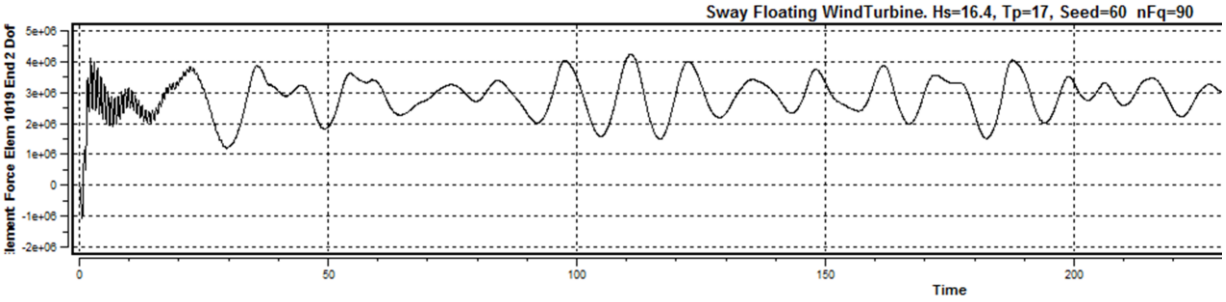

Figure 7-2 Illustration of initial response

7.2.1 SWAY in USFOS

The SWAY model in USFOS has real life dimensions together with specified hydrodynamic coefficients. The wind is modeled as a constant force, F= 117kN in the x-direction subjected to a node at the top of the cylinder that represents the actual force on the rotor turbine. X-Y-Z relationships and the SWAY turbine in USFOS are displayed in Figure 7-3. The diameter at sea surface is around 5m, resulting in mass dominated wave loads. The significant wave height is 16.4m and peak period is set to 17s when performing the ULS analysis. The water depth is set to 150m.

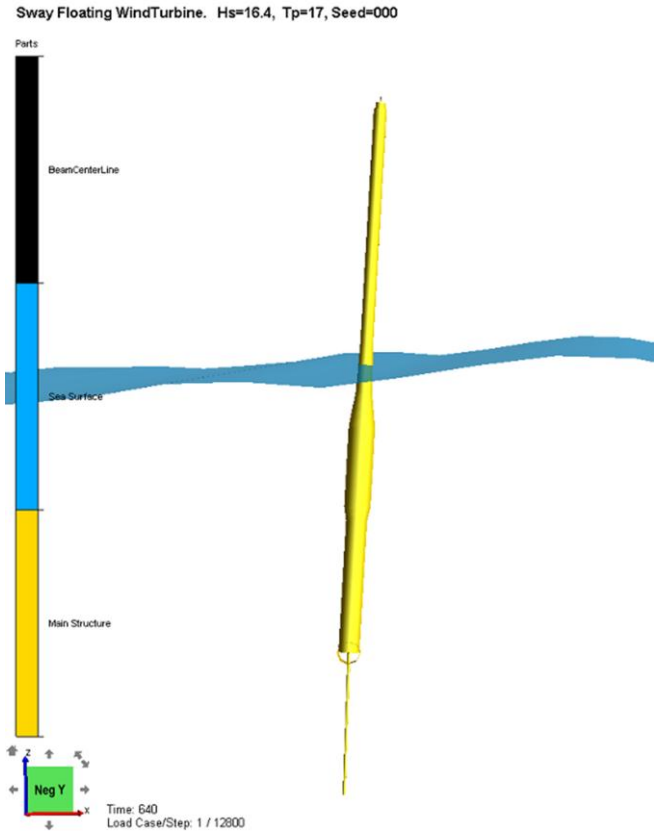

Figure 7-3 Model of the SWAY turbine in USFOS

7.2.2 Results from ULS Analysis in USFOS

When comparison of the results for the fixed cylinder for the two methods were made, a number of samples were required, and obviously the same holds true for the ULS analysis on the SWAY tower. 20 runs are executed from each method with appurtenant components. Results are found in Table 7-1. Table 7-2 shows the ratio between results from FFT and EAP and Table 7-3 gives the standard deviation of the response quantities. Results from each sample are found in Appendix E.

Table 7-1 Mean Values of Global Maximum from all Samples

Method	Disp top tower [m]	Acc top tower [m/s^2]	Cardan Force (top) [N]	Mz, sea surface [Nm]	Surface elevation [m]	Wave load [N]
FFT, 1000comp	42,49	4,86	4,24E+06	2,47E+08	12,17	1,46E+07
EAP, 90comp	44,34	5,48	4,26E+06	2,59E+08	12,70	1,60E+07
EAP, 60comp	45,59	5,42	4,30E+06	2,72E+08	13,25	1,58E+07
EAP, 30comp	50,00	5,50	4,37E+06	2,75E+08	12,97	1,57E+07

Table 7-2 Ratio between FFT and EAP when considering Mean Values

Method	Disp top tower [m]	Acc top tower [m/s^2]	Cardan Force (top) [N]	Mz, sea surface [Nm]	Surface elevation [m]	Wave load [N]
FFT, 1000comp	1,00	1,00	1,00	1,00	1,00	1,00
EAP, 90comp	1,04	1,13	1,01	1,05	1,04	1,10
EAP, 60comp	1,07	1,12	1,02	1,10	1,09	1,08
EAP, 30comp	1,18	1,13	1,03	1,11	1,07	1,08

Table 7-3 Standard Deviation

Method	Disp top tower [m]	Acc top tower [m/s^2]	Cardan Force (top) [N]	Mz, sea surface [Nm]	Surface elevation [m]	Wave load [N]
FFT, 1000comp	4,97	0,34	1,06E+05	1,72E+07	1,23	1,31E+06
EAP, 90comp	6,09	0,44	1,22E+05	3,25E+07	1,08	1,46E+06
EAP, 60comp	6,61	0,65	1,33E+05	3,60E+07	1,29	1,82E+06
EAP, 30comp	5,80	0,61	1,76E+05	2,57E+07	1,63	2,27E+06

To get a better understanding of the results, our main target quantity, the cardan force is plotted in Gumbel probability papers in the following page; refer Figure 7-4 to Figure 7-6. The results from the equal area method are plotted against FFT to obtain a visual comparison. In this thesis, one has chosen a 90 percentile estimate of the Gumbel distribution to compare the two methods. In practice, the 90 percentile estimate of a short term distribution for 3-hour extreme value distribution is used for obtaining the 10^-2 annual probability. In order to find a more accurate estimate, a long term analysis is required. The error for adopting 90% for 10^-2 annual probability for a short term distribution is within +/- 10% (Haver 2010). However, here, the duration of simulation is only in the order of 1000s and the choice of percentile is not analogous with an annual exceedance level, merely a way to compare FFT and EAP. Refer Table 7-4 for results of the 90% estimate of the distribution of the cardan force.

Using the relations to relate parameters to intercept and slopes of the estimated lines, Gumbel parameters and 90 percentile estimates are found. The estimate can be inaccurate because of the related statistical estimation uncertainty when only 20 samples are available. Also, the extreme value distribution is typically best close to peak, and may deviate in the tails (Leira 2010).

Table 7-4 Cardan Force results

Method	#comp	Mean Value	α=0.90
FFT	1000	4,24E+06	4,38E+06
EAP	30	4,37E+06	4,61E+06
EAP	60	4,30E+06	4,48E+06
EAP	90	4,26E+06	4,43E+06

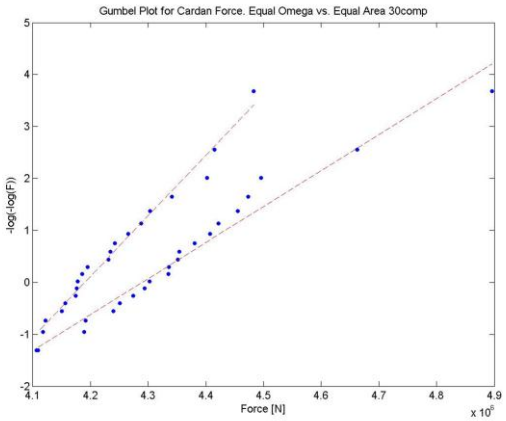

Figure 7-4 Gumbel Plot for Cardan Force. Equal Omega vs. Equal Area, 30comp

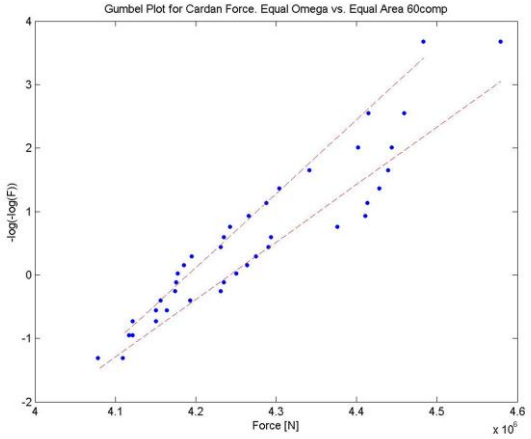

Figure 7-5 Gumbel Plot for Cardan Force. Equal Omega vs. Equal Area, 60comp

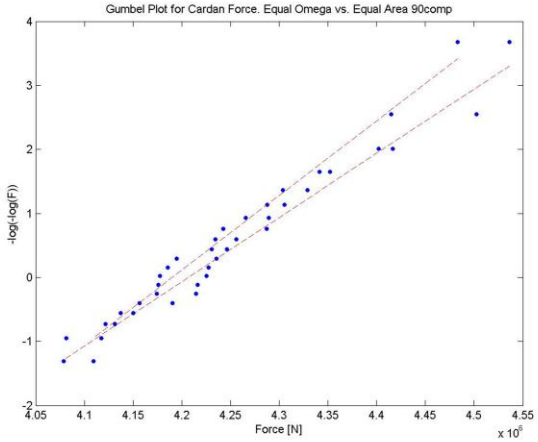

Figure 7-6 Gumbel Plot for Cardan Force. Equal Omega vs. Equal Area, 90comp

8 Discussion of Results from SWAY analysis

From Table 7-2, the equal area method gives very satisfactory results, especially considering the cardan force which differs with only some few percent. For a floating structure, it is common with large motions horizontally and a displacement of the top tower in the range of 40-50 meters is expected. All response quantities using the equal area method give larger values than for FFT, i.e. the equal area method is conservative. The reason lies in that the equal area method produces in average a higher surface elevation. This leads to larger wave loads, which again results in higher values for displacement, accelerations and forces.

In contrast to the dynamic analysis of the fixed cylinder where the natural periods lay well inside the wave spectrum, the natural periods of the SWAY turbine lay far away from the frequency range of the wave spectrum. SWAY's natural periods are 1s in heave motion, 30s with the clutch fixed and 80s for reversed pendulum at 150m water depth (the remaining natural periods are not found in USFOS). In other words, the frequency of the wave load is not so important when it comes to the floating solution, the SWAY turbine. However, when dealing with floating structures that are mass dominated, other loads from the waves become significant. In addition to the wave frequency load, there will also be a slowly varying force on the turbine corresponding to difference frequencies (slow-drift excitation loads) and a high frequency load corresponding to sum frequencies. Further descriptions of these effects are found in following subchapters.

8.1.1 Slow-Drift Motions in Irregular Waves

Slow-drift motions are resonance oscillations excited by nonlinear interaction effects between the waves and body motion according to Faltinsen (2009). Due to low damping of the SWAY turbine, large motions occur, and cause rather large forces in the cardan. When the mean wave loads are large, so are the slow-drift excitation loads, and can be of equal importance. For a moored structure, such as the SWAY turbine, slow drift resonance oscillations occur in surge, sway and yaw. Refer equation 8-1 for general formula of the slow-drift excitation loads F_i^{SV} (Faltinsen 2009).

$$\boldsymbol{F_i^{SV} = \sum_{j=1}^{N}\sum_{k=1}^{N} A_j A_k \left[T_{jk}^{ic}\cos\{(\omega_k-\omega_j)t+(\epsilon_k-\epsilon_j)\}+T_{jk}^{is}\sin\{(\omega_k-\omega_j)t+(\epsilon_k-\epsilon_j)\}\right]} \qquad \textbf{(8-1)}$$

Where:

A	Wave amplitudes
ω	Wave frequencies
ϵ	Random phase angles
T	Second order transfer function
N	Number of wave components
t	Time

8.1.2 Sum-Frequency Effects

Due to nonlinear effects, one gets excitation forces with higher frequencies than the dominant frequencies in the wave spectrum. This is because of terms oscillating with frequencies $2\omega_j$, $2\omega_k$, and $(\omega_j+\omega_k)$, where ω are the wave frequency. These may be important for exciting the resonance oscillations in heave, pitch and roll of the turbine. This is referred to as ringing. However, it is shown that the sum-frequency heave forces are small at the natural period in heave (Faltinsen 2009) and these forces are much lower than the wave frequency load.

8.2 Temporary Conclusion

It is clear from results given in Table 7-1 to Table 7-3 and Gumbel plots in Figure 7-4 to Figure 7-6 that the equal area method with 90 components gives the best results when compared with FFT. Not surprisingly, because of the highest number of components in the wave spectrum.

Since the equal area method produces almost the same results as FFT, one can conclude that the wave spectrums of the equal area method are able to produce the same or higher nonlinear effects that may compensate for the smaller linear effects found in Chapter 5. The equal area method produces slightly higher responses than FFT, i.e. the equal area method is conservative. The small difference between results from FFT and EAP suggests that the equal area method can be employed.

Considering the responses; cardan force, moment in the tower at sea surface and displacement at top tower, the minimum extreme using EAP always exceeds minimum extreme obtained when using FFT. Therefore, the chance for underestimating response is negligible and no safety factor is necessary, refers Appendix E. EAP and FFT have approximately the same results concerning these response quantities, and a correction factor is not required, refer Table 7-2.

Especially the cardan force gives very satisfying results. The 90 percentile estimate from the Gumbel distribution between FFT and EAP with 90 components is only in the order of 1%, i.e. negligible difference, refer Table 7-4. Concerning the wave load and the acceleration at top tower, a correction factor may be necessary because of higher ratio between FFT and EAP. One proposes a correction factor of 0.9 if it is important with an accurate result.

Take notice that the standard deviation is larger considering the equal area method. It is therefore recommended to run more than one simulation using the equal area method.

Together with a significantly reduction in computer time and non-conservative results, the equal area method is the preferable method in this case. It may be possible for further reduction in computer time by using a built-in command, *SpoolWave* in USFOS. This is investigated in the following chapter.

9 SpoolWave Command

A method for reducing the computational time is by using the command, *SpoolWave* in USFOS. With this record, the user defines how to search for the highest/lowest waves in an irregular wave field. The analysis time will be moved forward to the specified "time before peak", resulting in decreased computer time (USFOS User's Manual 2006), refer Figure 9-1 for illustration of the command. However, using the spoolwave command should be executed with caution and results given should not be accepted without reflection. Among other things is it necessary to have a long enough "time before peak" period to get the similar dynamic behavior and satisfactory results. Necessary start time length before specified wave peak depends on the type of structure. The user must also have knowledge about how the structure responds to waves i.e. whether or not the structure gives largest responses during highest, second highest wave peak or trough. The "spoolwave method" for reduction of computer time has not been fully tested and it is uncertain which types of results that can be used when employing the command. This Chapter tests the adequacy of the *SpoolWave* command on the SWAY turbine.

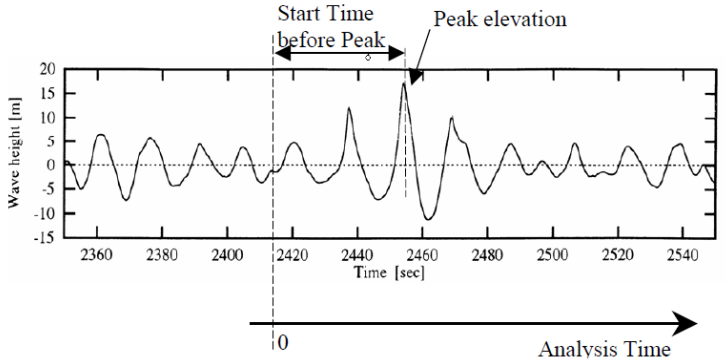

Figure 9-1 Illustration of the spoolwave command (USFOS User's Manual 2006)

9.1 Spoolwave on the SWAY Turbine

It is assumed that the extreme response will occur close to some of the extreme surface elevations, both peak trough and crest, refer USFOS Hydrodynamics (2010). The equal area method with 90 components gives satisfactory results when compared upon FFT, refer Chapter 7.2.2. Employing the spoolwave command with the equal area method with 90 components will decrease the computer time even further. The spoolwave command has been tested on all twenty samples with a simulation time 300s before specified trough or crest. The responses requested from this analysis are the same as for the original analysis; cardan force, displacement and acceleration at the top, moment in tower at sea surface, wave load and surface elevation. It will be shown that the history plots resemble those obtained from the full analysis, but the "spoolwave values" differ from exact to conservative and non-conservative results. This applies for both highest wave crest and trough, and it is therefore necessary to check the temporal variation of response and surface elevation to get a better understanding of these random deviations.

When performing the time-domain analyses with the spoolwave command it was observed that the specified peak/trough does not always appear after 300s as specified. This was found by comparing values for extreme surface elevation from the full analysis with extremes from the spoolwave analysis. The reason for this is that there is no specified peak/trough to "spool" i.e. the specified peak/trough occurs before 300s in these cases. 300s correspond to around one third of the full analysis, and the chance for this occurrence is much larger than for example applying the spoolwave command to a three hour time simulation, i.e. 300s cover only 2.8% of three hours. When comparing surface elevation results, it is seen that largest wave crest occur before 300s in seven samples and lowest

trough occur before 300s in five samples, i.e. thirteen samples are available for spoolwave with maximal crest and fifteen samples are available for lowest trough when attempting to verify the use of the spoolwave command.

It is also worth mentioning that maximum results given from the spoolwave command are from simulation time 250s to 350s. This is to eliminate results from the initial transient response and an attempt to narrow down the possibility that one would get maximum results that occur from other incidents than largest/smallest surface elevation.

9.2 Results

The moment in the tower at sea surface, acceleration at the top tower and tension in the rod are considered the most interesting and important responses to consider. Results, discussion and conclusion of the use of spoolwave regarding these quantities are found in the following pages. Results for displacement at tower top and wave load are given in Appendix F.

9.2.1 Moment in Tower at Sea Surface

Bending moments in the tower are important design parameters and are mainly caused by the inclination of the tower and by tower top accelerations. The movements of the tower top give a good picture of the source of these bending moments. The largest moment is assumed to come from largest crest and not the lowest trough. This is verified when comparing results from the full analysis against spoolwave results when asking for maximum trough and crest. Table 9-1 gives a full overview of the results using spoolwave versus results from the full analysis from the thirteen available samples.

Table 9-1 Spoolwave Analysis vs. Full Analysis. Mz at Sea Surface [Nm].

Case	Full Analysis	Spoolwave, Max Crest	Ratio
H=16.4_T=17_Seed=000_0090.max	2,80E+08	2,86E+08	1,02
H=16.4_T=17_Seed=030_0090.max	2,34E+08	2,26E+08	0,97
H=16.4_T=17_Seed=060_0090.max	2,34E+08	2,30E+08	0,98
H=16.4_T=17_Seed=080_0090.max	2,39E+08	2,51E+08	1,05
H=16.4_T=17_Seed=100_0090.max	2,52E+08	2,52E+08	1,00
H=16.4_T=17_Seed=110_0090.max	2,50E+08	2,44E+08	0,97
H=16.4_T=17_Seed=130_0090.max	2,78E+08	2,22E+08	0,80
H=16.4_T=17_Seed=140_0090.max	2,26E+08	2,91E+08	1,29
H=16.4_T=17_Seed=150_0090.max	2,87E+08	2,89E+08	1,00
H=16.4_T=17_Seed=160_0090.max	2,87E+08	2,87E+08	1,00
H=16.4_T=17_Seed=170_0090.max	2,17E+08	2,14E+08	0,99
H=16.4_T=17_Seed=180_0090.max	2,39E+08	2,42E+08	1,01
H=16.4_T=17_Seed=190_0090.max	2,21E+08	2,08E+08	0,94
Max	2,87E+08	2,91E+08	1,29
Min	2,17E+08	2,08E+08	0,80
Standard Deviation	2,52E+07	3,00E+07	0,10
Mean	**2,50E+08**	**2,49E+08**	**1,00**

Table 9-1 indicates that the *SpoolWave* option with the highest crest gives almost identical results for moment at sea surface. Results from the samples in the spoolwave analyses differ with only a few percent, and almost all maxima from the spoolwave analysis refer to the same moment maxima as for

the full analysis. In other words, the response history plots are visually the same with a minor difference in values. If an identical result from the spoolwave analysis is desired, one could try to increase the duration of the spoolwave analysis, but the cost is longer computational time and one should discuss if this is necessary. If the extreme response comes from another surface elevation, one can most likely expect that the second largest moment comes from the largest crest.

The reason for the large deviation in sample Seed=140 is because maximum surface elevation occurs at the very end of the full analysis and often the maximum moment occurs right after peak maxima, refer Figure 9-2. In contrast to the full analysis, the spoolwave analysis "captures" this extreme. Results from Seed=130 also deviates significantly. This shows that moments are not only dependent on maximum surface elevation but also that previous wave history plays a small role.

Gumbel plots are useful to see the different trends between the results from the spoolwave - and full analyses. Figure 9-3 compares the results from using the spoolwave command upon the correct results. The blue points represent results from the full analysis, and the cyan points represent results from the spoolwave analysis. The straight lines give a visual view of the trend.

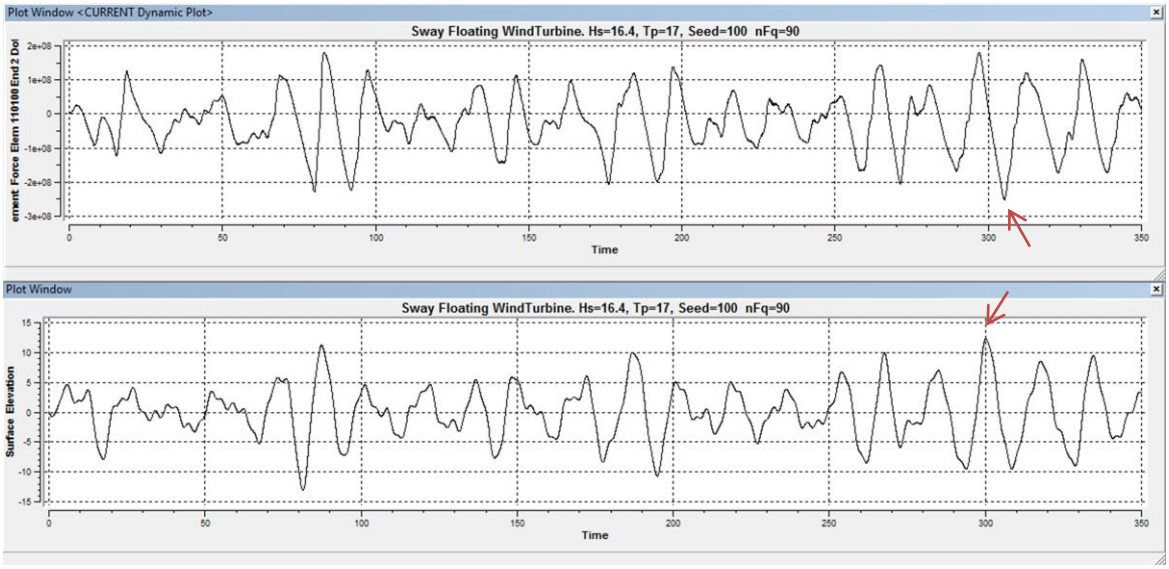

Figure 9-2 Time history plots for Moment at Sea Surface and Surface Elevation

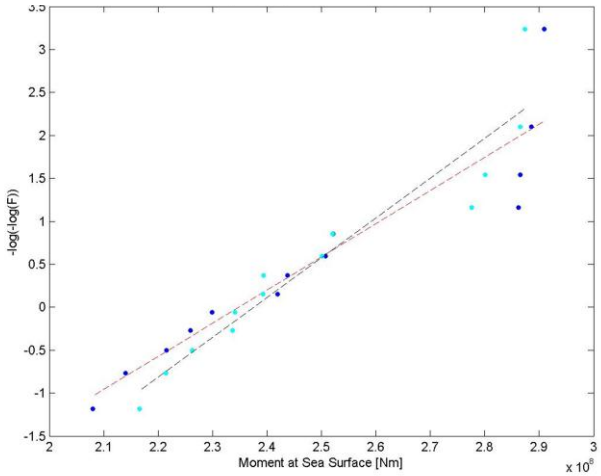

Figure 9-3 Gumbel Plot for Moment at Sea Surface. Full Analysis vs. Spoolwave Analysis with maximum surface elevation

9.2.2 Horizontal Movement of the Tower Top

Results for acceleration at top tower from the full analysis and the use of the spoolwave command are compared in Table 9-2. *Order* in Table 9-2 and Table 9-3 describes which kind of wave crest or trough that is selected in the spoolwave analysis. First, second, third etc. highest wave crest is selected by specifying 1, 2, 3 etc. in the head file in USFOS, refer Appendix A. A negative number represent the first, second, third etc. lowest wave trough (USFOS User's Manual 2006).

Table 9-2 Spoolwave Analysis vs. Full Analysis. Acceleration at Toper Top [m/s^2]

Case	Full Analysis	Spoolwave, Max Crest	Ratio	Best Result with Spoolwave	Ratio	Order
H=16.4_T=17_Seed=000_0090.max	5,60	5,62	1,00	5,61	1,00	1
H=16.4_T=17_Seed=030_0090.max	5,41	5,47	1,01	5,40	1,00	-1
H=16.4_T=17_Seed=060_0090.max	5,42	4,23	0,78	5,46	1,01	-1
H=16.4_T=17_Seed=080_0090.max	4,80	4,73	0,99	4,73	0,99	1
H=16.4_T=17_Seed=100_0090.max	6,12	4,73	0,77	5,20	0,85	-1
H=16.4_T=17_Seed=110_0090.max	5,37	4,52	0,84	5,31	0,99	-1
H=16.4_T=17_Seed=130_0090.max	5,39	5,34	0,99	5,34	0,99	1
H=16.4_T=17_Seed=140_0090.max	5,05	5,51	1,09	5,51	1,09	1
H=16.4_T=17_Seed=150_0090.max	5,16	5,16	1,00	5,16	1,00	1
H=16.4_T=17_Seed=160_0090.max	5,22	5,22	1,00	5,22	1,00	1
H=16.4_T=17_Seed=170_0090.max	5,34	5,34	1,00	5,34	1,00	1
H=16.4_T=17_Seed=180_0090.max	5,10	5,07	0,99	5,07	0,99	1
H=16.4_T=17_Seed=190_0090.max	5,73	4,07	0,71	5,80	1,01	-1
Max	6,12	5,62	1,09	5,80	1,09	
Min	4,80	4,07	0,71	4,73	0,85	
Standard Deviation	0,33	0,50	0,12	0,26	0,05	
Mean	**5,36**	**5,00**	**0,94**	**5,32**	**0,99**	

Usually the largest surface elevation leads to the largest acceleration in top tower. All samples from spoolwave analysis run with maximum crest gives satisfactory results except samples Seed=60, Seed=100, Seed=110 and Seed=190. Here, the lowest trough results in the maximum acceleration. Only sample Seed=100 have a significant deviation in both cases. Here the second lowest surface elevation results in the largest response. From *exact.exe* it is seen that the second largest trough has approximately the same dimensions as the largest trough.

The standard deviation is only 5% when considering the best results with use of the spoolwave command and is within an acceptable range.

9.2.3 Tension Rod Forces

The tension in the rod is a result of the difference between two big, opposite forces (gravity and buoyancy, static and dynamic). Some extreme responses are expected to occur for the extreme trough. However, this is not necessarily true sometimes the worst situation can come from another large elevation (both crest and trough). Therefore, the spoolwave command is employed with several different surface elevations when searching for the extreme for cardan force. Here, the spoolwave command is executed with the highest crest and 1st, 2st, 3st lowest troughs. Seed=100 was also run with the second highest wave crest since none of the above gave satisfactory results. Order with best result in sample Seed=90 was found after manually investigating the full dynamic plot in *exact.exe* because the crest occurs after only 200s.

Results from the full analysis and spoolwave analysis are found below in Table 9-3. Fifteen samples are available for deciding the adequacy of the spoolwave command considering cardan force.

Table 9-3 Overview of Cardan Force results from Full Analysis and Spoolwave Analysis

Cardan Force [N]						
Case	**Full Analysis**	**Spoolwave, Min Crest**	**Ratio**	**Best Results with Spoolwave**	**Ratio**	**Order**
H=16.4_T=17_Seed=000_0090.max	4,50E+06	4,57E+06	1,01	4,57E+06	1,01	-1
H=16.4_T=17_Seed=010_0090.max	4,35E+06	4,35E+06	1,00	4,35E+06	1,00	-1
H=16.4_T=17_Seed=030_0090.max	4,31E+06	4,10E+06	0,95	4,10E+06	0,95	-1
H=16.4_T=17_Seed=060_0090.max	4,54E+06	3,92E+06	0,86	4,56E+06	1,00	-2
H=16.4_T=17_Seed=070_0090.max	4,25E+06	4,26E+06	1,00	4,26E+06	1,00	-1
H=16.4_T=17_Seed=080_0090.max	4,22E+06	4,11E+06	0,97	4,22E+06	1,00	-3
H=16.4_T=17_Seed=090_0090.max	4,33E+06	3,88E+06	0,90	4,33E+06	1,00	1
H=16.4_T=17_Seed=100_0090.max	4,24E+06	3,95E+06	0,93	4,29E+06	1,01	2
H=16.4_T=17_Seed=110_0090.max	4,21E+06	3,94E+06	0,94	4,26E+06	1,01	1
H=16.4_T=17_Seed=120_0090.max	4,42E+06	3,92E+06	0,89	4,42E+06	1,00	-2
H=16.4_T=17_Seed=130_0090.max	4,23E+06	4,07E+06	0,96	4,07E+06	0,96	-1
H=16.4_T=17_Seed=140_0090.max	4,14E+06	4,02E+06	0,97	4,12E+06	1,00	-3
H=16.4_T=17_Seed=150_0090.max	4,23E+06	4,03E+06	0,95	4,03E+06	0,95	-1
H=16.4_T=17_Seed=180_0090.max	4,08E+06	4,12E+06	1,01	4,12E+06	1,01	-1
H=16.4_T=17_Seed=190_0090.max	4,26E+06	4,24E+06	1,00	4,24E+06	1,00	-1
Max	4,54E+06	4,57E+06	1,01	4,57E+06	1,01	
Min	4,08E+06	3,88E+06	0,86	4,03E+06	0,95	
Standard Deviation	1,25E+05	1,88E+05	0,05	1,64E+05	0,02	
Mean	**4,29E+06**	**4,10E+06**	**0,96**	**4,26E+06**	**0,99**	

Every sample from the spoolwave analysis found in Table 9-3 has also been checked visually in dynamic plots in *exact.exe* to get a better understanding of the behavior of the tension rod force. It is observed that two local peaks always occur simultaneously with largest trough and does not result in the largest outcome. The extreme responses occur right after or before specified surface elevation, refer Figure 9-4.

It is also worth mentioning that observed extreme result from the spoolwave analysis may refer to another extreme than the full analysis. The result from the spoolwave analysis may have be 1% larger (e.g. Seed=000) if the extreme from the spoolwave analysis refers to the same extreme in the full analysis, but this difference is negligible.

Gumbel plots in Figure 9-6 and Figure 9-7 visually compare the results from using spoolwave command with the correct results. Both regression lines from the spoolwave results are close to the regression line of the full analysis.

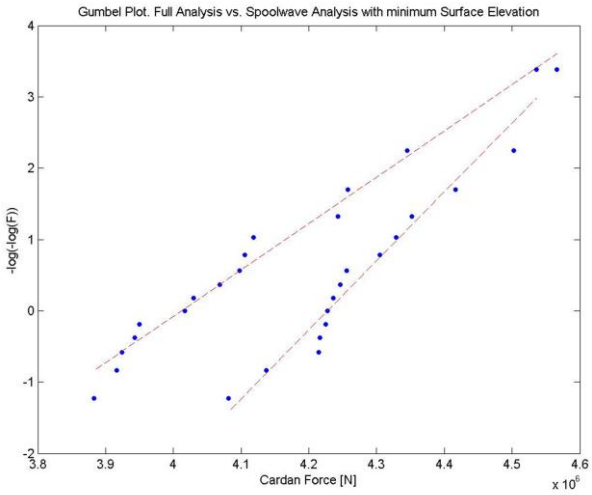

Figure 9-4 Gumbel Plot for Cardan Force. Full Analysis vs. Spoolwave Analysis with minimum surface elevation

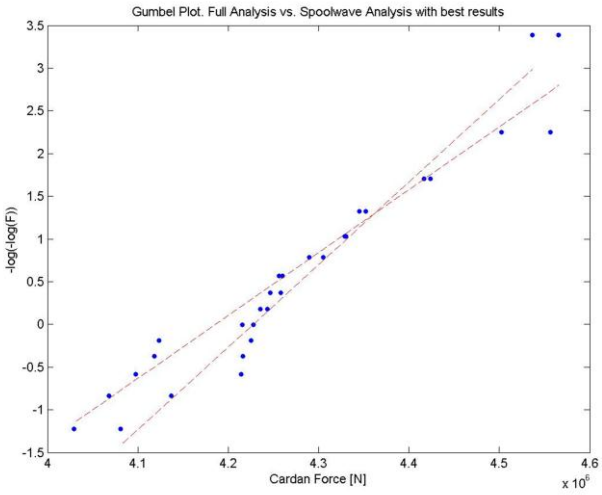

Figure 9-5 Gumbel Plot for Cardan Force. Full Analysis vs. Spoolwave Analysis with best results

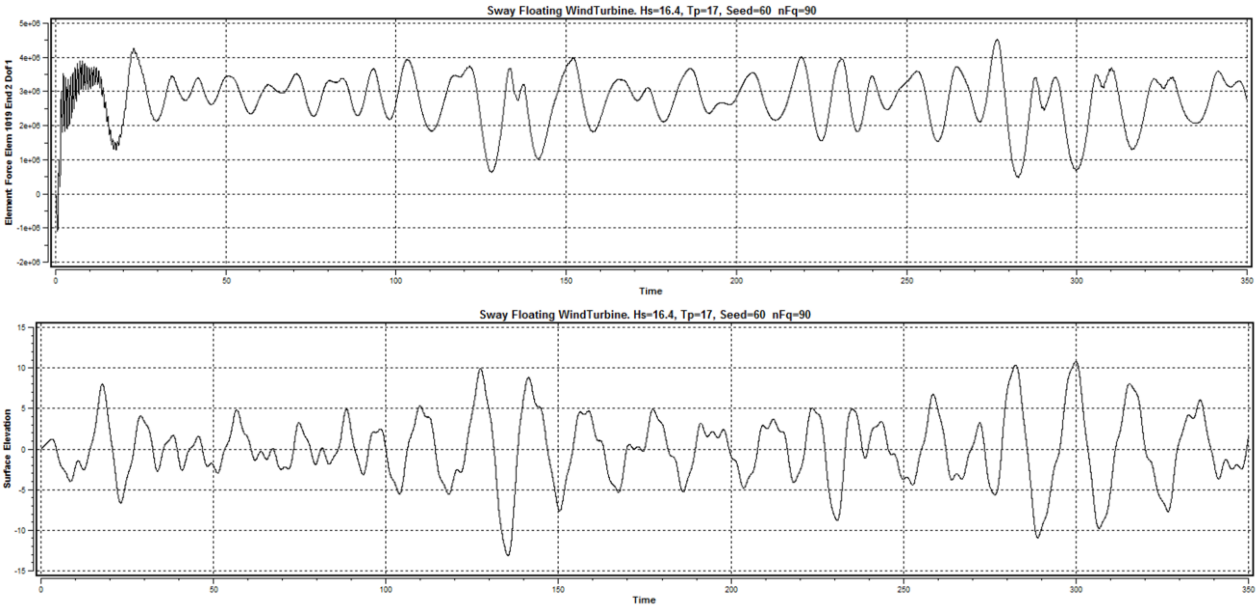

Figure 9-6 Illustration of cardan force behavior vs. surface elevation

9.3 Conclusion

9.3.1 Moment in Tower at Sea Surface

The results when using spoolwave is satisfactory since the mean ratio are equal to one. However, the standard deviation for the spoolwave results are somewhat high because of sample Seed=130 and Seed=140.

The hypothesis that was done before the analysis that an extreme response occur close to extreme surface elevations is confirmed when considering the moment in the tower at sea surface. Only sample Seed=130 have its extreme at a random place during full time-domain simulation. This implies that the

moments are not only dependent of current surface elevation, but are also slightly influenced by previous surface elevation history. The regression lines from the samples for the full analysis and spoolwave analysis intersects and have resembling gradients, and the results from the spoolwave command are therefore satisfactory, refer Figure 9-3.

It is only necessary to use the spoolwave command with maximum surface elevation. Using a scaling factor is not required here, but may be recommended if only running a few analyses because of a larger standard deviation.

9.3.2 Horizontal Movement of the Tower Top

When comparing the results from the spoolwave analysis and the full analysis it is seen that the spoolwave command gives in average, lower results when just using maximum surface elevation. Samples Seed=60, Seed=100, Seed=110 and Seed=180 deviates significantly and leads to a mean ratio of 0.96. When spoolwave is also run with minimum surface elevation, the samples mentioned above gives almost the identical results as the full analysis. Here, the mean ratio increases to 1.0. Plots from all these samples show that the lowest trough are together with a high crest indicating that the extreme acceleration are dependent of total wave height. The standard deviation decreases from 12% to 5% when spoolwave analysis is also run with minimum trough.

If one shall only execute the spoolwave command with maximum surface elevation, a correction factor of 1.10 is recommended because of a mean ratio difference of 0.94 and a larger standard deviation. However, a spoolwave analysis with minimum and maximum surface elevation is recommended.

9.3.3 Tension Rod Forces

Considering Table 9-3, best results comes from running the spoolwave command with several different surface elevations. Combining results from the spoolwave command with different surface elevations, one obtains a mean ratio of 0.99 between correct results and spoolwave results. With only maximum trough and crest one get a mean ratio of 0.96 and 0.97. Since the mean ratio are about the same, it may not be necessary to run many spoolwave analyses if several tests are to be executed. But if only a single test is run, one should use the spoolwave command with several different surface elevations because of a larger spreading in results for spoolwave command performed with only largest trough.

The Extremes from samples Seed=30, Seed=130 and Seed=150 deviates the most and occur in random locations in the full analysis, and the “order” of surface elevation that leads to largest response varies. One concludes therefore that the response is also highly dependent of previous surface elevation history.

The extreme in the spoolwave analysis does not always refer to the same extreme in the full analysis, but because of small variation in the cardan force, one obtains similar results. Figure 9-4 displays a visual view of the small variance in peaks for the cardan force.

The Gumbel plots for samples from the full analyses and spoolwave analyses are similar and satisfying.

The process with trying spoolwave with so many different wave heights are time consuming, and is not recommended unless one want to perform time-domain simulation with a duration in order of hours. One should select largest trough if only one spoolwave analysis are executed.

9.3.4 Summary

Considering all results and Gumbel plots, the spoolwave command is satisfactory for all three response quantities. Acceleration and moment behave similar; having a linear relationship between the response and surface elevation, refer Figure 9-2. The highest crest will in general lead to the largest response. This yield for general tower forces, but sometimes the largest response may occur during a

large wave height, refer chapter 9.3.2. The results for wave load and displacement when using the spoolwave command are found in Appendix F.

Of all three responses, the tension in the rod is most influenced by the previous wave history, and the spoolwave command should be performed with several different surface elevations to obtain good results.

Using the spoolwave command leads to conservative, non-conservative or exact results and it is necessary to use corrections factor to make sure that no underestimation of response occur. Combining results from standard deviation, mean and 90 percentile estimates, refer Appendix D, following safety factors are recommended:

- General tower forces/movements, using highest crest/trough — Scaling factor: 1.00
- Moment and displacement, using highest crest — Scaling factor: 1.05
- Wave load and acceleration, using highest crest — Scaling factor: 1.10
- Tension rod forces: Use both crest/trough. 1^{st}, 2^{st}, 3^{st} largest — Scaling factor: 1.05

The safety factors are proposed when assuming few simulations. More samples would lead to smaller standard deviation, and the scaling factors may then be unnecessary high.

It has been time consuming to go into *exact.exe* for each sample to check whether or not the specified crest/trough in spoolwave occur before the specified "spool time". A solution to this problem may be to have a start and end time of the storm length specified in the command, *SpoolWave*, instead of the total duration of the storm. Then one would avoid the possibility that the crest/trough occur before specified time and spurious large responses from the initial transient response.

In this comparison one should be aware of that the results from the spoolwave simulation covers one tenth of the full analysis and correct results can therefore come from a coincidence.

Having a three hour simulation that is common for a short term analysis, and using the spoolwave command together with the equal area method would reduce the computer time significantly.

10 Conclusions

This thesis has dealt with the adequacy of simulating waves with a method based on the equal area principle. The equal area method has been compared upon the traditional method, Fast Fourier Transform. Checking the validity of the equal area method has been performed in three steps. First the statistical parameters for the surface elevation have been discussed. Second, the method has been applied to a single bottom fixed, vertical cylinder where both a static and dynamic analysis has been carried out. Last, the equal area method has been tested on a floating structure, the SWAY turbine. The accuracy of the USFOS command *SpoolWave* has also been examined.

Statistical Parameters

Results and discussion of the statistical parameters are reviewed in Chapter 5. The simulated waves in the computer program, USFOS should approach a Gaussian process. Here, the distribution should have the following characteristics; a mean value of 0, standard deviation of 3, skewness of 0, and a kurtosis of 3. All resulting parameter quantities except the kurtosis are very satisfactory. FFT produces a kurtosis value less than 3 and less than the equal area method. EAP produces in fact "better" parameters than FFT. The mean extremes of surface elevation from FFT and EAP are respectively lower and higher than the theoretical value. However, the deviations are not significant, and one concludes that FFT and EAP results in an asymptotically Gaussian distribution, which is satisfactory.

Static and Dynamic Analysis of Fixed Cylinder

The equal area method result in both conservative and non-conservative responses in comparison to FFT, i.e. there is no consistent trend in the outcome of this method. Chapter 5 and Chapter 6 give a fully discussion and conclusion of the results. Safety factors are proposed if EAP is chosen for simulating irregular waves. However, the equal area method is unpredictable and is not recommended to be used on fixed structures.

Dynamic Analysis of SWAY turbine

Several responses have been focused when checking the adequacy of the equal area method on the SWAY turbine. These are the cardan force, displacement and acceleration at the top of the turbine, moment in the tower at sea surface, wave load and surface elevation.

The equal area method always produces higher responses than FFT, i.e. the equal area method is conservative when employed on the SWAY turbine. The small ratio between results from FFT and EAP suggests that the equal area method can be used when employing a potential correction factor. Using the equal area method on the SWAY turbine gives satisfactory results. Full conclusion is given in Chapter 8.

The SPOOLWAVE Command

The *SpoolWave* command in USFOS is used for reduction in computer time. It should be exercised that the startup time is sufficiently long ahead of the peak wave, so that the response versus time is equal to the original analysis and that the initial transient response has been properly damped out. Here, a startup period of 300 seconds is satisfactory.

The command leads to conservative, non-conservative or exact results and it is therefore necessary to use corrections factor to make sure that no underestimation of response occur. However, the deviation between the full analysis and the analysis performed with the *SpoolWave* command are small. The spoolwave command has therefore been found to be adequate if employed correctly.

Summary

The equal area method produces a satisfactory Gaussian trend in surface elevation and good responses considering the SWAY turbine. There are therefore no noticeable reasons for not using the equal area method on floating solutions.

The deviations in response between FFT and EAP when considering the fixed cylinder are too large. The equal area method is not recommended on fixed solutions.

11 Recommendations for Further Work

The thesis leaves some questions open. Several issues can be explored in more detail. Here a few recommendations for further work will be given.

It has been found that certain control parameters in USFOS may be benefited by being slightly altered. One suggestion is to expand the commands, *static*, *dynamic* and *spoolwave* in USFOS from total duration of the storm to a start and end time. During the startup period, the structure experiences responses as an effect of initial conditions. By specifying a start time after T=0s, one would be able to avoid these results.

There is also noticeable uncertainty when finding 90 percentile estimates from Gumbel plots with only 20 samples and a duration of 1000 seconds. Therefore a three hour simulation comparison between the equal area method and FFT would be more precise. Number of available components for splitting the wave spectrum in USFOS is therefore recommended to be extended.

The adequacy of the equal area method is not satisfying when the natural period of the structure lays in the low energy part of the wave spectrum. Here, the spreading in frequency, $\Delta\omega$, is too large to capture the dynamic amplification factors. Therefore an alternative method that emphasizes the part of the wave spectrum where the natural period of the structure is located may be an option.

The theory and reasons for different results obtained from FFT and the equal area method is incomplete. The specific reason for more accurate results when wave loads are drag dominated are still unknown. Hence, this should be investigated further to arrive at a final conclusion on the quality of the equal area method.

There may also be too little information basing all conclusions on simulations with duration of 1000 seconds and with only 20 samples available, i.e. statistical uncertainty. Therefore more samples with longer duration are recommended for a final conclusion.

References

Faltinsen, O. M. *Sea Loads on ships and offshore structures.* Cambridge: Cambridge University Press, 2009.

Haver, Sverre K. *Prediction of Characteristic Response for Design Purposes.* Stavanger: Statoil, 2010.

Langen, I., Sigbjørnsen, R. *Dynamisk Analyse av konstruksjoner.* Trondheim: SINTEF, 1979.

Larsen, Carl M. "Kompendium, TMR4180 Marin Dynamikk." Trondheim: Department of Marine Technology, 2009.

Larsen, Carl Martin. *Drag forces in Dynamic Analysis [Lecture Notes]*. Trondheim: Department of Marine Technology, NTNU, 08 09 2005.

Leira, Bernt J. "Kompendium, TMR4235 Probabilistic Modelling and Estimation." Trondheim: Department of Marine Technology, 2010.

M. J. Tucker, P.G. Challenor and D. J. T. Carter. "Numerical Simulation of a random sea; a common error and its effect upon wave group statistics." In *Applied Ocean Research, vol6, no.2* , pp. 118-122. 1984.

Myrhaug, Dag. "Kompendium, TMR4180 Marin Dynamikk Uregelmessig Sjø." Trondheim: Department of Marine Technology, 2007.

Myrhaug, Dag. "Kompendium, TMR4235 Statistics of Narrow Band Processes and Equivalent Linearization." Trondheim: Department of Marine Technology, 2005.

Pettersen, Bjørnar. "Kompendium, TMR4247, Hydrodynamikk." Trondheim: Department of Marine Technology, 2007.

Saha, N. Gao, Z. and Moan, T. *Sampling uncertainty of simulated stochastic sea elevation and response process of a vertical cylinder.* Paper, Trondheim: Norwegian University of Science and Technology, in press.

SINTEF marintek. *USFOS Getting Started.* Trondheim: SINTEF GROUP, 2001.

SINTEF marintek. *USFOS Hydrodynamics.* SINTEF Marintek. Trondheim: SINTEF GROUP, 10 02 2010.

SINTEF marintek. *USFOS User's Manual.* Trondheim: Available online from: www.usfos.no/manuals/usfos/users/documents/Usfos_UM_06.pdf, 2006.

SWAY AS. *sway.no.* Sway. n.d. http://sway.no/?page=166 (accessed 03 17, 2011).

Tore H. Søreide, Jørgen Amdahl, Ernst Eberg, Tore Holmås and Øyvind Hellan. *USFOS - A computer program for Progressive Collapse Analysis of Steel Offshore Structures. Theory Manual.* Trondheim: Sintef, 1993.

WAFO-Group. *WAFO, a MATLAB toolbox for Analysis of Random Waves and Loads.* Lund: Lund University, 2000.

Appendices

Appendix Figures

Appendix Tables

A USFOS FILES

The USFOS files used for performing time-domain analysis on the fixed cylinder and the SWAY turbine is given in this appendix. Subchapters A.1 and A.2 contains the control file and model file for the fixed cylinder, and subchapters A.3 and A.4 contains the control file and model file for the SWAY turbine. The load controls *STATIC* and *DYNAMIC* are altered when performing the static and dynamic analysis on the fixed cylinder. The *SpoolWave* command in Figure A.3 is made use of when performing the "spoolwave analysis".

Refer to USFOS User's Manual for description and use of the different commands.

A.1 Control File for Fixed Cylinder

```
HEAD       Project Thesis for Ine-Therese Binner.   Hs=HEIGHT,  Tp=PERIOD, Seed=SEED
                 I r r e g u l a r  W a v e   A n a l y s i s
           ------------------------------------------------------------
'
 Switches  Wave  TimeIncr   0.1    ! Compute Waves every 0.1s

 BeamType Riser All
'
'          EndT      dT    dTRes d TPri
DYNAMIC   1500.0   0.10    100     100
'
'           End_Time   Delta_T   Dt_Res  Dt_term   mxdisp   nstep   minstp
'STATIC     1000.0       0.1    100.     100.       0.0       0     0.001
'
'
' eigenval  Time     60
'
' ========================================================================
'     W A V E. Jonswap Spect. Hs=HEIGHT, Tp=PERIOD, Dir=SEED
'              frequency ranging from T=3-25s. Fix Gamma Param
' ------------------------------------------------------------------------
'        LCase  LoTyp   Hs      Tp      Dir   Seed  Surflev  Depth   n_ini
 WaveData  2    Spect  HEIGHT  PERIOD   000   SEED    90.0   90     4
'
     -1000   1
      -200   1
         0   0
       100   0
'
'     nfreq   Type     T_min  T_max   igrid  Gamma
      1000      Jonsw    3      25.0    1      3.3
'
'           Ratio_1  Ratio_2  Freq_1  Freq_2
DampRatio  0.03     0.03      0.07      0.5
'
 Buoyancy
'Rel_velo
 BuoyHist   2   Mat
'
'
'
'            ID      Type     T1     T2    Fac   Pow
 TimeHist     1    S_Curve     0     2     1     2    ! Gravity
'
'            ID   <type>    Dtime Factor   Start_time Ini_Time End_Time
 TIMEHIST     2    Switch   0.0   1.0       0.0             ! Wave
'
'
 LoadHist     1    1      !  Gravity
 LoadHist     2    2      !  Wave
'
'
'           Time
INI_TIME    500
'
Dynres_G   ReacOVTM
Dynres_G   WaveOVTM
DynRes_G   WaveElev
DynRes_G   WaveLoad
'
 CNODES     1
 '          nodex    idof     dfact
            2        1        1.00

' -----------------  e o f --------------------------
```

Figure A-1 USFOS Control file for Fixed Cylinder

A.2 Model File for Fixed Cylinder

```
HEAD
'
'            Node ID            X              Y              Z    Boundary code
 NODE              1            0.00          0.000          0.000   1 1 1 1 1 1
 NODE              2            0.00          0.000         50.000
 NODE              3            0.00          0.000         75.000
 NODE              4            0.00          0.000         90.000
 NODE              5            0.00          0.000        120.000

'
'            Elem ID     np1      np2   material   geom    lcoor    ecc1    ecc2
 BEAM             1        1        2        1        1
 BEAM             2        2        3        1        1
 BEAM             3        3        4        1        1
 BEAM             4        4        5        1        1
'
'
'            N_divide    Elem
REFINE         2         1
REFINE         5         3
REFINE         10        4
'
'            NIS         Elem
Wave_int       2         1
Wave_int       3         2
Wave_int       4         3
Wave_int       6         4
'
'         matno    E-mod     poiss  yield      density   term. expantion
'
 MISOIEP      1    0.21E14   0.3    10.0E+10    7.85E3   0.0       !Static Analysis
'
'MISOIEP      1    0.42E12   0.3    10.0E+10    0.82E5   0.0       !Mass Dominated. Tn=4.4s
'MISOIEP      1    0.42E12   0.3    10.0E+10    2.8E5    0.0       !Mass Dominated. Tn=8.
'MISOIEP      1    0.63E12   0.3    10.0E+10    8.7E5    0.0       !Mass Dominated. Tn=14s
'
'MISOIEP      1    3.20E12   0.3    10.0E+10    0.64E4   0.0       !Drag Dominated. Tn=4.4s
'MISOIEP      1    3.19E12   0.3    10.0E+10    2.18E4   0.0       !Drag Dominated. Tn=8.5s
'MISOIEP      1    3.69E12   0.3    10.0E+10    5.22E4   0.0       !Drag Dominated. Tn=14s
'
'            Geom ID       Do         Thick
 PIPE             1        8.00        0.10         !When Wave Loads are Mass Dominated
 PIPE             1        1.00        0.10         !When Wave Loads are Drag Dominated
'
 GRAVITY          1    0 0 -9.81
'
```

Figure A-2 USFOS Model File for Fixed Cylinder

A.3 Control File for SWAY Turbine

```
HEAD       Sway Floating. Const dArea Hs=HEIGHT, Tp=PERIOD, Seed=SEED  nFq=NFREQ
                 S w a y S i m   A n a l y s i s
               Virtual Prototyping AS 2009-12-01
'
 Switches  Wave  TimeIncr   0.1    ! Compute Waves every 0.1s
'
 BeamType Riser All
#liter
'
'          EndT      dT    dTRes d TPri
#Dynamic  1000.0   0.050    20     20
Dynamic   350.0   0.050     1      1
'
'            TimeBeforePeak   Order  dT  StormLength  Crit
SpoolWav          300           -1    0.5   1000      Elev
'
'        LCase  LoTyp   Hs      Tp     Dir   Seed  Surflev  Depth   n_ini
 WaveData  09  Spect  HEIGHT  PERIOD   000   SEED    0.0    150   4
'
     -1000   1
      -200   1
         0   0
       100   0
'
'     nfreq Type     T_min  T_max   igrid  Gamma
       NFREQ  Jonsw      3    50.0     3       3.3
'
'          Cd    Cm  Elno...
 Hyd_CdCm   1.4  2.0
 RaylDamp  0.00   3E-3        ! Gives 0.5% damp at 0.5Hz

'                           Z    NIS
 Wave_Int         Profile 10.0   10
                           0.0   10
                         -10.0    8
                         -20.0    4
                         -50.0    3
                        -100.0    3
'
 Rel_Velo
'
 Buoyancy
 BuoyHist   11   Mat
'
 BuoyForm  Panel  Group 100
 BuoyForm  Panel  Elem 110120
'
'         Elem
 Flooded  1019            ! Tension Rod
'
'            ID      Type     T1     T2    Fac   Pow
 TimeHist     1    S_Curve     0     2     1     2    ! Gravity
 TimeHist     3    S_Curve     0     2     1     2    ! Wind
 TimeHist    11    S_Curve     0     2     1     2    ! Buoyancy

'           ID   <type>    Dtime Factor   Start_time Ini_Time End_Time
 TIMEHIST     9    Switch   0.0   1.0       0.0             ! Wave and current
'
 LoadHist     1    1      !  Gravity
 LoadHist     9    9      !  Wave and current
 LoadHist     3    3      !  Wind
'
'           Type    Node   Dof
 DynRes_N   Disp   301     1    ! Top of tower            !1
 DynRes_N   Acc    301     1    ! Top of tower            !2
 DynRes_N   Disp   301     2    ! Top of tower            !3
 DynRes_N   Disp   19      1    ! Top of tension bar      !4
 DynRes_N   Acc    19      1    ! Top of tension bar      !5
 DynRes_N   Disp   19      2    ! Top of tension bar      !6
 DynRes_N   Disp   19      3    ! Top of tension bar      !7
'
'           Type    Elem   End  Dof
 DynRes_E   Force   1019    2    1    !  Cardan force Top                !8
 DynRes_E   Force   1019    2    4    !  Cardan torsional moment Top     !9
 Dynres_E   Force  110100   2    1                                       !10
 Dynres_E   Force  110100   2    5                                       !11
 Dynres_E   Force  110100   2    6                                       !12
'
 DynRes_G   WaveElev                                  !13
 Dynres_G   WaveLoad                                  !14
'
 CNODES     1
 '          nodex    idof     dfact
            301       1        1.00
```

Figure A-3 USFOS Control File for SWAY

A.4 Model File for SWAY Turbine

```
' wind force
'          LC  Node   Fx
 NodeLoad   3  300  117E3                  ! WindForce X-dir
 NodeMass      300  117E3/9.81  0  0  0 0 0 ! X-mass
'
 GroupDef      100 Mat       2 3 4 5 6 7 8 9 10
 Name   Group  100 Main_Buoy
'
'            Node ID            X              Y              Z    Boundary code
 NODE             10        -00.000         -0.800       -150.000   1  1  1  0  0  1
 NODE             19        -00.000         -0.800       -100.000
 NODE             20        -00.000         -0.800       -100.000
 NODE             30        -00.000         -0.800        -87.350
 NODE             40        -00.000         -0.800        -66.000
 NODE             50        -00.000         -0.800        -54.000
 NODE             60        -00.000         -0.800        -49.000
 NODE             61        -00.000         -0.800        -38.641
 NODE             62        -00.000         -0.800        -29.707
 NODE             70        -00.000         -0.800        -21.000
 NODE             80        -00.000         -0.800        -14.500
 NODE             90        -00.000         -0.800         -9.000
 NODE            100        -00.000         -0.800          0.920
 NODE            110        -00.000         -0.800          8.000
 NODE            120         -0.000         -0.800         27.281
 NODE            121         -0.000         -0.800         30.738
 NODE            122         -0.000         -0.800         33.701
 NODE            130         -0.000         -0.800         37.158
 NODE            131         -0.000         -0.800         41.603
 NODE            132         -0.000         -0.800         46.047
 NODE            140         -0.000         -0.800         50.492
 NODE            141         -0.000         -0.800         55.431
 NODE            142         -0.000         -0.800         59.200
 NODE            150         -0.000         -0.800         65.308
 NODE            160         -0.000         -0.800         75.185
 NODE            169          0.000         -0.800         90.100
 NODE            170          0.000         -0.800         90.450
 NODE            300          0.000         -0.800         92.450
 NODE            301          0.000         -0.800         94.410
#NODE             400        300.000         -0.800         92.450   0  1 1  1 1 1
#NODE            1111        -14.788         -2.003          9.973
#NODE            1112        -14.791         -2.005          9.975
#NODE            1113        -21.560         -7.232         13.527
#NODE            1121        -14.788          0.403          9.973
#NODE            1122        -14.791          0.405          9.975
#NODE            1123        -21.560          5.632         13.527
#NODE            1169          0.001         -0.800         90.000

'            Elem ID     np1      np2   material   geom    lcoor    ecc1    ecc2
 BEAM          1019       10       19       51      900   ! in PVC in tests! 900 mm diamter 1.4 x 45 thickness
 BEAM          1920       19       20     1200      940
 BEAM          2030       20       30        2    73530
 BEAM          3040       30       40        3    73530
 BEAM          4050       40       50        4    73530
 BEAM          5060       50       60        5   735301
 BEAM          6061       60       61        6     9230
 BEAM          6162       61       62        6     9230
 BEAM          6270       62       70        6     9230
 BEAM          8070       80       70        7   735301
 BEAM          9080       90       80        8     5750
 BEAM        100090      100       90        9     5060
 BEAM        110100      110      100       10     4550
 BEAM        110120      110      120       11     4535
 BEAM        120121      120      121       12     4530
 BEAM        121122      121      122       12     4528
 BEAM        122130      122      130       12     4526
 BEAM        130131      130      131       13     4525
 BEAM        131132      131      132       13     4524
 BEAM        132140      132      140       13     4522
 BEAM        140141      140      141       14     4520
 BEAM        141142      141      142       14     4518
 BEAM        142150      142      150       14     4518
 BEAM        150160      150      160       15     4516
 BEAM        160170      160      170       16     4514
 BEAM        170300      170      300       17     3050
 BEAM        300301      300      301       17      165
'
ElmTrans Loc 2 Elem 1920
'            Geom ID       Do          Thick   (Shear_y   Shear_z      Diam2 )
 PIPE           165       0.165       0.043
 PIPE           250       0.250       0.030
 PIPE           900       0.900       0.0675  ! PVC pipe in tests
 PIPE           940       0.940       0.030
 PIPE          1025       1.000       0.015
 PIPE          2000       2.000       0.025
 PIPE          3050       3.500       0.050
 PIPE          4514       4.500       0.0675   ! Changed al tube   0.014    correct value
```

Figure A-4 USFOS Model File for SWAY, part1

```
 PIPE          4516       4.500       0.0675   ! Changed al tube   0.016
 PIPE          4518       4.500       0.0675   ! Changed Al tube   0.018
 PIPE          4520       4.500       0.0675   ! Changed Al tube   0.020
 PIPE          4522       4.500       0.0675   ! Changed Al tube   0.022
 PIPE          4524       4.500       0.0675   ! Changed Al tube   0.024
 PIPE          4525       4.500       0.0675   ! Changed Al tube   0.025
 PIPE          4526       4.500       0.0675   ! Changed Al tube   0.026
 PIPE          4528       4.500       0.0675   ! Changed Al tube   0.028
 PIPE          4530       4.500       0.0675   ! Changed Al tube   0.030
 PIPE          4535       4.500       0.0675   ! Changed Al tube   0.035
 PIPE          4550       4.500       0.0675     0.00      0.00       5.000 ! Changed Al tube       0.050
 PIPE          5060       5.000       0.0675     0.00      0.00       5.700 ! Changed Al tube       0.060
 PIPE          5750       5.700       0.0675     0.00      0.00       7.350 ! Changed Al tube       0.050
 PIPE          7015       7.000       0.0675   ! Changed Al tube 0.015
 PIPE          7330       7.300       0.0675   ! Changed Al tube 0.030
 PIPE          9030       9.000       0.0675   ! Changed Al tube 0.030
 PIPE          9230       9.200       0.0675   ! Changed Al tube 0.030
 PIPE         70251       7.000       0.0675     0.00      0.00       9.000 ! Changed Al tube   0.025
 PIPE         73301       7.300       0.0675     0.00      0.00       9.000 ! Changed Al tube   0.030
 PIPE         73530       7.350       0.0675   ! Changed Al tube 0.030
 PIPE        735301       7.350       0.0675     0.00      0.00       9.200 ! Changed Al tube 0.030

'            Loc-Coo           dx             dy             dz
'            Ecc-ID            Ex             Ey             Ez
'
'            Mat  ID     E-mod       Poiss      Yield      Density     ThermX
 MISOIEP          1   0.700E+11   3.000E-01   4.000E+08   2.700E+03   0.000E+00
 MISOIEP          2   0.700E+13   3.000E-01   4.000E+18   2.700E+03   0.000E+00
 MISOIEP          3   0.700E+13   3.000E-01   4.000E+18   2.700E+03   0.000E+00
 MISOIEP          4   0.700E+13   3.000E-01   4.000E+18   2.700E+03   0.000E+00
 MISOIEP          5   0.700E+13   3.000E-01   4.000E+18   2.700E+03   0.000E+00
 MISOIEP          6   0.700E+13   3.000E-01   4.000E+18   2.700E+03   0.000E+00
 MISOIEP          7   0.700E+13   3.000E-01   4.000E+18   2.700E+03   0.000E+00
 MISOIEP          8   0.700E+13   3.000E-01   4.000E+18   2.700E+03   0.000E+00
 MISOIEP          9   0.700E+13   3.000E-01   4.000E+18   2.700E+03   0.000E+00
 MISOIEP         10   0.700E+13   3.000E-01   4.000E+18   2.700E+03   0.000E+00
 MISOIEP         11   0.700E+13   3.000E-01   4.000E+18   2.700E+03   0.000E+00
 MISOIEP         12   0.700E+13   3.000E-01   4.000E+18   2.700E+03   0.000E+00
 MISOIEP         13   0.700E+13   3.000E-01   4.000E+18   2.700E+03   0.000E+00
 MISOIEP         14   0.700E+13   3.000E-01   4.000E+18   2.700E+03   0.000E+00
 MISOIEP         15   0.700E+13   3.000E-01   4.000E+18   2.700E+03   0.000E+00
 MISOIEP         16   0.700E+13   3.000E-01   4.000E+08   2.700E+03   0.000E+00
 MISOIEP         17   0.700E+11   3.000E-01   4.000E+08   1.000E+02   0.000E+00
 MISOIEP         20   0.700E+11   3.000E-01   4.000E+08   2.700E+03   0.000E+00
 MISOIEP         30   1.391E+11   3.000E-01   4.000E+08   2.700E+03   1.000E-03
'
' Tension bar in pvc
'
 MISOIEP         51   1.380E+11   3.000E-01   4.000E+08   1.400E+03   1.000E-03
'
'            Mat  ID              P           Delta
 HYPELAST       201
                          -1.00000E+10   -1.00000E+00
                           1.00000E+10    1.00000E+00
 HYPELAST       204
                          -1.00000E+11   -1.00000E+00 ! Forandret fra E+09
                           1.00000E+11    1.00000E+00
 HYPELAST       205
                          -1.00000E+10   -1.00000E+00
                           1.00000E+10    1.00000E+00
 HYPELAST       206
                          -5.00000E+04   -1.00000E+00
                           5.00000E+04    1.00000E+00

'            Mat  ID          S P R I N G    R E F S.
 MREF          1200      204      201      201      205      206      206
'            Node ID               M A S S
 NODEMASS        30              2.19000E+06    2.19000E+06    2.19000E+06
 NODEMASS       300              3.03000E+05    3.03000E+05    3.03000E+05
'
 NodeMass  20   274.805E3 ! Ballast Water. Use Do to match old calc
 NodeMass  30   738.606E3 ! Ballast Water  Use Do to match old calc
 NodeMass  40   463.801E3 ! Ballast Water  Use Do to match old calc
'
'            Load Case   Acc_X       Acc_Y       Acc_Z
 GRAVITY           1  0.0000E+00  0.0000E+00 -9.8100E+00
'
'  *added  mass*
 node 8120    0   -5.3    -100   ! dY = -4.5m
 node 8220    0    3.7    -100   ! dY = +4.5m
 beam 8100   20  8120  8000  8000
 beam 8200   20  8220  8000  8000
 misoiep   8000  210000e6 0.3 1000.0e6  0 0
 pipe      8000  8  0.010
 flooded   8100  8200
 hydropar  Cd    0.0  Elem  8100 8200
 hydropar  Cm    2.0  Elem  8100 8200
```

Figure A-5 USFOS Model File for SWAY, part2

B MATLAB Scripts

MATLAB have been used for calculation of statistical parameters for wave profiles and plotting relevant Gumbel probability papers. This appendix displays the scripts that have been employed.

B.1 Calculation of Statistical Properties

MATLAB has built-in functions that calculate the mean, maximum, minimum, standard deviation, kurtosis, and skewness from a time series. Figure B-1 shows an example where these properties are calculated from a random time series sample for the surface elevation.

```
clear all

% Calculation of statistical parameters for a given time series.

load
C:\Documents\test\time_series_waveelevation\14s\omega_mass\H12_T14_Seed190_omega_waveelevation.txt;


waveelevation=H12_T14_Seed190_omega_waveelevation;

%----------------------------------------

time = waveelevation(:,1);
dt=time(20)-time(19);
n1=round(0.1/dt);
n2=length(time);

disp = waveelevation(:,2);


res(1,1) = mean(disp(n1:n2));
res(1,2) = std(disp(n1:n2));
res(1,3) = kurtosis(disp);
res(1,4) = skewness(disp);
res(1,5) = max(disp(n1:n2));
res(1,6) = min(disp(n1:n2));


format short eng
res;

xlswrite('C:\Users\Ine-Therese\Desktop\MASTER\Matlab\res\H12_T14_Seed190_omega_wave.xls', res,
'resultater');
```

Figure B-1 MATLAB Script for calculation of Statistical Properties

B.2 Gumbel Probability Papers

The MATLAB toolbox, WAFO contains several routines for statistical analysis. Figure B-2 shows the function, *wgumbplot.m* that is used for plotting extremes in a Gumbel probability paper. The last part of the script contains a built-in function that calculates the Gumbel parameters, which has been added manually. From these parameters, the extreme value for a 90 percentile estimate of the distribution is found.

The parameter estimation in *wgumplot()* is done by fitting a straight line to the empirical distribution functions in the diagrams and using the relations to relate parameters to intercept and slopes of the estimated lines. Refer WAFO Tutorial (2000) for more information.

This particular script plots the 20 maximum surface elevations for the equal area method with 30 components, refer Figure 5.1. Desired Gumbel plots of extremes are written into the function manually.

```
function phat = wgumbplot(x)
%WGUMBPLOT Plots data on a Gumbel distribution paper.
%
% CALL:  phat = wgumbplot(X)
%       phat = [a b] Parameters (see wgumbcdf) estimated from the plot by
%              least squares method
%          X = data vector or matrix
% Example:
%   R=wgumbrnd(2,0,[],1,100);
%   phat=wgumbplot(R)

% Reference:
%  Johnson  N.L., Kotz S. and Balakrishnan, N. (1994)
%  Continuous Univariate Distributions, Volume 2. Wiley.
% rewritten ms 20.06.2000

max_30=[8.85
 9.25
 9.53
 8.98
 11.13
 11.18
 9.39
 10.32
 9.30
 11.24
 11.33
 8.93
 9.85
 9.51
 11.54
 9.53
 10.39
 11.32
 9.16
 8.62]

x=max_30

figure(1)
F=empdistr(x,[],0);
plot(F(:,1),-log(-log(F(:,2))),'b.','markersize',12);
U=[ones(size(F(:,1))) F(:,1)];
c=U\(-log(-log(F(:,2))));
a=1/c(2);
b=-c(1)*a;
hold on
plot(F(:,1),U*c,'r--')
hold off
title('Gumbel Plot: Equal Area, 30comp for Surface Elevation')
xlabel('Surface Elevation [m]')
ylabel('-log(-log(F))')
if nargout > 0,
  phat=[a,b]
end

saveas(figure(1),'C:\Users\Ine-
Therese\Desktop\MASTER\Matlab\Gumbelplots\cylinder\static\gumbelplot_surfaceelevation_30.jpg');

gum=wgumbplot(x)
a=gum(1)
b=gum(2)

p=0.90
Extrem_percentile=b+(-log(-log(p)))*a
```

C Results from Analyses on Fixed Cylinder

This appendix shows all wave load results from the static and dynamic analysis performed on the fixed cylinder together with statistical parameters for the surface elevation.

C.1 Statistical parameters for Surface Elevation

Table C-1 to Table C-4 gives a total overview of the statistical parameters for each sample in the static analysis. Since similar observations are observed for the dynamic analysis, one finds it adequate to only show the parameters for the static analysis.

Table C-1 Statistical parameters for surface elevation with EAP with 30 components

Sample	Name	Mean	Standard Deviaton	Kurtosis	Skewness	Max (MATLAB)	Min (MATLAB)	Max (USFOS)
1	H12_T14_Seed000_30_waveelevation	-0,00	2,98	2,48	-0,03	8,85	-7,69	8,85
2	H12_T14_Seed010_30_waveelevation	0,00	2,99	2,73	-0,11	8,36	-9,25	9,25
3	H12_T14_Seed020_30_waveelevation	-0,00	3,10	2,71	-0,04	8,93	-9,53	9,53
4	H12_T14_Seed030_30_waveelevation	-0,00	2,95	2,66	0,09	8,89	-8,98	8,98
5	H12_T14_Seed040_30_waveelevation	0,01	3,04	3,04	0,08	11,13	-10,21	11,13
6	H12_T14_Seed050_30_waveelevation	-0,01	3,06	3,28	0,09	11,18	-10,34	11,18
7	H12_T14_Seed060_30_waveelevation	-0,01	3,06	2,73	-0,04	9,39	-9,10	9,39
8	H12_T14_Seed070_30_waveelevation	0,02	2,97	3,16	-0,01	9,33	-10,32	10,32
9	H12_T14_Seed080_30_waveelevation	0,00	3,05	2,65	-0,05	9,30	-9,25	9,30
10	H12_T14_Seed090_30_waveelevation	0,01	3,01	2,94	0,03	11,24	-9,65	11,24
11	H12_T14_Seed100_30_waveelevation	-0,00	3,07	3,26	-0,09	10,21	-11,33	11,33
12	H12_T14_Seed110_30_waveelevation	-0,01	2,85	2,88	-0,01	8,93	-8,23	8,93
13	H12_T14_Seed120_30_waveelevation	0,01	3,01	2,85	0,03	9,85	-8,40	9,85
14	H12_T14_Seed130_30_waveelevation	0,01	2,94	2,73	0,05	9,51	-8,68	9,51
15	H12_T14_Seed140_30_waveelevation	0,00	2,92	3,44	0,11	11,54	-10,49	11,54
16	H12_T14_Seed150_30_waveelevation	-0,01	2,99	2,87	-0,07	9,46	-9,53	9,53
17	H12_T14_Seed160_30_waveelevation	-0,00	2,98	2,95	-0,01	10,14	-10,39	10,39
18	H12_T14_Seed170_30_waveelevation	-0,00	2,95	3,47	0,10	11,32	-10,21	11,32
19	H12_T14_Seed180_30_waveelevation	0,01	2,88	3,03	-0,07	7,90	-9,16	9,16
20	H12_T14_Seed190_30_waveelevation	0,01	3,02	2,64	0,05	8,62	-8,11	8,62
	Max	0,02	3,10	3,47	0,11	11,54	-7,69	11,54
	Min	-0,01	2,85	2,48	-0,11	7,90	-11,33	8,62
	Standard Deviation	0,01	0,06	0,28	0,07	1,09	0,94	0,99
	Mean	**0,00**	**2,99**	**2,92**	**0,01**	**9,70**	**-9,44**	**9,97**

Table C-2 Statistical parameters for surface elevation with EAP with 60 components

Sample	Name	Mean	Standard Deviaton	Kurtosis	Skewness	Max (MATLAB)	Min (MATLAB)	Max (USFOS)
1	H12_T14_Seed000_60_waveelevation	0,00	2,86	2,70	-0,06	9,63	-8,16	9,63
2	H12_T14_Seed010_60_waveelevation	-0,01	2,84	2,71	0,04	8,71	-7,54	8,71
3	H12_T14_Seed020_60_waveelevation	0,00	3,02	2,62	0,04	7,91	-9,39	9,39
4	H12_T14_Seed030_60_waveelevation	0,00	2,86	2,88	0,15	9,48	-8,19	9,48
5	H12_T14_Seed040_60_waveelevation	-0,01	3,04	2,76	-0,00	9,45	-11,00	11,00
6	H12_T14_Seed050_60_waveelevation	0,01	3,02	3,21	0,07	10,96	-10,25	10,96
7	H12_T14_Seed060_60_waveelevation	-0,00	3,12	3,01	0,03	11,09	-8,92	11,09
8	H12_T14_Seed070_60_waveelevation	-0,01	2,94	2,48	0,07	8,55	-7,33	8,55
9	H12_T14_Seed080_60_waveelevation	0,01	2,90	2,97	0,11	10,72	-9,30	10,72
10	H12_T14_Seed090_60_waveelevation	-0,01	2,92	3,10	0,03	9,08	-9,60	9,60
11	H12_T14_Seed100_60_waveelevation	-0,01	2,98	2,71	0,08	9,60	-7,77	9,60
12	H12_T14_Seed110_60_waveelevation	-0,00	3,06	2,88	0,05	9,91	-9,86	9,91
13	H12_T14_Seed120_60_waveelevation	0,00	2,97	2,82	-0,16	8,26	-9,85	9,85
14	H12_T14_Seed130_60_waveelevation	-0,00	3,16	3,02	-0,06	8,88	-10,49	10,49
15	H12_T14_Seed140_60_waveelevation	0,00	3,06	2,83	0,04	9,67	-10,44	10,44
16	H12_T14_Seed150_60_waveelevation	-0,00	2,95	3,73	0,02	9,95	-11,01	11,01
17	H12_T14_Seed160_60_waveelevation	-0,00	2,80	3,24	-0,00	8,22	-10,09	10,09
18	H12_T14_Seed170_60_waveelevation	0,01	2,98	2,74	0,08	8,36	-8,17	8,36
19	H12_T14_Seed180_60_waveelevation	-0,00	2,69	2,87	-0,09	8,09	-8,99	8,99
20	H12_T14_Seed190_60_waveelevation	-0,01	2,77	3,00	-0,11	7,90	-8,79	8,79
	Max	0,01	3,16	3,73	0,15	11,09	-7,33	11,09
	Min	-0,01	2,69	2,48	-0,16	7,90	-11,01	8,36
	Standard Deviation	0,01	0,12	0,27	0,08	0,99	1,13	0,88
	Mean	**-0,00**	**2,95**	**2,92**	**0,02**	**9,22**	**-9,26**	**9,83**

Table C-3 Statistical parameters for surface elevation with EAP with 90 components

Sample	Name	Mean	Standard Deviaton	Kurtosis	Skewness	Max (MATLAB)	Min (MATLAB)	Max (USFOS)
1	H12_T14_Seed000_90_waveelevation	-0,01	2,89	2,75	0,05	9,36	-7,82	9,36
2	H12_T14_Seed010_90_waveelevation	0,01	2,92	3,09	0,07	9,08	-9,52	9,52
3	H12_T14_Seed020_90_waveelevation	0,00	3,09	3,08	-0,02	9,42	-10,50	10,50
4	H12_T14_Seed030_90_waveelevation	0,01	3,08	2,92	0,05	10,71	-8,54	10,71
5	H12_T14_Seed040_90_waveelevation	-0,01	3,07	2,67	-0,05	9,34	-10,10	10,10
6	H12_T14_Seed050_90_waveelevation	-0,02	3,03	3,38	0,01	10,43	-10,64	10,64
7	H12_T14_Seed060_90_waveelevation	-0,01	3,15	3,12	-0,02	9,64	-9,69	9,69
8	H12_T14_Seed070_90_waveelevation	-0,00	2,94	2,74	-0,01	8,56	-10,41	10,41
9	H12_T14_Seed080_90_waveelevation	0,00	2,99	2,84	0,08	8,89	-8,29	8,89
10	H12_T14_Seed090_90_waveelevation	0,01	2,88	2,97	-0,02	9,48	-9,02	9,48
11	H12_T14_Seed100_90_waveelevation	0,00	3,12	2,96	-0,06	9,79	-9,27	9,79
12	H12_T14_Seed110_90_waveelevation	0,00	2,93	2,66	-0,09	7,48	-8,11	8,11
13	H12_T14_Seed120_90_waveelevation	0,00	2,96	2,90	-0,03	8,88	-9,49	9,49
14	H12_T14_Seed130_90_waveelevation	0,01	2,91	3,11	0,02	10,60	-9,40	10,60
15	H12_T14_Seed140_90_waveelevation	-0,00	2,95	2,65	-0,11	7,84	-8,84	8,84
16	H12_T14_Seed150_90_waveelevation	-0,01	2,95	2,93	-0,01	8,84	-9,20	9,20
17	H12_T14_Seed160_90_waveelevation	0,01	2,83	3,39	0,13	11,90	-8,97	11,90
18	H12_T14_Seed170_90_waveelevation	-0,00	2,87	2,88	0,06	9,71	-8,42	9,71
19	H12_T14_Seed180_90_waveelevation	0,00	2,89	2,84	0,09	8,74	-8,15	8,74
20	H12_T14_Seed190_90_waveelevation	0,00	2,92	2,76	0,16	9,42	-8,27	9,42
	Max	0,01	3,15	3,39	0,16	11,90	-7,82	11,90
	Min	-0,02	2,83	2,65	-0,11	7,48	-10,64	8,11
	Standard Deviation	0,01	0,09	0,21	0,07	1,00	0,85	0,87
	Mean	**0,00**	**2,97**	**2,93**	**0,02**	**9,40**	**-9,13**	**9,75**

Table C-4 Statistical parameters for surface elevation with FFT with 1000 components

Sample	Name	Mean	Standard Deviaton	Kurtosis	Skewness	Max (MATLAB)	Min (MATLAB)	Max (USFOS)
1	H12_T14_Seed000_omega_waveelevation	0,00	2,85	2,64	-0,01	7,89	-8,01	8,01
2	H12_T14_Seed010_omega_waveelevation	0,00	3,06	2,89	0,03	9,87	-9,15	9,87
3	H12_T14_Seed020_omega_waveelevation	-0,00	3,17	2,89	0,01	9,66	-9,40	9,66
4	H12_T14_Seed030_omega_waveelevation	-0,00	2,90	2,68	0,08	9,13	-8,24	9,13
5	H12_T14_Seed040_omega_waveelevation	0,01	2,98	2,68	-0,05	9,60	-8,35	9,60
6	H12_T14_Seed050_omega_waveelevation	-0,01	3,01	2,77	0,01	8,28	-9,24	9,24
7	H12_T14_Seed060_omega_waveelevation	-0,01	3,13	2,74	-0,05	9,35	-9,36	9,36
8	H12_T14_Seed070_omega_waveelevation	-0,01	2,88	2,70	-0,08	7,95	-8,05	8,05
9	H12_T14_Seed080_omega_waveelevation	0,00	2,80	2,64	-0,07	7,71	-7,71	7,71
10	H12_T14_Seed090_omega_waveelevation	-0,01	2,87	2,75	-0,06	8,04	-8,02	8,04
11	H12_T14_Seed100_omega_waveelevation	-0,01	2,97	2,65	-0,05	8,76	-8,31	8,76
12	H12_T14_Seed110_omega_waveelevation	-0,00	3,12	2,70	0,06	9,08	-9,73	9,73
13	H12_T14_Seed120_omega_waveelevation	-0,00	3,26	2,96	0,01	9,48	-9,64	9,64
14	H12_T14_Seed130_omega_waveelevation	-0,01	3,24	2,85	0,00	10,09	-10,05	10,09
15	H12_T14_Seed140_omega_waveelevation	0,01	3,12	2,71	0,01	8,71	-9,83	9,83
16	H12_T14_Seed150_omega_waveelevation	-0,01	2,91	2,64	-0,05	8,15	-8,23	8,23
17	H12_T14_Seed160_omega_waveelevation	-0,00	2,94	2,58	0,06	8,47	-8,67	8,67
18	H12_T14_Seed170_omega_waveelevation	-0,01	2,94	2,83	-0,02	9,94	-8,60	9,94
19	H12_T14_Seed180_omega_waveelevation	-0,01	2,88	2,57	-0,09	7,68	-8,24	8,24
20	H12_T14_Seed190_omega_waveelevation	-0,01	2,86	2,67	0,03	7,74	-8,17	8,17
	Max	0,01	3,26	2,96	0,08	10,09	-7,71	10,09
	Min	-0,01	2,80	2,57	-0,09	7,68	-10,05	7,71
	Standard Deviation	0,01	0,14	0,11	0,05	0,82	0,72	0,79
	Mean	**-0,00**	**2,99**	**2,73**	**-0,01**	**8,78**	**-8,75**	**9,00**

C.2 Wave Load Results from Static Analysis

Overview of wave loads on the fixed cylinder for each sample is given in Table 6-5 and Table C-6.

Table C-5 Mass dominated Wave Loads on fixed Cylinder for all Samples

Sample Name	FFT, 1000 comp	EAP, 30 comp	EAP, 60 comp	EAP, 90 comp	Force
H=12.0_T=14_Seed=000.max: PeakValue for DynRes 2 :	7,37E+06	7,65E+06	7,49E+06	8,02E+06	[N]
H=12.0_T=14_Seed=010.max: PeakValue for DynRes 2 :	9,64E+06	8,86E+06	8,63E+06	8,33E+06	[N]
H=12.0_T=14_Seed=020.max: PeakValue for DynRes 2 :	8,58E+06	8,95E+06	8,00E+06	9,52E+06	[N]
H=12.0_T=14_Seed=030.max: PeakValue for DynRes 2 :	7,83E+06	7,58E+06	9,01E+06	9,72E+06	[N]
H=12.0_T=14_Seed=040.max: PeakValue for DynRes 2 :	7,94E+06	9,98E+06	8,78E+06	8,54E+06	[N]
H=12.0_T=14_Seed=050.max: PeakValue for DynRes 2 :	8,12E+06	9,39E+06	9,54E+06	9,60E+06	[N]
H=12.0_T=14_Seed=060.max: PeakValue for DynRes 2 :	8,93E+06	8,49E+06	8,54E+06	9,19E+06	[N]
H=12.0_T=14_Seed=070.max: PeakValue for DynRes 2 :	7,59E+06	9,73E+06	8,24E+06	8,35E+06	[N]
H=12.0_T=14_Seed=080.max: PeakValue for DynRes 2 :	7,14E+06	7,98E+06	9,59E+06	7,90E+06	[N]
H=12.0_T=14_Seed=090.max: PeakValue for DynRes 2 :	7,16E+06	9,22E+06	8,45E+06	9,07E+06	[N]
H=12.0_T=14_Seed=100.max: PeakValue for DynRes 2 :	8,45E+06	9,49E+06	8,37E+06	9,19E+06	[N]
H=12.0_T=14_Seed=110.max: PeakValue for DynRes 2 :	8,54E+06	7,71E+06	9,38E+06	8,09E+06	[N]
H=12.0_T=14_Seed=120.max: PeakValue for DynRes 2 :	9,18E+06	9,56E+06	9,37E+06	9,02E+06	[N]
H=12.0_T=14_Seed=130.max: PeakValue for DynRes 2 :	9,29E+06	7,26E+06	9,18E+06	8,34E+06	[N]
H=12.0_T=14_Seed=140.max: PeakValue for DynRes 2 :	8,55E+06	9,25E+06	8,28E+06	7,60E+06	[N]
H=12.0_T=14_Seed=150.max: PeakValue for DynRes 2 :	8,12E+06	1,09E+07	8,61E+06	7,58E+06	[N]
H=12.0_T=14_Seed=160.max: PeakValue for DynRes 2 :	7,33E+06	8,45E+06	9,34E+06	9,68E+06	[N]
H=12.0_T=14_Seed=170.max: PeakValue for DynRes 2 :	8,05E+06	1,08E+07	8,54E+06	8,33E+06	[N]
H=12.0_T=14_Seed=180.max: PeakValue for DynRes 2 :	6,92E+06	8,00E+06	7,81E+06	8,52E+06	[N]
H=12.0_T=14_Seed=190.max: PeakValue for DynRes 2 :	7,16E+06	8,59E+06	8,01E+06	9,98E+06	[N]
Standard Deviation	7,93E+05	1,03E+06	6,06E+05	7,38E+05	[N]
Mean	**8,09E+06**	**8,89E+06**	**8,66E+06**	**8,73E+06**	[N]

Table C-6 Drag dominated Wave Loads on fixed Cylinder for all Samples

Sample Name	FFT, 1000 comp	EAP, 30 comp	EAP, 60 comp	EAP, 90 comp	Force
H=12.0_T=14_Seed=000.max: PeakValue for DynRes 2 :	1,40E+05	1,60E+05	1,82E+05	1,83E+05	[N]
H=12.0_T=14_Seed=010.max: PeakValue for DynRes 2 :	1,91E+05	1,98E+05	1,71E+05	1,85E+05	[N]
H=12.0_T=14_Seed=020.max: PeakValue for DynRes 2 :	1,94E+05	1,79E+05	1,72E+05	2,20E+05	[N]
H=12.0_T=14_Seed=030.max: PeakValue for DynRes 2 :	1,61E+05	1,69E+05	1,99E+05	2,31E+05	[N]
H=12.0_T=14_Seed=040.max: PeakValue for DynRes 2 :	1,91E+05	2,47E+05	2,24E+05	1,99E+05	[N]
H=12.0_T=14_Seed=050.max: PeakValue for DynRes 2 :	1,66E+05	2,46E+05	2,16E+05	2,28E+05	[N]
H=12.0_T=14_Seed=060.max: PeakValue for DynRes 2 :	1,72E+05	1,71E+05	2,27E+05	2,00E+05	[N]
H=12.0_T=14_Seed=070.max: PeakValue for DynRes 2 :	1,45E+05	2,00E+05	1,62E+05	2,22E+05	[N]
H=12.0_T=14_Seed=080.max: PeakValue for DynRes 2 :	1,40E+05	1,73E+05	2,21E+05	1,60E+05	[N]
H=12.0_T=14_Seed=090.max: PeakValue for DynRes 2 :	1,46E+05	2,46E+05	1,79E+05	1,86E+05	[N]
H=12.0_T=14_Seed=100.max: PeakValue for DynRes 2 :	1,48E+05	2,38E+05	1,98E+05	2,08E+05	[N]
H=12.0_T=14_Seed=110.max: PeakValue for DynRes 2 :	1,84E+05	1,63E+05	2,16E+05	1,42E+05	[N]
H=12.0_T=14_Seed=120.max: PeakValue for DynRes 2 :	1,80E+05	2,07E+05	2,18E+05	1,89E+05	[N]
H=12.0_T=14_Seed=130.max: PeakValue for DynRes 2 :	2,22E+05	1,85E+05	2,04E+05	2,20E+05	[N]
H=12.0_T=14_Seed=140.max: PeakValue for DynRes 2 :	1,99E+05	2,54E+05	2,13E+05	1,68E+05	[N]
H=12.0_T=14_Seed=150.max: PeakValue for DynRes 2 :	1,54E+05	2,18E+05	2,28E+05	1,78E+05	[N]
H=12.0_T=14_Seed=160.max: PeakValue for DynRes 2 :	1,48E+05	1,97E+05	2,00E+05	2,52E+05	[N]
H=12.0_T=14_Seed=170.max: PeakValue for DynRes 2 :	2,05E+05	2,28E+05	1,46E+05	1,94E+05	[N]
H=12.0_T=14_Seed=180.max: PeakValue for DynRes 2 :	1,42E+05	1,70E+05	1,54E+05	1,68E+05	[N]
H=12.0_T=14_Seed=190.max: PeakValue for DynRes 2 :	1,45E+05	1,54E+05	1,67E+05	2,05E+05	[N]
Standard Deviation	2,52E+04	3,33E+04	2,61E+04	2,71E+04	[N]
Mean	**1,69E+05**	**2,00E+05**	**1,95E+05**	**1,97E+05**	**[N]**

C.3 Results from Dynamic Analysis

The dynamic analyses on the fixed cylinder were performed three times with varying natural period. The wave loads were both mass – and drag dominated. Following tables shows the results for all these analyses, and is divided into subchapters for each of the natural periods.

C.3.1 Results when T_n=4.4s

Table C-7 Mass dominated wave loads and OVTM when Tn=4.4s

Case	Mass dominated wave loads [N]				Overturning Moment [Nm]			
	FFT	EAP, 30comp	EAP, 60comp	EAP, 90comp	FFT	EAP, 30comp	EAP, 60comp	EAP, 90comp
H12_T14_Seed000.max: PeakValue for DynRes	8,11E+06	1,04E+07	8,62E+06	8,02E+06	1,38E+09	1,06E+09	8,67E+08	7,82E+08
H12_T14_Seed010.max: PeakValue for DynRes	7,86E+06	8,86E+06	8,05E+06	9,39E+06	1,09E+09	8,51E+08	8,15E+08	9,10E+08
H12_T14_Seed020.max: PeakValue for DynRes	8,33E+06	8,98E+06	8,83E+06	8,54E+06	1,30E+09	9,76E+08	9,52E+08	7,20E+08
H12_T14_Seed030.max: PeakValue for DynRes	8,80E+06	9,73E+06	8,87E+06	9,77E+06	1,23E+09	9,37E+08	9,19E+08	8,67E+08
H12_T14_Seed040.max: PeakValue for DynRes	8,31E+06	9,31E+06	8,80E+06	7,21E+06	1,13E+09	1,04E+09	9,95E+08	7,22E+08
H12_T14_Seed050.max: PeakValue for DynRes	8,21E+06	8,84E+06	9,53E+06	1,03E+07	1,36E+09	1,01E+09	1,05E+09	1,39E+09
H12_T14_Seed060.max: PeakValue for DynRes	7,61E+06	8,89E+06	8,52E+06	8,99E+06	1,01E+09	7,86E+08	1,07E+09	8,36E+08
H12_T14_Seed070.max: PeakValue for DynRes	7,15E+06	9,73E+06	9,10E+06	8,40E+06	1,23E+09	9,75E+08	9,01E+08	7,49E+08
H12_T14_Seed080.max: PeakValue for DynRes	7,04E+06	8,44E+06	7,56E+06	1,05E+07	1,29E+09	9,40E+08	8,85E+08	9,19E+08
H12_T14_Seed090.max: PeakValue for DynRes	6,99E+06	9,28E+06	7,85E+06	7,60E+06	1,21E+09	8,94E+08	8,97E+08	7,76E+08
H12_T14_Seed100.max: PeakValue for DynRes	8,59E+06	8,32E+06	8,08E+06	1,04E+07	1,14E+09	1,01E+09	7,21E+08	1,07E+09
H12_T14_Seed110.max: PeakValue for DynRes	8,01E+06	7,60E+06	9,41E+06	9,53E+06	1,18E+09	9,84E+08	8,56E+08	9,49E+08
H12_T14_Seed120.max: PeakValue for DynRes	8,64E+06	7,59E+06	9,13E+06	9,06E+06	1,30E+09	8,64E+08	1,00E+09	8,42E+08
H12_T14_Seed130.max: PeakValue for DynRes	9,33E+06	8,07E+06	9,29E+06	1,00E+07	1,13E+09	8,30E+08	9,16E+08	9,99E+08
H12_T14_Seed140.max: PeakValue for DynRes	7,95E+06	8,01E+06	8,09E+06	8,41E+06	1,18E+09	1,02E+09	8,33E+08	7,75E+08
H12_T14_Seed150.max: PeakValue for DynRes	8,24E+06	1,06E+07	8,63E+06	9,92E+06	1,23E+09	9,26E+08	9,06E+08	9,97E+08
H12_T14_Seed160.max: PeakValue for DynRes	8,99E+06	9,96E+06	7,80E+06	9,29E+06	1,42E+09	1,12E+09	7,98E+08	9,26E+08
H12_T14_Seed170.max: PeakValue for DynRes	8,24E+06	9,01E+06	8,54E+06	7,67E+06	1,17E+09	1,09E+09	8,98E+08	7,63E+08
H12_T14_Seed180.max: PeakValue for DynRes	8,57E+06	8,35E+06	8,86E+06	9,97E+06	1,38E+09	8,23E+08	1,06E+09	1,10E+09
H12_T14_Seed190.max: PeakValue for DynRes	8,11E+06	7,48E+06	9,25E+06	1,01E+07	1,28E+09	8,46E+08	8,71E+08	8,16E+08
Standard Deviation	6,17E+05	9,11E+05	5,76E+05	1,00E+06	1,07E+08	9,59E+07	9,09E+07	1,62E+08
Mean	**8,15E+06**	**8,87E+06**	**8,64E+06**	**9,15E+06**	**1,23E+09**	**9,50E+08**	**9,11E+08**	**8,95E+08**

Table C-8 Drag dominated wave loads and OVTM when Tn=4.4s

Case	Drag dominated wave loads [N]				Overturning Moment [Nm]			
	FFT	EAP, 30comp	EAP, 60comp	EAP, 90comp	FFT	EAP, 30comp	EAP, 60comp	EAP, 90comp
H12_T14_Seed000.max: PeakValue for DynRes	1,63E+05	2,72E+05	1,76E+05	1,55E+05	2,36E+07	3,71E+07	2,20E+07	1,89E+07
H12_T14_Seed010.max: PeakValue for DynRes	1,58E+05	1,96E+05	2,05E+05	2,45E+05	2,20E+07	2,19E+07	2,42E+07	2,71E+07
H12_T14_Seed020.max: PeakValue for DynRes	1,62E+05	1,82E+05	1,72E+05	1,80E+05	2,07E+07	2,18E+07	2,31E+07	1,78E+07
H12_T14_Seed030.max: PeakValue for DynRes	2,12E+05	2,26E+05	2,01E+05	2,28E+05	3,24E+07	2,12E+07	2,36E+07	2,22E+07
H12_T14_Seed040.max: PeakValue for DynRes	1,66E+05	2,04E+05	2,40E+05	1,62E+05	2,34E+07	3,36E+07	2,40E+07	1,77E+07
H12_T14_Seed050.max: PeakValue for DynRes	1,68E+05	1,84E+05	2,34E+05	2,33E+05	2,12E+07	2,30E+07	2,63E+07	3,28E+07
H12_T14_Seed060.max: PeakValue for DynRes	1,69E+05	1,64E+05	2,14E+05	1,99E+05	2,02E+07	1,74E+07	2,69E+07	2,04E+07
H12_T14_Seed070.max: PeakValue for DynRes	1,39E+05	2,25E+05	2,09E+05	2,30E+05	1,98E+07	3,35E+07	2,49E+07	1,67E+07
H12_T14_Seed080.max: PeakValue for DynRes	1,42E+05	1,59E+05	2,07E+05	2,52E+05	2,26E+07	1,70E+07	2,11E+07	2,55E+07
H12_T14_Seed090.max: PeakValue for DynRes	1,47E+05	2,54E+05	1,71E+05	1,66E+05	2,05E+07	2,17E+07	3,17E+07	2,65E+07
H12_T14_Seed100.max: PeakValue for DynRes	1,81E+05	2,35E+05	1,44E+05	2,92E+05	2,78E+07	2,64E+07	1,68E+07	2,70E+07
H12_T14_Seed110.max: PeakValue for DynRes	1,56E+05	1,84E+05	1,76E+05	2,33E+05	2,29E+07	2,39E+07	1,93E+07	1,77E+07
H12_T14_Seed120.max: PeakValue for DynRes	1,82E+05	1,47E+05	1,95E+05	1,93E+05	2,29E+07	2,32E+07	2,55E+07	1,91E+07
H12_T14_Seed130.max: PeakValue for DynRes	2,14E+05	1,59E+05	2,09E+05	3,18E+05	2,28E+07	1,88E+07	1,88E+07	2,68E+07
H12_T14_Seed140.max: PeakValue for DynRes	1,90E+05	1,81E+05	1,61E+05	1,78E+05	2,46E+07	2,31E+07	1,91E+07	1,85E+07
H12_T14_Seed150.max: PeakValue for DynRes	1,78E+05	2,30E+05	2,34E+05	2,46E+05	2,33E+07	2,18E+07	2,19E+07	3,29E+07
H12_T14_Seed160.max: PeakValue for DynRes	2,09E+05	2,38E+05	1,40E+05	2,13E+05	2,58E+07	2,78E+07	2,15E+07	2,20E+07
H12_T14_Seed170.max: PeakValue for DynRes	1,88E+05	2,22E+05	1,78E+05	1,50E+05	1,97E+07	2,96E+07	2,25E+07	2,03E+07
H12_T14_Seed180.max: PeakValue for DynRes	2,04E+05	1,72E+05	2,41E+05	3,14E+05	2,61E+07	1,90E+07	2,64E+07	2,82E+07
H12_T14_Seed190.max: PeakValue for DynRes	1,60E+05	1,67E+05	1,89E+05	2,13E+05	2,22E+07	2,09E+07	2,83E+07	1,76E+07
Standard Deviation	2,30E+04	3,55E+04	2,99E+04	4,94E+04	3,05E+06	5,56E+06	3,59E+06	5,16E+06
Mean	**1,74E+05**	**2,00E+05**	**1,95E+05**	**2,20E+05**	**2,32E+07**	**2,41E+07**	**2,34E+07**	**2,28E+07**

C.3.2 Results when T_n=8.5s

Table C-9 Mass dominated wave loads and OVTM when Tn=8.5s

Case	Mass dominated wave loads [N]				Overturning Moment [Nm]			
	FFT	EAP, 30comp	EAP, 60comp	EAP, 90comp	FFT	EAP, 30comp	EAP, 60comp	EAP, 90comp
H12_T14_Seed000.max: PeakValue for DynRes	8,11E+06	1,04E+07	8,61E+06	8,18E+06	2,98E+09	2,17E+09	2,31E+09	2,52E+09
H12_T14_Seed010.max: PeakValue for DynRes	7,84E+06	8,92E+06	8,03E+06	9,45E+06	2,56E+09	1,88E+09	2,32E+09	2,27E+09
H12_T14_Seed020.max: PeakValue for DynRes	8,32E+06	8,92E+06	8,83E+06	8,46E+06	2,49E+09	1,93E+09	2,21E+09	2,60E+09
H12_T14_Seed030.max: PeakValue for DynRes	8,88E+06	9,77E+06	9,04E+06	9,77E+06	2,04E+09	2,26E+09	2,57E+09	2,55E+09
H12_T14_Seed040.max: PeakValue for DynRes	8,30E+06	9,30E+06	8,85E+06	7,18E+06	2,56E+09	2,06E+09	2,57E+09	2,34E+09
H12_T14_Seed050.max: PeakValue for DynRes	8,28E+06	8,80E+06	9,53E+06	1,06E+07	2,43E+09	2,33E+09	2,37E+09	2,83E+09
H12_T14_Seed060.max: PeakValue for DynRes	7,61E+06	8,77E+06	8,75E+06	8,99E+06	2,12E+09	1,97E+09	2,69E+09	2,56E+09
H12_T14_Seed070.max: PeakValue for DynRes	6,95E+06	9,75E+06	9,05E+06	8,34E+06	2,81E+09	2,01E+09	2,91E+09	2,65E+09
H12_T14_Seed080.max: PeakValue for DynRes	7,09E+06	8,45E+06	7,56E+06	1,05E+07	2,82E+09	2,15E+09	2,41E+09	2,58E+09
H12_T14_Seed090.max: PeakValue for DynRes	6,97E+06	9,11E+06	7,76E+06	7,65E+06	2,99E+09	2,13E+09	2,28E+09	3,02E+09
H12_T14_Seed100.max: PeakValue for DynRes	8,58E+06	8,32E+06	8,05E+06	1,04E+07	2,25E+09	2,04E+09	2,50E+09	2,90E+09
H12_T14_Seed110.max: PeakValue for DynRes	8,04E+06	7,63E+06	9,36E+06	9,47E+06	2,33E+09	1,96E+09	2,61E+09	2,62E+09
H12_T14_Seed120.max: PeakValue for DynRes	8,63E+06	7,63E+06	9,09E+06	9,03E+06	2,57E+09	2,00E+09	2,18E+09	2,16E+09
H12_T14_Seed130.max: PeakValue for DynRes	9,29E+06	8,06E+06	9,30E+06	1,00E+07	2,49E+09	2,00E+09	2,33E+09	2,96E+09
H12_T14_Seed140.max: PeakValue for DynRes	7,92E+06	7,92E+06	8,10E+06	8,45E+06	2,42E+09	2,04E+09	2,53E+09	2,54E+09
H12_T14_Seed150.max: PeakValue for DynRes	8,21E+06	1,06E+07	8,61E+06	9,82E+06	2,55E+09	2,08E+09	2,40E+09	2,70E+09
H12_T14_Seed160.max: PeakValue for DynRes	8,99E+06	9,99E+06	7,84E+06	9,24E+06	2,60E+09	2,72E+09	2,33E+09	2,71E+09
H12_T14_Seed170.max: PeakValue for DynRes	8,49E+06	9,06E+06	8,44E+06	7,59E+06	2,83E+09	1,82E+09	2,34E+09	2,70E+09
H12_T14_Seed180.max: PeakValue for DynRes	8,53E+06	8,36E+06	8,80E+06	9,96E+06	2,81E+09	2,05E+09	2,48E+09	3,15E+09
H12_T14_Seed190.max: PeakValue for DynRes	8,09E+06	7,47E+06	9,32E+06	1,01E+07	2,97E+09	1,82E+09	2,30E+09	2,68E+09
Standard Deviation	6,36E+05	9,07E+05	5,85E+05	1,02E+06	2,76E+08	2,01E+08	1,77E+08	2,44E+08
Mean	**8,16E+06**	**8,86E+06**	**8,65E+06**	**9,16E+06**	**2,58E+09**	**2,07E+09**	**2,43E+09**	**2,65E+09**

Table C-10 Drag dominated wave loads and OVTM when Tn=8.5s

Case	Drag dominated wave loads [N]				Overturning Moment [Nm]			
	FFT	EAP, 30comp	EAP, 60comp	EAP, 90comp	FFT	EAP, 30comp	EAP, 60comp	EAP, 90comp
H12_T14_Seed000.max: PeakValue for DynRes	1,66E+05	2,31E+05	1,58E+05	1,47E+05	4,35E+07	5,62E+07	4,31E+07	3,91E+07
H12_T14_Seed010.max: PeakValue for DynRes	1,56E+05	1,98E+05	2,23E+05	2,70E+05	3,66E+07	3,62E+07	4,18E+07	3,55E+07
H12_T14_Seed020.max: PeakValue for DynRes	1,68E+05	1,71E+05	1,78E+05	1,63E+05	3,62E+07	3,52E+07	3,55E+07	4,37E+07
H12_T14_Seed030.max: PeakValue for DynRes	2,10E+05	2,05E+05	1,93E+05	2,18E+05	4,28E+07	4,27E+07	3,87E+07	4,27E+07
H12_T14_Seed040.max: PeakValue for DynRes	1,67E+05	1,80E+05	2,10E+05	1,43E+05	3,96E+07	4,02E+07	5,06E+07	3,69E+07
H12_T14_Seed050.max: PeakValue for DynRes	1,73E+05	2,01E+05	2,11E+05	2,50E+05	3,91E+07	4,14E+07	4,46E+07	4,45E+07
H12_T14_Seed060.max: PeakValue for DynRes	1,76E+05	1,62E+05	2,36E+05	1,95E+05	3,46E+07	3,08E+07	4,02E+07	4,14E+07
H12_T14_Seed070.max: PeakValue for DynRes	1,36E+05	2,07E+05	1,95E+05	2,06E+05	4,09E+07	3,99E+07	4,73E+07	4,25E+07
H12_T14_Seed080.max: PeakValue for DynRes	1,37E+05	1,61E+05	1,92E+05	2,27E+05	4,61E+07	3,43E+07	3,89E+07	4,77E+07
H12_T14_Seed090.max: PeakValue for DynRes	1,47E+05	2,36E+05	1,75E+05	1,58E+05	4,26E+07	3,83E+07	4,01E+07	4,61E+07
H12_T14_Seed100.max: PeakValue for DynRes	1,97E+05	2,25E+05	1,40E+05	2,84E+05	3,60E+07	3,18E+07	3,86E+07	4,85E+07
H12_T14_Seed110.max: PeakValue for DynRes	1,67E+05	1,74E+05	1,55E+05	2,10E+05	3,83E+07	3,99E+07	4,55E+07	4,41E+07
H12_T14_Seed120.max: PeakValue for DynRes	1,78E+05	1,45E+05	2,30E+05	1,92E+05	3,70E+07	3,54E+07	4,01E+07	3,48E+07
H12_T14_Seed130.max: PeakValue for DynRes	2,13E+05	1,70E+05	2,11E+05	2,89E+05	3,94E+07	3,52E+07	3,92E+07	5,27E+07
H12_T14_Seed140.max: PeakValue for DynRes	1,91E+05	1,77E+05	1,49E+05	1,67E+05	4,23E+07	3,48E+07	4,01E+07	3,67E+07
H12_T14_Seed150.max: PeakValue for DynRes	1,97E+05	2,15E+05	2,18E+05	2,35E+05	4,16E+07	3,25E+07	4,15E+07	5,30E+07
H12_T14_Seed160.max: PeakValue for DynRes	2,13E+05	2,52E+05	1,35E+05	1,93E+05	4,18E+07	4,94E+07	4,07E+07	4,92E+07
H12_T14_Seed170.max: PeakValue for DynRes	1,92E+05	2,27E+05	1,54E+05	1,50E+05	4,13E+07	3,61E+07	4,37E+07	4,02E+07
H12_T14_Seed180.max: PeakValue for DynRes	2,23E+05	1,69E+05	2,48E+05	2,81E+05	4,29E+07	3,47E+07	3,91E+07	6,09E+07
H12_T14_Seed190.max: PeakValue for DynRes	1,61E+05	1,58E+05	1,83E+05	1,88E+05	4,05E+07	3,20E+07	4,92E+07	4,16E+07
Standard Deviation	2,55E+04	3,05E+04	3,35E+04	4,75E+04	2,99E+06	6,20E+06	3,86E+06	6,58E+06
Mean	**1,78E+05**	**1,93E+05**	**1,90E+05**	**2,08E+05**	**4,02E+07**	**3,79E+07**	**4,19E+07**	**4,41E+07**

C.3.3 Results when T_n=14

Table C-11 Mass dominated wave loads and OVTM when Tn=14s

Case	Mass dominated wave loads [N]				Overturning Moment [Nm]			
	FFT	EAP, 30comp	EAP, 60comp	EAP, 90comp	FFT	EAP, 30comp	EAP, 60comp	EAP, 90comp
H12_T14_Seed000.max: PeakValue for DynRes	8,02E+06	1,03E+07	8,74E+06	8,16E+06	4,43E+09	3,55E+09	3,82E+09	3,27E+09
H12_T14_Seed010.max: PeakValue for DynRes	7,86E+06	8,67E+06	8,01E+06	9,49E+06	4,15E+09	4,17E+09	3,42E+09	3,97E+09
H12_T14_Seed020.max: PeakValue for DynRes	8,37E+06	8,86E+06	9,19E+06	8,67E+06	4,69E+09	3,57E+09	3,62E+09	3,73E+09
H12_T14_Seed030.max: PeakValue for DynRes	8,84E+06	9,54E+06	8,99E+06	9,69E+06	4,80E+09	4,22E+09	5,14E+09	3,83E+09
H12_T14_Seed040.max: PeakValue for DynRes	8,16E+06	9,24E+06	8,85E+06	7,17E+06	3,93E+09	3,27E+09	3,54E+09	3,93E+09
H12_T14_Seed050.max: PeakValue for DynRes	8,22E+06	8,75E+06	9,76E+06	1,03E+07	4,00E+09	4,19E+09	4,91E+09	4,73E+09
H12_T14_Seed060.max: PeakValue for DynRes	7,66E+06	8,87E+06	8,75E+06	8,98E+06	4,19E+09	3,77E+09	4,34E+09	5,40E+09
H12_T14_Seed070.max: PeakValue for DynRes	7,13E+06	9,71E+06	9,08E+06	8,34E+06	3,71E+09	4,26E+09	5,04E+09	3,19E+09
H12_T14_Seed080.max: PeakValue for DynRes	7,07E+06	8,30E+06	7,52E+06	1,07E+07	3,34E+09	3,63E+09	3,68E+09	3,98E+09
H12_T14_Seed090.max: PeakValue for DynRes	6,90E+06	9,26E+06	7,73E+06	7,63E+06	4,19E+09	4,00E+09	3,85E+09	4,12E+09
H12_T14_Seed100.max: PeakValue for DynRes	8,56E+06	8,34E+06	8,03E+06	1,01E+07	4,44E+09	4,14E+09	3,58E+09	3,69E+09
H12_T14_Seed110.max: PeakValue for DynRes	8,02E+06	7,62E+06	9,38E+06	9,55E+06	4,06E+09	3,72E+09	4,76E+09	4,37E+09
H12_T14_Seed120.max: PeakValue for DynRes	8,62E+06	7,51E+06	9,21E+06	8,97E+06	4,45E+09	3,73E+09	4,95E+09	4,09E+09
H12_T14_Seed130.max: PeakValue for DynRes	9,22E+06	8,05E+06	9,30E+06	9,98E+06	4,08E+09	4,44E+09	5,42E+09	5,67E+09
H12_T14_Seed140.max: PeakValue for DynRes	8,01E+06	7,99E+06	8,20E+06	8,57E+06	4,31E+09	4,37E+09	4,11E+09	4,63E+09
H12_T14_Seed150.max: PeakValue for DynRes	8,34E+06	1,07E+07	8,77E+06	9,84E+06	3,67E+09	3,47E+09	3,52E+09	3,84E+09
H12_T14_Seed160.max: PeakValue for DynRes	9,29E+06	9,80E+06	7,92E+06	9,08E+06	4,52E+09	3,49E+09	3,62E+09	4,21E+09
H12_T14_Seed170.max: PeakValue for DynRes	8,24E+06	9,07E+06	8,49E+06	7,57E+06	4,96E+09	4,25E+09	3,51E+09	2,99E+09
H12_T14_Seed180.max: PeakValue for DynRes	8,55E+06	8,33E+06	8,84E+06	9,98E+06	4,51E+09	4,68E+09	4,46E+09	3,64E+09
H12_T14_Seed190.max: PeakValue for DynRes	8,03E+06	7,65E+06	9,35E+06	1,00E+07	4,36E+09	3,81E+09	4,95E+09	3,47E+09
Standard Deviation	6,39E+05	8,89E+05	6,21E+05	9,99E+05	3,95E+08	3,86E+08	6,76E+08	6,77E+08
Mean	**8,16E+06**	**8,83E+06**	**8,70E+06**	**9,14E+06**	**4,24E+09**	**3,94E+09**	**4,21E+09**	**4,04E+09**

Table C-12 Drag dominated wave loads and OVTM when Tn=14s

Case	Drag dominated wave loads [N]				Overturning Moment [Nm]			
	FFT	EAP, 30comp	EAP, 60comp	EAP, 90comp	FFT	EAP, 30comp	EAP, 60comp	EAP, 90comp
H12_T14_Seed000.max: PeakValue for DynRes	1,78E+05	2,22E+05	1,67E+05	1,45E+05	7,26E+07	6,92E+07	6,99E+07	5,29E+07
H12_T14_Seed010.max: PeakValue for DynRes	1,78E+05	1,69E+05	1,91E+05	2,35E+05	6,89E+07	7,14E+07	5,98E+07	7,27E+07
H12_T14_Seed020.max: PeakValue for DynRes	1,79E+05	1,69E+05	1,63E+05	1,67E+05	7,95E+07	5,97E+07	6,26E+07	6,24E+07
H12_T14_Seed030.max: PeakValue for DynRes	1,98E+05	1,92E+05	1,63E+05	1,98E+05	9,12E+07	7,08E+07	8,78E+07	6,89E+07
H12_T14_Seed040.max: PeakValue for DynRes	1,96E+05	1,77E+05	2,12E+05	1,38E+05	6,74E+07	6,01E+07	6,02E+07	7,09E+07
H12_T14_Seed050.max: PeakValue for DynRes	1,85E+05	1,54E+05	1,79E+05	2,19E+05	7,07E+07	6,75E+07	8,37E+07	9,30E+07
H12_T14_Seed060.max: PeakValue for DynRes	1,62E+05	1,51E+05	1,88E+05	1,88E+05	7,18E+07	6,43E+07	8,38E+07	9,79E+07
H12_T14_Seed070.max: PeakValue for DynRes	1,77E+05	1,83E+05	1,94E+05	2,13E+05	6,73E+07	7,29E+07	9,82E+07	5,79E+07
H12_T14_Seed080.max: PeakValue for DynRes	1,78E+05	1,50E+05	1,67E+05	2,15E+05	5,59E+07	5,71E+07	6,57E+07	6,60E+07
H12_T14_Seed090.max: PeakValue for DynRes	1,68E+05	2,21E+05	1,57E+05	1,43E+05	7,02E+07	7,65E+07	6,66E+07	7,74E+07
H12_T14_Seed100.max: PeakValue for DynRes	1,94E+05	2,07E+05	1,48E+05	2,63E+05	8,57E+07	7,09E+07	6,47E+07	6,86E+07
H12_T14_Seed110.max: PeakValue for DynRes	1,96E+05	1,53E+05	1,57E+05	2,10E+05	7,23E+07	7,08E+07	7,64E+07	7,10E+07
H12_T14_Seed120.max: PeakValue for DynRes	1,33E+05	1,37E+05	1,71E+05	1,85E+05	7,97E+07	6,51E+07	8,81E+07	7,50E+07
H12_T14_Seed130.max: PeakValue for DynRes	1,44E+05	1,51E+05	1,79E+05	2,92E+05	8,33E+07	7,61E+07	9,00E+07	1,01E+08
H12_T14_Seed140.max: PeakValue for DynRes	1,93E+05	1,53E+05	1,44E+05	1,55E+05	7,47E+07	7,38E+07	6,98E+07	7,16E+07
H12_T14_Seed150.max: PeakValue for DynRes	1,96E+05	1,92E+05	2,14E+05	1,92E+05	6,99E+07	6,38E+07	5,89E+07	7,49E+07
H12_T14_Seed160.max: PeakValue for DynRes	2,11E+05	2,05E+05	1,33E+05	2,02E+05	8,66E+07	6,77E+07	6,00E+07	7,13E+07
H12_T14_Seed170.max: PeakValue for DynRes	1,91E+05	1,87E+05	1,50E+05	1,36E+05	9,05E+07	8,17E+07	6,01E+07	4,99E+07
H12_T14_Seed180.max: PeakValue for DynRes	1,91E+05	1,64E+05	1,92E+05	2,62E+05	8,31E+07	7,69E+07	8,58E+07	6,61E+07
H12_T14_Seed190.max: PeakValue for DynRes	1,66E+05	1,48E+05	1,92E+05	1,98E+05	7,50E+07	6,68E+07	8,81E+07	6,49E+07
Standard Deviation	1,90E+04	2,57E+04	2,22E+04	4,35E+04	8,96E+06	6,34E+06	1,29E+07	1,31E+07
Mean	**1,81E+05**	**1,74E+05**	**1,73E+05**	**1,98E+05**	**7,58E+07**	**6,92E+07**	**7,40E+07**	**7,17E+07**

D 90 Percentile estimates from Gumbel Distributions

This Appendix contains tables of all relevant 90 percentile estimates from the Gumbel distributions in the rapport. These values may be important for deciding adequate safety factors if using the equal area method.

The parameter estimation, α and b is done in WAFO. Then the 90 percentile estimates are found by equation D-1.

$$y_{0,90} = b + \frac{-\ln(-\ln(0,90))}{a} \qquad \textbf{(D-1)}$$

D.1 90 Percentile estimates for Fixed Cylinder

Table D-1 90 Percentile estimates for Surface elevation (static analysis)

Method	Number of comp	Mean [m]	90percentile [m]	Ratio
Equal Area	30	9,97	12,15	1,03
Equal Area	60	9,83	12,42	1,05
Equal Area	90	9,75	12,53	1,06
Equal Omega	1000	9,00	11,83	1,00

Table D-2 90 percentile estimates for static mass - and drag dominated wave loads

	Method	Number of comp	Mean	90percentile	Ratio
Mass dominated [N]	Equal Area	30	8,89E+06	1,02E+07	1,12
	Equal Area	60	8,66E+06	9,45E+06	1,04
	Equal Area	90	8,73E+06	9,70E+06	1,06
	Equal Omega	1000	8,09E+06	9,13E+06	1,00
Drag Dominated [N]	Equal Area	30	2,00E+05	2,44E+05	1,21
	Equal Area	60	1,95E+05	2,29E+05	1,13
	Equal Area	90	1,97E+05	2,33E+05	1,15
	Equal Omega	1000	1,69E+05	2,02E+05	1,00

Table D-3 90 percentile estimates for OVTM when wave loads are mass dominated

OVTM [Nm]	Method	Number of comp.	Mean	90 percentile	Ratio
Tn=4,4s	Equal Area	30	9,50E+08	1,08E+09	0,78
	Equal Area	60	9,11E+08	1,03E+09	0,75
	Equal Area	90	8,95E+08	1,11E+09	0,80
	Equal Omega	1000	1,23E+09	1,38E+09	1,00
Tn=8,5s	Equal Area	30	2,07E+09	2,34E+09	0,79
	Equal Area	60	2,43E+09	2,67E+09	0,91
	Equal Area	90	2,65E+09	2,97E+09	1,01
	Equal Omega	1000	2,58E+09	2,95E+09	1,00
Tn=14s	Equal Area	30	3,94E+09	4,45E+09	0,93
	Equal Area	60	4,21E+09	5,10E+09	1,07
	Equal Area	90	4,04E+09	4,93E+09	1,04
	Equal Omega	1000	4,24E+09	4,76E+09	1,00

Table D-4 90 percentile estimates for OVTM when wave loads are drag dominated

OVTM [Nm]	Method	Number of comp.	Mean	90 percentile	Ratio
Tn=4,4s	Equal Area	30	2,41E+07	3,14E+07	1,15
	Equal Area	60	2,34E+07	2,81E+07	1,03
	Equal Area	90	2,28E+07	2,96E+07	1,08
	Equal Omega	1000	2,32E+07	2,73E+07	1,00
Tn=8,5s	Equal Area	30	3,79E+07	4,60E+07	1,04
	Equal Area	60	4,19E+07	4,70E+07	1,07
	Equal Area	90	4,41E+07	5,27E+07	1,20
	Equal Omega	1000	4,02E+07	4,41E+07	1,00
Tn=14s	Equal Area	30	6,92E+07	7,75E+07	0,88
	Equal Area	60	7,40E+07	9,09E+07	1,04
	Equal Area	90	7,17E+07	8,89E+07	1,01
	Equal Omega	1000	7,58E+07	8,76E+07	1,00

D.2 90 percentile estimates on SWAY when using SPOOLWAVE

Table D-5 90 percentile estimates for cardan force, full - and spoolwave analysis

Method	Cardan Force [N]		
	mean	90percentile	Ratio
Spoolwave, min crest	4,10E+06	4,34E+06	0,98
Best results with Spoolwave	4,26E+06	4,48E+06	1,01
Full analysis	4,29E+06	4,45E+06	1,00

Table D-6 90 percentile estimates for Moment at sea surface, full - and spoolwave analysis

Method	Moment at Sea surface [Nm]		
	mean	90percentile	Ratio
Spoolwave, max crest	2,49E+08	2,89E+08	1,02
Full analysis	2,50E+08	2,83E+08	1,00

E Results from analyses on SWAY

Here, one finds the response quantities for all analyses performed on SWAY.

Table E-1 SWAY Responses when using EAP, 30 components

Case	Disp top tower [m]	Acc top tower [m/s^2]	Cardan Force (top) [N]	Mz at sea surface [Nm]	Surface elevation [m]	Wave load [N]
H=16.4_T=17_Seed=000_0030.max:	50,62	4,61	4,47E+06	2,77E+08	11,09	1,23E+07
H=16.4_T=17_Seed=010_0030.max:	45,64	4,76	4,35E+06	2,69E+08	12,50	1,32E+07
H=16.4_T=17_Seed=020_0030.max:	49,84	5,36	4,50E+06	2,72E+08	11,24	1,58E+07
H=16.4_T=17_Seed=030_0030.max:	43,66	4,92	4,25E+06	2,60E+08	11,33	1,38E+07
H=16.4_T=17_Seed=040_0030.max:	54,72	5,49	4,33E+06	2,73E+08	14,81	1,78E+07
H=16.4_T=17_Seed=050_0030.max:	48,63	6,38	4,41E+06	2,48E+08	14,82	1,98E+07
H=16.4_T=17_Seed=060_0030.max:	49,76	4,94	4,35E+06	2,79E+08	12,69	1,49E+07
H=16.4_T=17_Seed=070_0030.max:	45,75	5,33	4,34E+06	2,81E+08	12,42	1,45E+07
H=16.4_T=17_Seed=080_0030.max:	39,25	5,21	4,11E+06	2,57E+08	12,06	1,55E+07
H=16.4_T=17_Seed=090_0030.max:	47,82	5,15	4,30E+06	2,75E+08	11,52	1,43E+07
H=16.4_T=17_Seed=100_0030.max:	66,18	6,28	4,90E+06	3,57E+08	14,82	1,61E+07
H=16.4_T=17_Seed=110_0030.max:	48,07	5,65	4,19E+06	2,20E+08	12,40	1,54E+07
H=16.4_T=17_Seed=120_0030.max:	50,76	6,13	4,29E+06	2,59E+08	12,45	1,72E+07
H=16.4_T=17_Seed=130_0030.max:	47,93	5,50	4,19E+06	2,94E+08	12,46	1,49E+07
H=16.4_T=17_Seed=140_0030.max:	48,44	6,54	4,42E+06	2,79E+08	15,47	1,92E+07
H=16.4_T=17_Seed=150_0030.max:	54,88	5,07	4,27E+06	2,88E+08	11,78	1,36E+07
H=16.4_T=17_Seed=160_0030.max:	48,83	6,01	4,24E+06	2,57E+08	14,88	1,66E+07
H=16.4_T=17_Seed=170_0030.max:	57,17	6,55	4,46E+06	2,95E+08	16,58	2,08E+07
H=16.4_T=17_Seed=180_0030.max:	45,37	5,20	4,38E+06	2,76E+08	11,57	1,39E+07
H=16.4_T=17_Seed=190_0030.max:	56,74	4,94	4,66E+06	2,82E+08	12,48	1,44E+07
Max	66,18	6,55	4,90E+06	3,57E+08	16,58	2,08E+07
Min	39,25	4,61	4,11E+06	2,20E+08	11,09	1,23E+07
Standard Deviation	5,80	0,61	1,76E+05	2,57E+07	1,63	2,27E+06
Mean	**50,00**	**5,50**	**4,37E+06**	**2,75E+08**	**12,97**	**1,57E+07**

Table E-2 SWAY Responses when using EAP, 60 components

Case	Disp top tower [m]	Acc top tower [m/s^2]	Cardan Force (top) [N]	Mz at sea surface [Nm]	Surface elevation [m]	Wave load [N]
H=16.4_T=17_Seed=000_0060.max:	40,08	5,09E+00	4,25E+06	2,58E+08	1,30E+01	1,43E+07
H=16.4_T=17_Seed=010_0060.max:	32,83	4,64E+00	4,29E+06	2,12E+08	1,29E+01	1,41E+07
H=16.4_T=17_Seed=020_0060.max:	43,91	5,03E+00	4,23E+06	2,61E+08	1,24E+01	1,57E+07
H=16.4_T=17_Seed=030_0060.max:	47,62	5,19E+00	4,19E+06	2,63E+08	1,40E+01	1,59E+07
H=16.4_T=17_Seed=040_0060.max:	41,22	5,00E+00	4,43E+06	2,71E+08	1,19E+01	1,26E+07
H=16.4_T=17_Seed=050_0060.max:	50,45	5,62E+00	4,15E+06	2,73E+08	1,62E+01	1,78E+07
H=16.4_T=17_Seed=060_0060.max:	52,83	6,55E+00	4,44E+06	2,66E+08	1,44E+01	1,93E+07
H=16.4_T=17_Seed=070_0060.max:	39,92	4,58E+00	4,08E+06	2,41E+08	1,15E+01	1,30E+07
H=16.4_T=17_Seed=080_0060.max:	45,52	5,83E+00	4,41E+06	2,63E+08	1,43E+01	1,91E+07
H=16.4_T=17_Seed=090_0060.max:	41,33	5,04E+00	4,44E+06	2,64E+08	1,27E+01	1,56E+07
H=16.4_T=17_Seed=100_0060.max:	39,75	4,73E+00	4,16E+06	2,55E+08	1,10E+01	1,40E+07
H=16.4_T=17_Seed=110_0060.max:	55,47	6,77E+00	4,46E+06	3,60E+08	1,53E+01	1,73E+07
H=16.4_T=17_Seed=120_0060.max:	51,01	5,80E+00	4,38E+06	3,14E+08	1,48E+01	1,66E+07
H=16.4_T=17_Seed=130_0060.max:	43,85	4,60E+00	4,23E+06	2,36E+08	1,26E+01	1,51E+07
H=16.4_T=17_Seed=140_0060.max:	46,67	5,95E+00	4,58E+06	2,82E+08	1,31E+01	1,78E+07
H=16.4_T=17_Seed=150_0060.max:	60,60	6,06E+00	4,41E+06	3,42E+08	1,40E+01	1,56E+07
H=16.4_T=17_Seed=160_0060.max:	48,85	6,00E+00	4,26E+06	3,14E+08	1,29E+01	1,63E+07
H=16.4_T=17_Seed=170_0060.max:	44,18	5,93E+00	4,29E+06	2,43E+08	1,25E+01	1,61E+07
H=16.4_T=17_Seed=180_0060.max:	37,03	5,00E+00	4,12E+06	2,46E+08	1,31E+01	1,58E+07
H=16.4_T=17_Seed=190_0060.max:	48,65	5,05E+00	4,28E+06	2,83E+08	1,24E+01	1,46E+07
Max	60,60	6,77	4,58E+06	3,60E+08	16,19	1,93E+07
Min	32,83	4,58	4,08E+06	2,12E+08	11,05	1,26E+07
Standard Deviation	6,61	0,65	1,33E+05	3,60E+07	1,29	1,82E+06
Mean	**45,59**	**5,42**	**4,30E+06**	**2,72E+08**	**13,25**	**1,58E+07**

Table E-3 SWAY Responses when using EAP, 90 components

Case	Disp top tower [m]	Acc top tower [m/s^2]	Cardan Force (top) [N]	Mz at sea surface [Nm]	Surface elevation [m]	Wave load [N]
H=16.4_T=17_Seed=000_0090.max:	49,20	5,60	4,50E+06	2,80E+08	12,15	1,72E+07
H=16.4_T=17_Seed=010_0090.max:	51,82	5,68	4,35E+06	2,82E+08	13,93	1,69E+07
H=16.4_T=17_Seed=020_0090.max:	41,11	4,70	4,19E+06	2,18E+08	10,16	1,31E+07
H=16.4_T=17_Seed=030_0090.max:	46,49	5,41	4,31E+06	2,34E+08	14,04	1,82E+07
H=16.4_T=17_Seed=040_0090.max:	40,65	5,48	4,13E+06	2,49E+08	12,64	1,58E+07
H=16.4_T=17_Seed=050_0090.max:	36,26	6,50	4,29E+06	2,67E+08	14,12	1,76E+07
H=16.4_T=17_Seed=060_0090.max:	40,87	5,42	4,54E+06	2,34E+08	13,14	1,69E+07
H=16.4_T=17_Seed=070_0090.max:	37,52	5,49	4,25E+06	2,83E+08	11,85	1,48E+07
H=16.4_T=17_Seed=080_0090.max:	44,83	4,80	4,22E+06	2,39E+08	11,69	1,43E+07
H=16.4_T=17_Seed=090_0090.max:	48,21	5,84	4,33E+06	3,07E+08	13,35	1,75E+07
H=16.4_T=17_Seed=100_0090.max:	44,53	6,12	4,24E+06	2,52E+08	13,08	1,80E+07
H=16.4_T=17_Seed=110_0090.max:	38,38	5,37	4,21E+06	2,50E+08	11,92	1,54E+07
H=16.4_T=17_Seed=120_0090.max:	52,02	6,14	4,42E+06	3,37E+08	12,70	1,52E+07
H=16.4_T=17_Seed=130_0090.max:	41,83	5,39	4,23E+06	2,78E+08	13,34	1,67E+07
H=16.4_T=17_Seed=140_0090.max:	41,39	5,05	4,14E+06	2,26E+08	11,49	1,41E+07
H=16.4_T=17_Seed=150_0090.max:	52,84	5,16	4,23E+06	2,87E+08	12,99	1,44E+07
H=16.4_T=17_Seed=160_0090.max:	57,89	5,22	4,29E+06	2,87E+08	14,56	1,61E+07
H=16.4_T=17_Seed=170_0090.max:	35,65	5,34	4,08E+06	2,17E+08	12,27	1,61E+07
H=16.4_T=17_Seed=180_0090.max:	40,47	5,10	4,08E+06	2,39E+08	12,96	1,46E+07
H=16.4_T=17_Seed=190_0090.max:	44,91	5,73	4,26E+06	2,21E+08	11,56	1,70E+07
Max	57,89	6,50	4,54E+06	3,37E+08	14,56	1,82E+07
Min	35,65	4,70	4,08E+06	2,17E+08	10,16	1,31E+07
Standard Deviation	6,09	0,44	1,22E+05	3,25E+07	1,08	1,46E+06
Mean	**44,34**	**5,48**	**4,26E+06**	**2,59E+08**	**12,70**	**1,60E+07**

Table E-4 SWAY Responses when using FFT, 1000 components

Case	Disp top tower [m]	Acc top tower [m/s^2]	Cardan Force (top) [N]	Mz at sea surface [Nm]	Surface elevation [m]	Wave load [N]
H=16.4_T=17_Seed=000_1000.max:	36,35	4,57	4,11E+06	2,31E+08	11,68	1,30E+07
H=16.4_T=17_Seed=010_1000.max:	49,48	5,77	4,40E+06	2,65E+08	15,10	1,77E+07
H=16.4_T=17_Seed=020_1000.max:	49,97	4,91	4,30E+06	2,56E+08	12,40	1,52E+07
H=16.4_T=17_Seed=030_1000.max:	42,38	4,74	4,12E+06	2,47E+08	12,57	1,46E+07
H=16.4_T=17_Seed=040_1000.max:	42,12	4,72	4,48E+06	2,55E+08	13,61	1,45E+07
H=16.4_T=17_Seed=050_1000.max:	40,88	4,49	4,16E+06	2,43E+08	11,17	1,21E+07
H=16.4_T=17_Seed=060_1000.max:	42,37	5,14	4,17E+06	2,56E+08	13,13	1,56E+07
H=16.4_T=17_Seed=070_1000.max:	38,46	4,14	4,15E+06	2,19E+08	11,93	1,28E+07
H=16.4_T=17_Seed=080_1000.max:	40,64	4,52	4,20E+06	2,41E+08	10,73	1,38E+07
H=16.4_T=17_Seed=090_1000.max:	36,48	4,51	4,12E+06	2,38E+08	10,94	1,35E+07
H=16.4_T=17_Seed=100_1000.max:	37,19	4,96	4,24E+06	2,55E+08	11,28	1,52E+07
H=16.4_T=17_Seed=110_1000.max:	45,45	4,82	4,23E+06	2,63E+08	11,96	1,39E+07
H=16.4_T=17_Seed=120_1000.max:	42,69	5,11	4,18E+06	2,32E+08	11,29	1,60E+07
H=16.4_T=17_Seed=130_1000.max:	52,75	5,13	4,41E+06	2,75E+08	15,02	1,53E+07
H=16.4_T=17_Seed=140_1000.max:	48,00	5,09	4,29E+06	2,57E+08	12,35	1,54E+07
H=16.4_T=17_Seed=150_1000.max:	43,50	4,79	4,23E+06	2,33E+08	12,15	1,52E+07
H=16.4_T=17_Seed=160_1000.max:	40,56	5,09	4,34E+06	2,70E+08	10,98	1,34E+07
H=16.4_T=17_Seed=170_1000.max:	47,26	5,01	4,18E+06	2,54E+08	12,16	1,57E+07
H=16.4_T=17_Seed=180_1000.max:	36,72	4,75	4,27E+06	2,07E+08	11,23	1,50E+07
H=16.4_T=17_Seed=190_1000.max:	36,57	4,91	4,19E+06	2,35E+08	11,72	1,39E+07
Max	52,75	5,77	4,48E+06	2,75E+08	15,10	1,77E+07
Min	36,35	4,14	4,11E+06	2,07E+08	10,73	1,21E+07
Standard Deviation	4,97	0,34	1,06E+05	1,72E+07	1,23	1,31E+06
Mean	**42,49**	**4,86**	**4,24E+06**	**2,47E+08**	**12,17**	**1,46E+07**

F Additional Results from Analyses with Spoolwave

The responses; the cardan force, moment in the tower at sea surface, and acceleration at tower top are considered the most interesting response quantities and is displayed and discussed in the rapport. However, the results from wave load and tower top displacement may also be of importance, and are therefore given in this Appendix.

Table F-1 Overview of Wave Load results from Full and Spoolwave Analysis

Case	Full Analysis	Spoolwave, Max Crest	Ratio	Best Result with Spoolwave	Ratio	Order
H=16.4_T=17_Seed=000_0090.max:	1,72E+07	1,72E+07	1,00	1,72E+07	1,00	1
H=16.4_T=17_Seed=030_0090.max:	1,82E+07	1,82E+07	1,00	1,82E+07	1,00	1
H=16.4_T=17_Seed=060_0090.max:	1,69E+07	1,28E+07	0,76	1,69E+07	1,00	-1
H=16.4_T=17_Seed=080_0090.max:	1,43E+07	1,41E+07	0,99	1,41E+07	0,99	1
H=16.4_T=17_Seed=100_0090.max:	1,80E+07	1,44E+07	0,80	1,65E+07	0,92	-1
H=16.4_T=17_Seed=110_0090.max:	1,54E+07	1,36E+07	0,88	1,54E+07	1,00	-1
H=16.4_T=17_Seed=130_0090.max:	1,67E+07	1,67E+07	1,00	1,67E+07	1,00	1
H=16.4_T=17_Seed=140_0090.max:	1,41E+07	1,50E+07	1,06	1,50E+07	1,06	1
H=16.4_T=17_Seed=150_0090.max:	1,44E+07	1,43E+07	0,99	1,43E+07	0,99	1
H=16.4_T=17_Seed=160_0090.max:	1,61E+07	1,61E+07	1,00	1,61E+07	1,00	1
H=16.4_T=17_Seed=170_0090.max:	1,61E+07	1,61E+07	1,00	1,61E+07	1,00	1
H=16.4_T=17_Seed=180_0090.max:	1,46E+07	1,47E+07	1,01	1,47E+07	1,01	1
H=16.4_T=17_Seed=190_0090.max:	1,70E+07	1,32E+07	0,78	1,70E+07	1,00	-1
Max	1,82E+07	1,82E+07	1,06	1,82E+07	1,06	
Min	1,41E+07	1,28E+07	0,76	1,41E+07	0,92	
Standard Deviation	1,42E+06	1,63E+06	0,10	1,25E+06	0,03	
Mean	**1,61E+07**	**1,51E+07**	**0,94**	**1,60E+07**	**1,00**	

Table F-2 Overview of Tower top Displacement results from Full and Spoolwave Analysis

Case	Full Analysis	Spoolwave, Max Crest	Ratio	Best Result with Spoolwave	Ratio	Order
H=16.4_T=17_Seed=000_0090.max:	49,20	50,61	1,03	50,61	1,03	1
H=16.4_T=17_Seed=030_0090.max:	46,49	46,15	0,99	46,15	0,99	1
H=16.4_T=17_Seed=060_0090.max:	40,87	40,42	0,99	40,42	0,99	1
H=16.4_T=17_Seed=080_0090.max:	44,83	40,40	0,90	44,87	1,00	-1
H=16.4_T=17_Seed=100_0090.max:	44,53	42,67	0,96	42,67	0,96	1
H=16.4_T=17_Seed=110_0090.max:	38,38	40,97	1,07	40,97	1,07	1
H=16.4_T=17_Seed=130_0090.max:	41,83	42,24	1,01	42,24	1,01	1
H=16.4_T=17_Seed=140_0090.max:	41,39	43,85	1,06	43,85	1,06	1
H=16.4_T=17_Seed=150_0090.max:	52,84	53,25	1,01	53,25	1,01	1
H=16.4_T=17_Seed=160_0090.max:	57,89	57,89	1,00	57,89	1,00	1
H=16.4_T=17_Seed=170_0090.max:	35,65	35,65	1,00	35,65	1,00	1
H=16.4_T=17_Seed=180_0090.max:	40,47	35,80	0,88	35,80	0,88	1
H=16.4_T=17_Seed=190_0090.max:	44,91	42,27	0,94	44,18	0,98	-1
Max	57,89	57,89	1,07	57,89	1,07	
Min	35,65	35,65	0,88	35,65	0,88	
Standard Deviation	6,04	6,50	0,05	6,38	0,05	
Mean	**44,56**	**44,01**	**0,99**	**44,50**	**1,00**	